

R-VGAL: A Sequential Variational Bayes Algorithm for Generalised Linear Mixed Models

Bao Anh Vu^{1, 2, *}, David Gunawan¹, and Andrew Zammit-Mangion^{1, 2}

¹School of Mathematics and Statistics, University of Wollongong, Wollongong, New South
Wales, Australia

²Securing Antarctica’s Environmental Future, University of Wollongong, Wollongong, New
South Wales, Australia

April 19, 2024

Abstract

Models with random effects, such as generalised linear mixed models (GLMMs), are often used for analysing clustered data. Parameter inference with these models is difficult because of the presence of cluster-specific random effects, which must be integrated out when evaluating the likelihood function. Here, we propose a sequential variational Bayes algorithm, called Recursive Variational Gaussian Approximation for Latent variable models (R-VGAL), for estimating parameters in GLMMs. The R-VGAL algorithm operates on the data sequentially, requires only a single pass through the data, and can provide parameter updates as new data are collected without the need of re-processing the previous data. At each update, the R-VGAL algorithm requires the gradient and Hessian of a “partial” log-likelihood function evaluated at the new observation, which are generally not available in closed form for GLMMs. To circumvent this issue, we propose using an importance-sampling-based approach for estimating the gradient and Hessian via Fisher’s and Louis’ identities. We find that R-VGAL can be unstable when traversing the first few data points, but that this issue can be mitigated by introducing a damping factor in the initial steps of the algorithm. Through illustrations on both simulated and real datasets, we show that R-VGAL provides good approximations to posterior distributions, that it can be made robust through damping, and that it is computationally efficient.

* Corresponding author
E-mail address: bavu@uow.edu.au

Keywords: Fisher’s identity, intractable gradient, latent variable model, Louis’ identity, damped Newton’s method

1 Introduction

Mixed models are useful for analysing clustered data, wherein observations that come from the same cluster/group are likely to be correlated. Example datasets include records of students clustered within schools, and repeated measurements of biomarkers on patients. Mixed models account for intra-group dependencies by incorporating cluster/group-specific “random effects”. Inference with these models is made challenging by the fact that the likelihood function involves integrals over the random effects that are not usually tractable except for the few cases where the distribution of the random effects is conjugate to the distribution of the data, such as in the linear mixed model (Verbeke et al., 1997), the beta-binomial model (Crowder, 1979), and Rasch’s Poisson count model (Jansen, 1994). Notably, there is no closed-form expression for the likelihood function in the case of the ubiquitous logistic mixed model.

Maximum-likelihood-based approaches are often used for parameter inference in mixed models. In the case of linear mixed models, parameter inference via maximum likelihood estimation is straightforward (e.g., Wakefield, 2013). For mixed models with an intractable likelihood, integrals over random effects need to be numerically approximated, for example by using Gaussian quadrature (Naylor and Smith, 1982) or the Laplace approximation (Tierney and Kadane, 1986). The likelihood may also be indirectly maximised using an expectation-maximisation type algorithm (Dempster et al., 1977), which treats the random effects as missing, and iteratively maximises the “expected complete-data log-likelihood” of the data and the random effects. Quasi-likelihood approaches such as penalised quasi-likelihood (PQL, Breslow and Clayton, 1993) and marginal quasi-likelihood (MQL, Goldstein, 1991) approximate nonlinear mixed models with linear mixed models, so that well-developed estimation routines for linear mixed models can be applied; see Tuerlinckx et al. (2006) for a detailed discussion of these methods. These maximum-likelihood-based methods provide point estimates and not full posterior distributions over the parameters.

Full posterior distributions can be obtained using Markov chain Monte Carlo (MCMC, e.g., Zhao et al., 2006; Fong et al., 2010). MCMC provides exact, sample-based posterior distributions, but at a higher computational cost than maximum-likelihood-based methods. Alternatively, variational Bayes (VB) methods (e.g., Ong et al., 2018; Tan and Nott, 2018) are becoming increasingly popular for estimating parameters in complex statistical models. These methods approximate the exact posterior distribution with a member from a simple and tractable family of distributions; this family is usually chosen to balance the accuracy

of the approximation against the computational cost required to obtain the approximation. VB methods are usually computationally cheaper than MCMC methods. VB approaches can either batch-process the data (e.g., Tran et al., 2016; Ong et al., 2018; Tan and Nott, 2018) or sequentially process data points (e.g., Broderick et al., 2013; Gunawan et al., 2021; Lambert et al., 2022). For settings with large amounts of data, a method that targets the posterior distribution via sequential processing of the data offers several advantages. The so-called Recursive Variational Gaussian Approximation (R-VGA, Lambert et al., 2022) algorithm is a recently-developed sequential variational Bayes method that provides a fast and accurate approximation to the posterior distribution with only one pass through the data, making it computationally efficient when compared to MCMC or batch variational Bayes. Lambert et al. (2022) apply the R-VGA algorithm to linear and logistic regression models without random effects.

In this paper, we build on the R-VGA algorithm by proposing a novel recursive variational Gaussian approximation, called Recursive Variational Gaussian Approximation for Latent variable models (R-VGAL), for estimating the parameters in GLMMs. At each update, R-VGAL requires the gradient and Hessian of the “partial” log-likelihood evaluated at the new observation, which are often not available in closed form. To circumvent this issue, we propose an importance-sampling-based approach for estimating the gradient and Hessian that uses Fisher’s and Louis’ identities (Cappé et al., 2005). This approach was inspired by the work of Nemeth et al. (2016), who used Fisher’s and Louis’ identities to approximate the gradient and Hessian in a sequential Monte Carlo context. The efficacy of R-VGAL is illustrated using linear, logistic and Poisson mixed effect models on simulated and real datasets. The examples show that R-VGAL provides good approximations to the exact posterior distributions estimated using Hamiltonian Monte Carlo (HMC, Neal, 2011; Betancourt and Girolami, 2015) and at a low computational cost.

The paper is organised as follows. Sect. 2 provides some background on the sequential variational Bayes framework and presents the R-VGAL algorithm. Sect. 3 applies the R-VGAL algorithm to simulated and real datasets. Sect. 4 concludes with a discussion of our results and an overview of future research directions. This article has an online supplement containing additional technical details, and the code to reproduce results from the simulation and real-data experiments is available on <https://github.com/bao-anh-vu/R-VGAL>.

2 The R-VGAL algorithm

This section reviews GLMMs (e.g. Demidenko, 2013; Faraway, 2016) and provides some background on the R-VGA algorithm of Lambert et al. (2022), and then introduces the R-VGAL algorithm for making parameter inference with GLMMs.

2.1 Generalised linear mixed models

GLMMs are statistical models that contain both fixed effects and random effects. Typically, the fixed effects are common across groups, while the random effects are group-specific, and this is the setting we focus on. We briefly discuss the potential application of R-VGAL to models with more complicated random effect structures, such as crossed or nested random effects, in Sect. S7 of the online supplement.

Denote by y_{ij} the j th response in the i th group, for $i = 1, \dots, N$ groups and $j = 1, \dots, n_i$, where n_i is the number of responses in group i . Let $\mathbf{y} \equiv (\mathbf{y}_1^\top, \dots, \mathbf{y}_N^\top)^\top$ be a vector of observations, where $\mathbf{y}_i \equiv (y_{i1}, \dots, y_{in_i})^\top$ are the responses from the i th group. The GLMMs we consider are constructed by first assigning each y_{ij} a distribution $y_{ij} \mid \boldsymbol{\beta}, \boldsymbol{\alpha}_i, \phi \sim p(\cdot)$, where $p(\cdot)$ is a member of the exponential family with a dispersion parameter ϕ that is usually related to the variance of the datum, $\boldsymbol{\beta}$ are the fixed effect parameters, and $\boldsymbol{\alpha}_i$ are the group-specific random effects for $i = 1, \dots, N$. Then, the mean of the responses, $\mu_{ij} \equiv \mathbb{E}(y_{ij} \mid \boldsymbol{\beta}, \boldsymbol{\alpha}_i, \phi)$, is modelled as

$$g(\mu_{ij}) = \mathbf{x}_{ij}^\top \boldsymbol{\beta} + \mathbf{z}_{ij}^\top \boldsymbol{\alpha}_i, \quad i = 1, \dots, N, \quad j = 1, \dots, n_i, \quad (1)$$

where \mathbf{x}_{ij} is a vector of fixed effect covariates corresponding to the j th response in the i th group; \mathbf{z}_{ij} is a vector of predictor variables corresponding to the j th response and the i th random effect; and $g(\cdot)$ is a link function that links the response mean μ_{ij} to the linear predictor $\mathbf{x}_{ij}^\top \boldsymbol{\beta} + \mathbf{z}_{ij}^\top \boldsymbol{\alpha}_i$. We further assume that $\boldsymbol{\alpha}_i \perp \boldsymbol{\alpha}_{i'}$ for $i \neq i'$. The random effects $\boldsymbol{\alpha}_i$, for $i = 1, \dots, N$, are assumed to follow a normal distribution with mean $\mathbf{0}$ and covariance matrix $\boldsymbol{\Sigma}_\alpha$, that is, each $\boldsymbol{\alpha}_i \mid \boldsymbol{\Sigma}_\alpha \sim \text{Gau}(\mathbf{0}, \boldsymbol{\Sigma}_\alpha)$. In practice, some structure is often assumed for the random effects covariance matrix so that it is parameterised in terms of a smaller number of parameters $\boldsymbol{\tau}$, that is, $\boldsymbol{\Sigma}_\alpha = \boldsymbol{\Sigma}_\alpha(\boldsymbol{\tau})$. Inference is then made on the parameters $\boldsymbol{\theta} = (\boldsymbol{\beta}^\top, \boldsymbol{\tau}^\top, \phi)^\top$.

The main objective of Bayesian inference is to obtain the posterior distribution of the model parameters $\boldsymbol{\theta}$ given the observations \mathbf{y} and the prior distribution $p(\boldsymbol{\theta})$. Through Bayes' rule, the posterior distribution of $\boldsymbol{\theta}$ is

$$p(\boldsymbol{\theta} \mid \mathbf{y}) = p(\boldsymbol{\beta}, \boldsymbol{\tau}, \phi \mid \mathbf{y}) \propto p(\mathbf{y} \mid \boldsymbol{\beta}, \boldsymbol{\tau}, \phi) p(\boldsymbol{\beta}, \boldsymbol{\tau}, \phi). \quad (2)$$

The likelihood function,

$$p(\mathbf{y} \mid \boldsymbol{\beta}, \boldsymbol{\tau}, \phi) = \prod_{i=1}^N \int p(\mathbf{y}_i \mid \boldsymbol{\alpha}_i, \boldsymbol{\beta}, \phi) p(\boldsymbol{\alpha}_i \mid \boldsymbol{\tau}) d\boldsymbol{\alpha}_i, \quad (3)$$

involves integrals over the random effects $\boldsymbol{\alpha}_i, i = 1, \dots, N$. The likelihood function can be calculated exactly for the linear mixed model with normally distributed random effects, for which

$$y_{ij} = \mathbf{x}_{ij}^\top \boldsymbol{\beta} + \mathbf{z}_{ij}^\top \boldsymbol{\alpha}_i + \epsilon_{ij}, \quad \boldsymbol{\alpha}_i \sim \text{Gau}(\mathbf{0}, \boldsymbol{\Sigma}_\alpha(\boldsymbol{\tau})), \quad \epsilon_{ij} \sim \text{Gau}(0, \sigma_\epsilon^2), \quad (4)$$

for $i = 1, \dots, N$ and $j = 1, \dots, n_i$, where ϵ_{ij} is a zero-mean, independent, normally distributed error term with variance σ_ϵ^2 that is associated with the j th response from the i th group. At the group level, this model can be written as

$$\mathbf{y}_i = \mathbf{X}_i \boldsymbol{\beta} + \mathbf{Z}_i \boldsymbol{\alpha}_i + \boldsymbol{\epsilon}_i, \quad \boldsymbol{\alpha}_i \sim \text{Gau}(\mathbf{0}, \boldsymbol{\Sigma}_\alpha(\boldsymbol{\tau})), \quad \boldsymbol{\epsilon}_i \sim \text{Gau}(\mathbf{0}, \sigma_\epsilon^2 \mathbf{I}_{n_i}),$$

where $\mathbf{X}_i \equiv (\mathbf{x}_{i1}, \dots, \mathbf{x}_{in_i})^\top$, $\mathbf{Z}_i \equiv (\mathbf{z}_{i1}, \dots, \mathbf{z}_{in_i})^\top$, and $\boldsymbol{\epsilon}_i \equiv (\epsilon_{i1}, \dots, \epsilon_{in_i})^\top$, with n_i being the number of observations in the i th group, for $i = 1, \dots, N$, and \mathbf{I}_m denotes an identity matrix of size $m \times m$. The likelihood function for this linear mixed model is

$$p(\mathbf{y} \mid \boldsymbol{\beta}, \boldsymbol{\tau}, \sigma_\epsilon^2) = \prod_{i=1}^N p(\mathbf{y}_i \mid \boldsymbol{\beta}, \boldsymbol{\tau}, \sigma_\epsilon^2) = \prod_{i=1}^N \text{Gau}(\mathbf{X}_i \boldsymbol{\beta}, \mathbf{Z}_i \boldsymbol{\Sigma}_\alpha(\boldsymbol{\tau}) \mathbf{Z}_i^\top + \sigma_\epsilon^2 \mathbf{I}_{n_i}). \quad (5)$$

The gradient and Hessian of the log-likelihood for the linear mixed model are also available in closed form. However, the likelihood $p(\mathbf{y}_i \mid \boldsymbol{\alpha}_i, \boldsymbol{\beta}, \phi)$ in (3) cannot be computed exactly for general random effects models. One important case is the logistic mixed model given by

$$y_{ij} \sim \text{Bernoulli}(\pi_{ij}), \quad \text{logit}(\pi_{ij}) = \mathbf{x}_{ij}^\top \boldsymbol{\beta} + \mathbf{z}_{ij}^\top \boldsymbol{\alpha}_i, \quad i = 1, \dots, N, \quad j = 1, \dots, n_i, \quad (6)$$

where $\text{logit}(\pi_{ij}) = \log\left(\frac{\pi_{ij}}{1-\pi_{ij}}\right)$. The gradient and Hessian of the log-likelihood function for this model can, however, be estimated unbiasedly, as we show in Sects. 2.3.1 and 2.3.2.

2.2 Sequential VB and R-VGA

We begin this section with a review of VB and the sequential VB framework. We then present the main steps in the derivations of the R-VGA algorithm of Lambert et al. (2022), on which our algorithm is based.

2.2.1 Sequential VB

VB is usually used for posterior inference in complex statistical models when inference using asymptotically exact methods such as MCMC is too costly; for a review see, for example, Blei et al. (2017). Let $\boldsymbol{\theta}$ be a vector of model parameters. Here, we consider the class of VB methods where the posterior distribution $p(\boldsymbol{\theta} \mid \mathbf{y})$ is approximated by a tractable density $q(\boldsymbol{\theta}; \boldsymbol{\lambda})$ parameterised by $\boldsymbol{\lambda}$. The variational parameters $\boldsymbol{\lambda}$ are optimised by minimising the Kullback-Leibler (KL) divergence between the variational distribution and

the posterior distribution, that is, by minimising

$$\text{KL}(q(\boldsymbol{\theta}; \boldsymbol{\lambda}) \parallel p(\boldsymbol{\theta} \mid \mathbf{y})) \equiv \int q(\boldsymbol{\theta}; \boldsymbol{\lambda}) \log \frac{q(\boldsymbol{\theta}; \boldsymbol{\lambda})}{p(\boldsymbol{\theta} \mid \mathbf{y})} d\boldsymbol{\theta}. \quad (7)$$

Many VB algorithms require processing the data as a batch; see, for example, Ong et al. (2018) and Tan and Nott (2018). The variational parameters $\boldsymbol{\lambda}$ are typically updated in an iterative manner using stochastic gradient descent (SGD, Hoffman et al., 2013; Kingma and Welling, 2013). In settings with large amounts of data or continuously-arriving data, it is often more practical to use online or sequential variational Bayes algorithms that update the approximation to the posterior distribution sequentially as new observations become available. These online/sequential algorithms are designed to handle data that are too large to fit in memory or that arrive in a continuous stream.

In a sequential VB framework, such as that proposed by Broderick et al. (2013), the observations $\mathbf{y}_1, \dots, \mathbf{y}_N$ are incorporated sequentially so that at iteration i , $i = 1, \dots, N$, one targets an approximation $q_i(\boldsymbol{\theta}) \equiv q(\boldsymbol{\theta}; \boldsymbol{\lambda}_i)$ that is closest in a KL sense to the “pseudo-posterior” $p(\mathbf{y}_i \mid \boldsymbol{\theta})q_{i-1}(\boldsymbol{\theta})/\mathcal{Z}_i$, where

$$\mathcal{Z}_i \equiv \int p(\mathbf{y}_i \mid \boldsymbol{\theta})q_{i-1}(\boldsymbol{\theta}) d\boldsymbol{\theta}. \quad (8)$$

In this framework, $q_{i-1}(\boldsymbol{\theta})$ is treated as the “prior” for the next iteration i , and the KL divergence between $q_i(\boldsymbol{\theta})$ and the “pseudo-posterior” is minimised at each iteration. Broderick et al. (2013) use a mean field VB approach (e.g., Ormerod and Wand, 2010), which assumes no posterior dependence between the elements of $\boldsymbol{\theta}$. The R-VGA algorithm proposed by Lambert et al. (2022) follows closely that of Broderick et al. (2013), but uses a variational distribution of the form $q_i(\boldsymbol{\theta}) = \text{Gau}(\boldsymbol{\mu}_i, \boldsymbol{\Sigma}_i)$, where $\boldsymbol{\Sigma}_i$ is a full covariance matrix, and seeks closed-form updates for $\boldsymbol{\lambda}_i \equiv \{\boldsymbol{\mu}_i, \boldsymbol{\Sigma}_i\}$ that minimise the KL divergence between $q_i(\boldsymbol{\theta})$ and $p(\mathbf{y}_i \mid \boldsymbol{\theta})q_{i-1}(\boldsymbol{\theta})/\mathcal{Z}_i$ for $i = 1, \dots, N$. Another sequential VB algorithm that is similar to that of Broderick et al. (2013) is the Updating Variational Bayes (UVB, Tomasetti et al., 2022) algorithm, which uses SGD (Bottou, 2010) at every iteration, $i = 1, \dots, N$, to minimise the KL divergence between $q_i(\boldsymbol{\theta})$ and $p(\mathbf{y}_i \mid \boldsymbol{\theta})q_{i-1}(\boldsymbol{\theta})/\mathcal{Z}_i$. One advantage of UVB compared to R-VGA is that it does not have to assume that the prior and variational distributions are Gaussian; see Sect. 5.2 of Tomasetti et al. (2022) for an example of UVB where a beta prior is used for one of the parameters and the variational distribution is a mixture of multivariate normal distributions. However, due to the lack of restrictions on the form of the variational distribution, UVB requires running a full optimisation algorithm at each iteration, whereas the R-VGAL updates are available in closed form.

Detailed derivations for the R-VGA algorithm can be found in Lambert et al. (2022). We provide below a sketch of the derivations to aid the exposition of the methodology in subsequent sections.

2.2.2 The R-VGA algorithm

Denote by $\mathbf{y}_{1:i} \equiv (\mathbf{y}_1^\top, \dots, \mathbf{y}_i^\top)^\top$ a collection of observations from groups 1 to i , $i = 1, \dots, N$. By assumption of conditional independence between observations $\mathbf{y}_1, \dots, \mathbf{y}_i$ given the parameters $\boldsymbol{\theta}$, the KL divergence between the variational distribution $q_i(\boldsymbol{\theta})$ and the posterior distribution $p(\boldsymbol{\theta} \mid \mathbf{y}_{1:i})$ can be expressed as

$$\begin{aligned} \text{KL}(q_i(\boldsymbol{\theta}) \parallel p(\boldsymbol{\theta} \mid \mathbf{y}_{1:i})) &\equiv \int q_i(\boldsymbol{\theta}) \log \frac{q_i(\boldsymbol{\theta})}{p(\boldsymbol{\theta} \mid \mathbf{y}_{1:i})} d\boldsymbol{\theta} \\ &= \mathbb{E}_{q_i}(\log q_i(\boldsymbol{\theta}) - \log p(\boldsymbol{\theta} \mid \mathbf{y}_{1:i-1}) - \log p(\mathbf{y}_i \mid \boldsymbol{\theta})) + \log p(\mathbf{y}_{1:i}) - \log p(\mathbf{y}_{1:i-1}). \end{aligned}$$

The posterior distribution after incorporating the first $i - 1$ groups of observations, $p(\boldsymbol{\theta} \mid \mathbf{y}_{1:i-1})$, is approximated by the variational distribution $q_{i-1}(\boldsymbol{\theta})$ to give

$$\text{KL}(q_i(\boldsymbol{\theta}) \parallel p(\boldsymbol{\theta} \mid \mathbf{y}_{1:i})) \approx \mathbb{E}_{q_i}(\log q_i(\boldsymbol{\theta}) - \log q_{i-1}(\boldsymbol{\theta}) - \log p(\mathbf{y}_i \mid \boldsymbol{\theta})) + \log p(\mathbf{y}_{1:i}) - \log p(\mathbf{y}_{1:i-1}). \quad (9)$$

The R-VGA algorithm assumes a variational distribution of the form $q_i(\boldsymbol{\theta}) = \text{Gau}(\boldsymbol{\mu}_i, \boldsymbol{\Sigma}_i)$ and seeks parameters $\boldsymbol{\mu}_i$ and $\boldsymbol{\Sigma}_i$ that minimise (9). As the last two terms in the right hand side of (9) do not depend on $\boldsymbol{\theta}$, the optimisation problem is equivalent to finding

$$\arg \min_{\boldsymbol{\mu}_i, \boldsymbol{\Sigma}_i} \mathbb{E}_{q_i}(\log q_i(\boldsymbol{\theta}) - \log q_{i-1}(\boldsymbol{\theta}) - \log p(\mathbf{y}_i \mid \boldsymbol{\theta})). \quad (10)$$

Differentiating the expectation (10) with respect to $\boldsymbol{\mu}_i$ and $\boldsymbol{\Sigma}_i$, setting the derivatives to zero, and rearranging the resulting equations, yields the following recursive updates for the variational mean $\boldsymbol{\mu}_i$ and precision matrix $\boldsymbol{\Sigma}_i^{-1}$:

$$\boldsymbol{\mu}_i = \boldsymbol{\mu}_{i-1} + \boldsymbol{\Sigma}_{i-1} \nabla_{\boldsymbol{\mu}_i} \mathbb{E}_{q_i}(\log p(\mathbf{y}_i \mid \boldsymbol{\theta})), \quad (11)$$

$$\boldsymbol{\Sigma}_i^{-1} = \boldsymbol{\Sigma}_{i-1}^{-1} - 2 \nabla_{\boldsymbol{\Sigma}_i} \mathbb{E}_{q_i}(\log p(\mathbf{y}_i \mid \boldsymbol{\theta})). \quad (12)$$

Then, using Bonnet’s Theorem (Bonnet, 1964) on (11) and Price’s Theorem (Price, 1958) on (12), we rewrite the gradient terms as

$$\nabla_{\boldsymbol{\mu}_i} \mathbb{E}_{q_i}(\log p(\mathbf{y}_i | \boldsymbol{\theta})) = \mathbb{E}_{q_i}(\nabla_{\boldsymbol{\theta}} \log p(\mathbf{y}_i | \boldsymbol{\theta})), \quad (13)$$

$$\nabla_{\boldsymbol{\Sigma}_i} \mathbb{E}_{q_i}(\log p(\mathbf{y}_i | \boldsymbol{\theta})) = \frac{1}{2} \mathbb{E}_{q_i}(\nabla_{\boldsymbol{\theta}}^2 \log p(\mathbf{y}_i | \boldsymbol{\theta})). \quad (14)$$

Thus the updates (11) and (12) become

$$\boldsymbol{\mu}_i = \boldsymbol{\mu}_{i-1} + \boldsymbol{\Sigma}_{i-1} \mathbb{E}_{q_i}(\nabla_{\boldsymbol{\theta}} \log p(\mathbf{y}_i | \boldsymbol{\theta})), \quad (15)$$

$$\boldsymbol{\Sigma}_i^{-1} = \boldsymbol{\Sigma}_{i-1}^{-1} - \mathbb{E}_{q_i}(\nabla_{\boldsymbol{\theta}}^2 \log p(\mathbf{y}_i | \boldsymbol{\theta})). \quad (16)$$

These updates are implicit as they require the evaluation of expectations with respect to $q_i(\boldsymbol{\theta})$. Under the assumption that $q_i(\boldsymbol{\theta})$ is close to $q_{i-1}(\boldsymbol{\theta})$, Lambert et al. (2022) propose replacing $q_i(\boldsymbol{\theta})$ with $q_{i-1}(\boldsymbol{\theta})$ in (15) and (16), and replacing $\boldsymbol{\Sigma}_{i-1}$ with $\boldsymbol{\Sigma}_i$ on the right hand side of (15), to yield an explicit scheme

$$\boldsymbol{\mu}_i = \boldsymbol{\mu}_{i-1} + \boldsymbol{\Sigma}_i \mathbb{E}_{q_{i-1}}(\nabla_{\boldsymbol{\theta}} \log p(\mathbf{y}_i | \boldsymbol{\theta})), \quad (17)$$

$$\boldsymbol{\Sigma}_i^{-1} = \boldsymbol{\Sigma}_{i-1}^{-1} - \mathbb{E}_{q_{i-1}}(\nabla_{\boldsymbol{\theta}}^2 \log p(\mathbf{y}_i | \boldsymbol{\theta})). \quad (18)$$

Equations (17) and (18) form the so-called R-VGA algorithm of Lambert et al. (2022).

We note that an “order 1 form” of the R-VGA algorithm exists, which allows the variational precision matrix to be updated using the first order derivatives of the log-likelihood without the need for the Hessian matrix. However, these updates are implicit and not directly implementable. Corollary 1 of Lambert et al. (2022) provides more details on this Hessian-free form.

2.3 R-VGAL

The R-VGA updates in (17) and (18) require the gradient $\nabla_{\boldsymbol{\theta}} \log p(\mathbf{y}_i | \boldsymbol{\theta})$ and Hessian $\nabla_{\boldsymbol{\theta}}^2 \log p(\mathbf{y}_i | \boldsymbol{\theta})$ of the “partial” log-likelihood for the i th observation. However, for the GLMMs discussed in Sect. 2.1, there are usually no closed-form expressions for said quantities, as evaluation of the partial log-likelihood involves an intractable integral over the random effects $\boldsymbol{\alpha}_i$. Our R-VGAL algorithm circumvents this issue by replacing $\nabla_{\boldsymbol{\theta}} \log p(\mathbf{y}_i | \boldsymbol{\theta})$ and $\nabla_{\boldsymbol{\theta}}^2 \log p(\mathbf{y}_i | \boldsymbol{\theta})$ with their unbiased estimates, $\widehat{\nabla_{\boldsymbol{\theta}} \log p(\mathbf{y}_i | \boldsymbol{\theta})}$ and $\widehat{\nabla_{\boldsymbol{\theta}}^2 \log p(\mathbf{y}_i | \boldsymbol{\theta})}$, respectively. These unbiased estimates are obtained by using an importance-sampling-based approach applied to Fisher’s and Louis’ identities (Cappé et al., 2005), which we discuss in more detail in Sects. 2.3.1 and 2.3.2.

Algorithm 1 R-VGAL

Input: observations $\mathbf{y}_1, \dots, \mathbf{y}_N$, initial values $\boldsymbol{\mu}_0$ and $\boldsymbol{\Sigma}_0$.
Output: variational parameters $\boldsymbol{\mu}_i$ and $\boldsymbol{\Sigma}_i$, for $i = 1, \dots, N$.
Set $q_0(\boldsymbol{\theta}) = \text{Gau}(\boldsymbol{\mu}_0, \boldsymbol{\Sigma}_0)$.
for $i = 1, \dots, N$ **do**
 $\boldsymbol{\mu}_i = \boldsymbol{\mu}_{i-1} + \boldsymbol{\Sigma}_i \mathbb{E}_{q_{i-1}}(\overline{\nabla_{\boldsymbol{\theta}} \log p(\mathbf{y}_i | \boldsymbol{\theta})})$
 $\boldsymbol{\Sigma}_i^{-1} = \boldsymbol{\Sigma}_{i-1}^{-1} - \mathbb{E}_{q_{i-1}}(\overline{\nabla_{\boldsymbol{\theta}}^2 \log p(\mathbf{y}_i | \boldsymbol{\theta})})$
end for

We summarise the R-VGAL algorithm in Algorithm 1.

To approximate the expectations with respect to $q_{i-1}(\boldsymbol{\theta})$ in the updates of the variational mean and precision matrix in Algorithm 1, we generate Monte Carlo samples, $\boldsymbol{\theta}^{(l)} \sim q_{i-1}(\boldsymbol{\theta})$, $l = 1, \dots, S$, and compute:

$$\mathbb{E}_{q_{i-1}}(\overline{\nabla_{\boldsymbol{\theta}} \log p(\mathbf{y}_i | \boldsymbol{\theta})}) \approx \frac{1}{S} \sum_{l=1}^S \overline{\nabla_{\boldsymbol{\theta}} \log p(\mathbf{y}_i | \boldsymbol{\theta}^{(l)})},$$

$$\mathbb{E}_{q_{i-1}}(\overline{\nabla_{\boldsymbol{\theta}}^2 \log p(\mathbf{y}_i | \boldsymbol{\theta})}) \approx \frac{1}{S} \sum_{l=1}^S \overline{\nabla_{\boldsymbol{\theta}}^2 \log p(\mathbf{y}_i | \boldsymbol{\theta}^{(l)})},$$

for $i = 1, \dots, N$.

The following sections discuss approaches to obtain unbiased estimates of the gradient and the Hessian of the log-likelihood with respect to the parameters.

2.3.1 Approximation of the gradient with Fisher's identity

Consider the i th iteration. Fisher's identity (Cappé et al., 2005) for the gradient of $\log p(\mathbf{y}_i | \boldsymbol{\theta})$ is

$$\nabla_{\boldsymbol{\theta}} \log p(\mathbf{y}_i | \boldsymbol{\theta}) = \int p(\boldsymbol{\alpha}_i | \mathbf{y}_i, \boldsymbol{\theta}) \nabla_{\boldsymbol{\theta}} \log p(\mathbf{y}_i, \boldsymbol{\alpha}_i | \boldsymbol{\theta}) d\boldsymbol{\alpha}_i. \quad (19)$$

If it is possible to sample directly from $p(\boldsymbol{\alpha}_i | \mathbf{y}_i, \boldsymbol{\theta})$ (e.g., as it is with the linear random effects model in Sect. 3.1), the above identity can be approximated by

$$\nabla_{\boldsymbol{\theta}} \log p(\mathbf{y}_i | \boldsymbol{\theta}) \approx \frac{1}{S_{\alpha}} \sum_{s=1}^{S_{\alpha}} \nabla_{\boldsymbol{\theta}} \log p(\mathbf{y}_i, \boldsymbol{\alpha}_i^{(s)} | \boldsymbol{\theta}), \quad \boldsymbol{\alpha}_i^{(s)} \sim p(\boldsymbol{\alpha}_i | \mathbf{y}_i, \boldsymbol{\theta}). \quad (20)$$

In the case where direct sampling from $p(\boldsymbol{\alpha}_i | \mathbf{y}_i, \boldsymbol{\theta})$ is difficult, we use importance sampling (e.g., Tokdar and Kass, 2010) to estimate the gradient of the log-likelihood in (19). Specifically, we draw samples

$\{\boldsymbol{\alpha}_i^{(s)} : s = 1, \dots, S_\alpha\}$ from an importance distribution $r(\boldsymbol{\alpha}_i | \mathbf{y}_i, \boldsymbol{\theta})$, and then compute the weights

$$w_i^{(s)} = \frac{p(\mathbf{y}_i | \boldsymbol{\alpha}_i^{(s)}, \boldsymbol{\theta})p(\boldsymbol{\alpha}_i^{(s)} | \boldsymbol{\theta})}{r(\boldsymbol{\alpha}_i^{(s)} | \mathbf{y}_i, \boldsymbol{\theta})}, \quad s = 1, \dots, S_\alpha.$$

The gradient of the log-likelihood is then approximated as

$$\nabla_{\boldsymbol{\theta}} \log p(\mathbf{y}_i | \boldsymbol{\theta}) \approx \sum_{s=1}^{S_\alpha} \bar{w}_i^{(s)} \nabla_{\boldsymbol{\theta}} \log p(\mathbf{y}_i, \boldsymbol{\alpha}_i^{(s)} | \boldsymbol{\theta}), \quad (21)$$

where $\mathcal{W}_i \equiv \{\bar{w}_i^{(s)} : s = 1, \dots, S_\alpha\}$ are the normalised weights given by

$$\bar{w}_i^{(s)} = \frac{w_i^{(s)}}{\sum_{q=1}^{S_\alpha} w_i^{(q)}}, \quad s = 1, \dots, S_\alpha.$$

One possible choice for the importance distribution is the distribution of the random effects, that is, $p(\boldsymbol{\alpha}_i | \boldsymbol{\theta})$.

In this case, the weights \mathcal{W}_i reduce to

$$w_i^{(s)} = p(\mathbf{y}_i | \boldsymbol{\alpha}_i^{(s)}, \boldsymbol{\theta}), \quad s = 1, \dots, S_\alpha.$$

We use this importance distribution in all of the case studies illustrated in Sect. 3.

2.3.2 Approximation of the Hessian with Louis' identity

Consider again the i th iteration. Louis' identity (Cappé et al., 2005) for the Hessian $\nabla_{\boldsymbol{\theta}}^2 \log p(\mathbf{y}_i | \boldsymbol{\theta})$ is

$$-\nabla_{\boldsymbol{\theta}}^2 \log p(\mathbf{y}_i | \boldsymbol{\theta}) = \nabla_{\boldsymbol{\theta}} \log p(\mathbf{y}_i | \boldsymbol{\theta}) \nabla_{\boldsymbol{\theta}} \log p(\mathbf{y}_i | \boldsymbol{\theta})^\top - \frac{\nabla_{\boldsymbol{\theta}}^2 p(\mathbf{y}_i | \boldsymbol{\theta})}{p(\mathbf{y}_i | \boldsymbol{\theta})}, \quad (22)$$

where

$$\begin{aligned} \frac{\nabla_{\boldsymbol{\theta}}^2 p(\mathbf{y}_i | \boldsymbol{\theta})}{p(\mathbf{y}_i | \boldsymbol{\theta})} &= \int p(\boldsymbol{\alpha}_i | \mathbf{y}_i, \boldsymbol{\theta}) \nabla_{\boldsymbol{\theta}} \log p(\mathbf{y}_i, \boldsymbol{\alpha}_i | \boldsymbol{\theta}) \nabla_{\boldsymbol{\theta}} \log p(\mathbf{y}_i, \boldsymbol{\alpha}_i | \boldsymbol{\theta})^\top d\boldsymbol{\alpha}_i \\ &+ \int p(\boldsymbol{\alpha}_i | \mathbf{y}_i, \boldsymbol{\theta}) \nabla_{\boldsymbol{\theta}}^2 \log p(\mathbf{y}_i, \boldsymbol{\alpha}_i | \boldsymbol{\theta}) d\boldsymbol{\alpha}_i. \end{aligned} \quad (23)$$

The first term on the right-hand side of (22) is obtained using Fisher's identity, as discussed in Sect. 2.3.1.

The second term consists of two integrals (see (23)), which can also be approximated using samples. Specif-

ically,

$$\frac{\nabla_{\boldsymbol{\theta}}^2 p(\mathbf{y}_i | \boldsymbol{\theta})}{p(\mathbf{y}_i | \boldsymbol{\theta})} \approx \frac{1}{S_\alpha} \sum_{s=1}^{S_\alpha} \left(\nabla_{\boldsymbol{\theta}} \log p(\mathbf{y}_i, \boldsymbol{\alpha}_i^{(s)} | \boldsymbol{\theta}) \nabla_{\boldsymbol{\theta}} \log p(\mathbf{y}_i, \boldsymbol{\alpha}_i^{(s)} | \boldsymbol{\theta})^\top + \nabla_{\boldsymbol{\theta}}^2 \log p(\mathbf{y}_i, \boldsymbol{\alpha}_i^{(s)} | \boldsymbol{\theta}) \right),$$

where $\boldsymbol{\alpha}_i^{(s)} \sim p(\boldsymbol{\alpha}_i | \mathbf{y}_i, \boldsymbol{\theta})$ for $s = 1, \dots, S_\alpha$. If obtaining samples from $p(\boldsymbol{\alpha}_i | \mathbf{y}_i, \boldsymbol{\theta})$ is not straightforward, importance sampling (as in Sect. 2.3.1) can be used instead. Following Nemeth et al. (2016), for computational efficiency, we use the same samples $\{\boldsymbol{\alpha}_i^{(s)} : s = 1, \dots, S_\alpha\}$ that were used to approximate the score using Fisher’s identity and their corresponding normalised weights \mathcal{W}_i to obtain the estimates of the second term in Louis’ identity. Then

$$\frac{\nabla_{\boldsymbol{\theta}}^2 p(\mathbf{y}_i | \boldsymbol{\theta})}{p(\mathbf{y}_i | \boldsymbol{\theta})} \approx \sum_{s=1}^{S_\alpha} \bar{w}_i^{(s)} \left(\nabla_{\boldsymbol{\theta}} \log p(\mathbf{y}_i, \boldsymbol{\alpha}_i^{(s)} | \boldsymbol{\theta}) \nabla_{\boldsymbol{\theta}} \log p(\mathbf{y}_i, \boldsymbol{\alpha}_i^{(s)} | \boldsymbol{\theta})^\top + \nabla_{\boldsymbol{\theta}}^2 \log p(\mathbf{y}_i, \boldsymbol{\alpha}_i^{(s)} | \boldsymbol{\theta}) \right).$$

2.4 Damped R-VGAL

A possible problem with R-VGAL is its instability in the first few observations, making it sensitive to the ordering of the observations. In Sect. S3 of the online supplement, we run the R-VGAL algorithm on a dataset in its original order, and also on a random reordering of the observations, and find that the R-VGAL parameter estimates from these two runs differ. Figures S13 and S14 in Sect. S3 show that the first few observations can heavily influence the trajectory of the variational mean. Here, we propose a damping approach to stabilise the R-VGAL algorithm during the initial few steps.

In damped R-VGAL, the updates of the mean and precision matrix for each observation are split into K steps, where K is selected on a case by case basis. In each step, we multiply the gradient and the Hessian of $\log p(\mathbf{y}_i | \boldsymbol{\theta})$ by a factor $a = \frac{1}{K}$ (which acts as a “step size”), and then update the variational parameters K times during the i th iteration. Intuitively, in this way, one observation is split into K “parts” and incorporated into the updates one part at a time. Using a smaller step size helps stabilise the R-VGAL algorithm, particularly for the first few observations. Sect. S3 of the online supplement shows that damping the first few iterations makes the R-VGAL algorithm more robust to different orderings of the data.

The damped R-VGAL approach we present here is inspired by the so-called *damped Newton’s method*. In the case where the model is linear and the likelihood is Gaussian, the original R-VGA algorithm, upon which R-VGAL is based, can be shown to be equivalent to an online version of Newton’s method; see Appendix 8.2 of Lambert et al. (2022) for a proof. Newton’s method seeks the minimiser of a continuously differentiable function $f : \mathbb{R}^d \rightarrow \mathbb{R}, d \in \mathbb{N}$, by beginning with some starting value $\mathbf{u}_0 \in \mathbb{R}^d$ and sequentially minimising the

quadratic approximation of the function $f(\cdot)$ around the current value in order to find the next value:

$$\mathbf{u}_{k+1} = \arg \min_{\mathbf{u}} f(\mathbf{u}_k) + \nabla_{\mathbf{u}} f(\mathbf{u}_k)^\top (\mathbf{u} - \mathbf{u}_k) + \frac{1}{2} (\mathbf{u} - \mathbf{u}_k)^\top \nabla_{\mathbf{u}}^2 f(\mathbf{u}_k) (\mathbf{u} - \mathbf{u}_k), \quad k = 0, 1, 2, \dots$$

Provided that $\nabla_{\mathbf{u}}^2 f(\mathbf{u}_k)$ is positive definite, the minimiser of $f(\cdot)$ is unique and can be computed iteratively as

$$\mathbf{u}_{k+1} = \mathbf{u}_k - (\nabla_{\mathbf{u}}^2 f(\mathbf{u}_k))^{-1} \nabla_{\mathbf{u}} f(\mathbf{u}_k), \quad k = 0, 1, 2, \dots \quad (24)$$

These iterations stop when $\|\nabla f(\mathbf{u}_{k+1})\| \leq \epsilon_0$, where ϵ_0 is some small tolerance parameter. Often, in practice, Newton's method is modified to include a step size $0 < \rho \leq 1$ to improve convergence:

$$\mathbf{u}_{k+1} = \mathbf{u}_k - \rho (\nabla_{\mathbf{u}}^2 f(\mathbf{u}_k))^{-1} \nabla_{\mathbf{u}} f(\mathbf{u}_k), \quad k = 0, 1, 2, \dots, \quad (25)$$

resulting in the damped Newton's method. This step size ρ is similar to the multiplicative factor a in our damped R-VGAL approach.

We also note that, in the case where the model is linear or when the likelihood function comes from an exponential family and the model is linearised, the R-VGA algorithm of Lambert et al. (2022) is equivalent to an online natural gradient algorithm with step size $\frac{1}{1+t}$, where t denotes the iteration. A proof of this equivalence can be found in Appendix 8.3 of Lambert et al. (2022). Viewed from the perspective of natural gradient optimisation, the damping factor a in damped R-VGAL can be interpreted as a reduction of the step size in natural gradient updates.

We summarise the damped R-VGAL algorithm in Algorithm 2.

3 Applications of R-VGAL

In this section, we apply R-VGAL to estimate parameters in linear, logistic and Poisson mixed models using three simulated datasets and two real datasets: the Six City dataset from Fitzmaurice and Laird (1993), and the Polypharmacy dataset from Hosmer et al. (2013). The linear and logistic models have univariate random effects, while the Poisson model has bivariate random effects. There are two additional examples in Sect. S6 of the online supplement: a real data example with the Poisson model applied to the Epilepsy dataset from Thall and Vail (1990), and a synthetic data example with a high number of observations simulated from the logistic mixed model.

Algorithm 2 Damped R-VGAL

Input: observations $\mathbf{y}_1, \dots, \mathbf{y}_N$, initial values $\boldsymbol{\mu}_0$ and $\boldsymbol{\Sigma}_0$, number of observations to damp n_{damp} , number of damping steps K .

Output: variational parameters $\boldsymbol{\mu}_i$ and $\boldsymbol{\Sigma}_i$, for $i = 1, \dots, N$.

Set $q_0(\boldsymbol{\theta}) = \text{Gau}(\boldsymbol{\mu}_0, \boldsymbol{\Sigma}_0)$.

for $i = 1, \dots, N$ **do**

if $i \leq n_{damp}$ **then**

 Set $a = 1/K$, $\boldsymbol{\mu}_{i,0} = \boldsymbol{\mu}_{i-1}$, $\boldsymbol{\Sigma}_{i,0} = \boldsymbol{\Sigma}_{i-1}$

for $k = 1, \dots, K$ **do**

 Set $q_{i,k-1}(\boldsymbol{\theta}) = \text{Gau}(\boldsymbol{\mu}_{i,k-1}, \boldsymbol{\Sigma}_{i,k-1})$.

$\boldsymbol{\mu}_{i,k} = \boldsymbol{\mu}_{i,k-1} + a\boldsymbol{\Sigma}_{i,k}\mathbb{E}_{q_{i,k-1}}(\overline{\nabla_{\boldsymbol{\theta}} \log p(\mathbf{y}_i | \boldsymbol{\theta})})$

$\boldsymbol{\Sigma}_{i,k}^{-1} = \boldsymbol{\Sigma}_{i,k-1}^{-1} - a\mathbb{E}_{q_{i,k-1}}(\overline{\nabla_{\boldsymbol{\theta}}^2 \log p(\mathbf{y}_i | \boldsymbol{\theta})})$

end for

 Set $\boldsymbol{\mu}_i = \boldsymbol{\mu}_{i,K}$, $\boldsymbol{\Sigma}_i = \boldsymbol{\Sigma}_{i,K}$, $q_i(\boldsymbol{\theta}) = \text{Gau}(\boldsymbol{\mu}_i, \boldsymbol{\Sigma}_i)$.

else

$\boldsymbol{\mu}_i = \boldsymbol{\mu}_{i-1} + \boldsymbol{\Sigma}_i\mathbb{E}_{q_{i-1}}(\overline{\nabla_{\boldsymbol{\theta}} \log p(\mathbf{y}_i | \boldsymbol{\theta})})$

$\boldsymbol{\Sigma}_i^{-1} = \boldsymbol{\Sigma}_{i-1}^{-1} - \mathbb{E}_{q_{i-1}}(\overline{\nabla_{\boldsymbol{\theta}}^2 \log p(\mathbf{y}_i | \boldsymbol{\theta})})$

end if

end for

We validate R-VGAL against Hamiltonian Monte Carlo (HMC, Neal, 2011; Betancourt and Girolami, 2015), which is implemented using the Stan programming language (Stan Development Team, 2023) in R (R Core Team, 2022). In examples with real data, the true parameters are unknown. We instead compute the maximum likelihood estimates for the parameters using the R package `lme4` (Bates et al., 2015), and also treat results from HMC as the “ground truth”, as HMC provides samples from the true posterior distributions. For all examples, we run 2 HMC chains for 15000 iterations each, and discard the first 5000 from each chain as burn in. We find that the effective sample sizes are high and the \hat{R} statistics are close to 1 for all examples, indicating that the HMC chains are well-mixed and have converged; see Sect. S5 of the online supplement for further details. Reproducible R code for all examples is available on <https://github.com/bao-anh-vu/R-VGAL>.

For all applications in this paper, we use the damped R-VGAL algorithm described in Sect. 2.4. We show that damping makes the algorithm more robust to different orderings of the observations in Sect. S3 of the online supplement. The values of n_{damp} and K used in damping observations should be kept as small as possible to limit the extra computational overhead, while also be sufficiently large to reduce the instability

observed with the R-VGAL algorithm in the initial stages. In our applications, we experimented with a few different settings of n_{damp} and K and plotted the trajectories of the variational mean under those settings. We found that the trajectories were most unstable during the first 10 observations, so we chose $n_{damp} = 10$ observations and the number of steps $K = 4$ to reduce the initial instability at the expense of a small additional computational cost. These values are used throughout our examples. Adaptive schemes for selecting the values of n_{damp} and K are left as future research directions.

3.1 Linear mixed effect model

In this example, we generate data from a linear mixed model with $N = 200$ groups and $n = 10$ responses per group. The j th response from the i th group is modelled as

$$y_{ij} = \mathbf{x}_{ij}^\top \boldsymbol{\beta} + z_{ij} \alpha_i + \epsilon_{ij}, \quad \alpha_i \sim \text{Gau}(0, \sigma_\alpha^2), \quad \epsilon_{ij} \sim \text{Gau}(0, \sigma_\epsilon^2), \quad (26)$$

for $i = 1, \dots, N$ and $j = 1, \dots, n$, where \mathbf{x}_{ij} is drawn from a $\text{Gau}(\mathbf{0}, \mathbf{I}_4)$ distribution and z_{ij} is drawn from a $\text{Gau}(0, 1)$ distribution. For this example, we did not include an intercept term, but it can be added if necessary. The true parameter values are $\boldsymbol{\beta} = (-1.5, 1.5, 0.5, 0.25)^\top$, $\sigma_\alpha = 0.9$, and $\sigma_\epsilon = 0.7$. Since R-VGAL uses a multivariate normal distribution as the variational approximation, we consider the log-transformed variables $\phi_\alpha \equiv \log(\sigma_\alpha^2)$ and $\phi_\epsilon \equiv \log(\sigma_\epsilon^2)$ so that ϕ_α and ϕ_ϵ are unconstrained. We then make inference on the parameters $\boldsymbol{\theta} = (\boldsymbol{\beta}^\top, \phi_\alpha, \phi_\epsilon)^\top$ using R-VGAL.

At the group level, the linear mixed model is

$$\mathbf{y}_i = \mathbf{X}_i \boldsymbol{\beta} + \mathbf{z}_i \alpha_i + \boldsymbol{\epsilon}_i, \quad i = 1, \dots, N, \quad (27)$$

where $\mathbf{y}_i \equiv (y_{i1}, \dots, y_{in})^\top$, $\mathbf{X}_i \equiv (\mathbf{x}_{i1}, \dots, \mathbf{x}_{in})^\top$, $\mathbf{z}_i \equiv (z_{i1}, \dots, z_{in})^\top$, and $\boldsymbol{\epsilon}_i \equiv (\epsilon_{i1}, \dots, \epsilon_{in})^\top$. At each iteration, $i = 1, \dots, N$, the R-VGAL algorithm makes use of the ‘‘partial’’ likelihood of the observations from the i th group, $p(\mathbf{y}_i | \boldsymbol{\theta}) = \text{Gau}(\boldsymbol{\mu}_{y|\theta}, \boldsymbol{\Sigma}_{y|\theta})$, where $\boldsymbol{\mu}_{y|\theta} = \mathbf{X}_i \boldsymbol{\beta}$ and $\boldsymbol{\Sigma}_{y|\theta} = \sigma_\alpha^2 \mathbf{z}_i \mathbf{z}_i^\top + \sigma_\epsilon^2 \mathbf{I}_n$. For this model, the gradient and Hessian of $\log p(\mathbf{y}_i | \boldsymbol{\theta})$ with respect to each of the parameters are available in closed form; see Sect. S1.1 of the online supplement. In this case, we are therefore able to compare the accuracy of R-VGAL implemented using approximate gradients and Hessians with that of R-VGAL implemented using exact gradients and Hessians.

The prior distribution we use, which is also the “initial” variational distribution, is

$$p(\boldsymbol{\theta}) = q_0(\boldsymbol{\theta}) = \text{Gau} \left(\begin{bmatrix} \mathbf{0} \\ \log(0.5^2) \\ \log(0.5^2) \end{bmatrix}, \begin{bmatrix} 10\mathbf{I}_4 & \mathbf{0} & \mathbf{0} \\ \mathbf{0}^\top & 1 & 0 \\ \mathbf{0}^\top & 0 & 1 \end{bmatrix} \right). \quad (28)$$

A $\text{Gau}(\log(0.5^2), 1)$ prior distribution for ϕ_α and ϕ_ϵ is equivalent to a log-normal prior distribution with mean 0.41 and variance 0.29 for both σ_α^2 and σ_ϵ^2 . Using this prior distribution, the 2.5th and 97.5th percentiles for both σ_α^2 and σ_ϵ^2 are (0.035, 1.775).

At each iteration $i = 1, \dots, 200$, we use $S_\alpha = 100$ Monte Carlo samples (of α_i) to approximate the gradient and Hessian of $\log p(\mathbf{y}_i | \boldsymbol{\theta})$ using Fisher’s and Louis’ identities. We use $S = 100$ Monte Carlo samples (of $\boldsymbol{\theta}$) to approximate the expectations with respect to $q_{i-1}(\boldsymbol{\theta})$ in the R-VGAL updates of the mean and precision matrix. These values were chosen based on an experimental study on the effect of S and S_α on the posterior estimates of R-VGAL in Sect. S2 of the online supplement.

We validate R-VGAL against HMC, which we implemented in Stan. Figure 1 shows the marginal posterior distributions of the parameters, along with bivariate posterior distributions as estimated using R-VGAL with approximate gradients and Hessians, R-VGAL with exact gradients and Hessians, and HMC. The posterior distributions obtained using R-VGAL are clearly very similar to those obtained using HMC, irrespective of whether exact or approximate gradients and Hessians are used.

3.2 Logistic mixed effect model

In this example, we generate simulated data from a random effects logistic regression model with $N = 500$ groups and $n = 10$ responses per group. The random effect logistic regression model we use is

$$y_{ij} \sim \text{Bernoulli}(\pi_{ij}), \quad \pi_{ij} \equiv \Pr(y_{ij} = 1 | \boldsymbol{\beta}, \tau^2) = \frac{\exp(\mathbf{x}_{ij}^\top \boldsymbol{\beta} + \alpha_i)}{1 + \exp(\mathbf{x}_{ij}^\top \boldsymbol{\beta} + \alpha_i)}, \quad \alpha_i \sim \text{Gau}(0, \tau^2), \quad (29)$$

where \mathbf{x}_{ij} is drawn from a $\text{Gau}(\mathbf{0}, \mathbf{I}_4)$ distribution, for $i = 1, \dots, N$ and $j = 1, \dots, n$. For this example, we did not include an intercept term, but it can be added if necessary. The true parameter values are $\boldsymbol{\beta} = (-1.5, 1.5, 0.5, 0.25)^\top$ and $\tau = 0.9$.

As in the linear case, although the parameters of the model are $\boldsymbol{\beta}$ and τ , we work with $\boldsymbol{\theta} = (\boldsymbol{\beta}^\top, \phi_\tau)^\top$ where $\phi_\tau \equiv \log(\tau^2)$. The gradient and Hessian of the “partial” log-likelihood $\log p(\mathbf{y}_i | \boldsymbol{\theta})$ in this model are not analytically tractable, but can be estimated unbiasedly using Fisher’s and Louis’ identities as discussed in

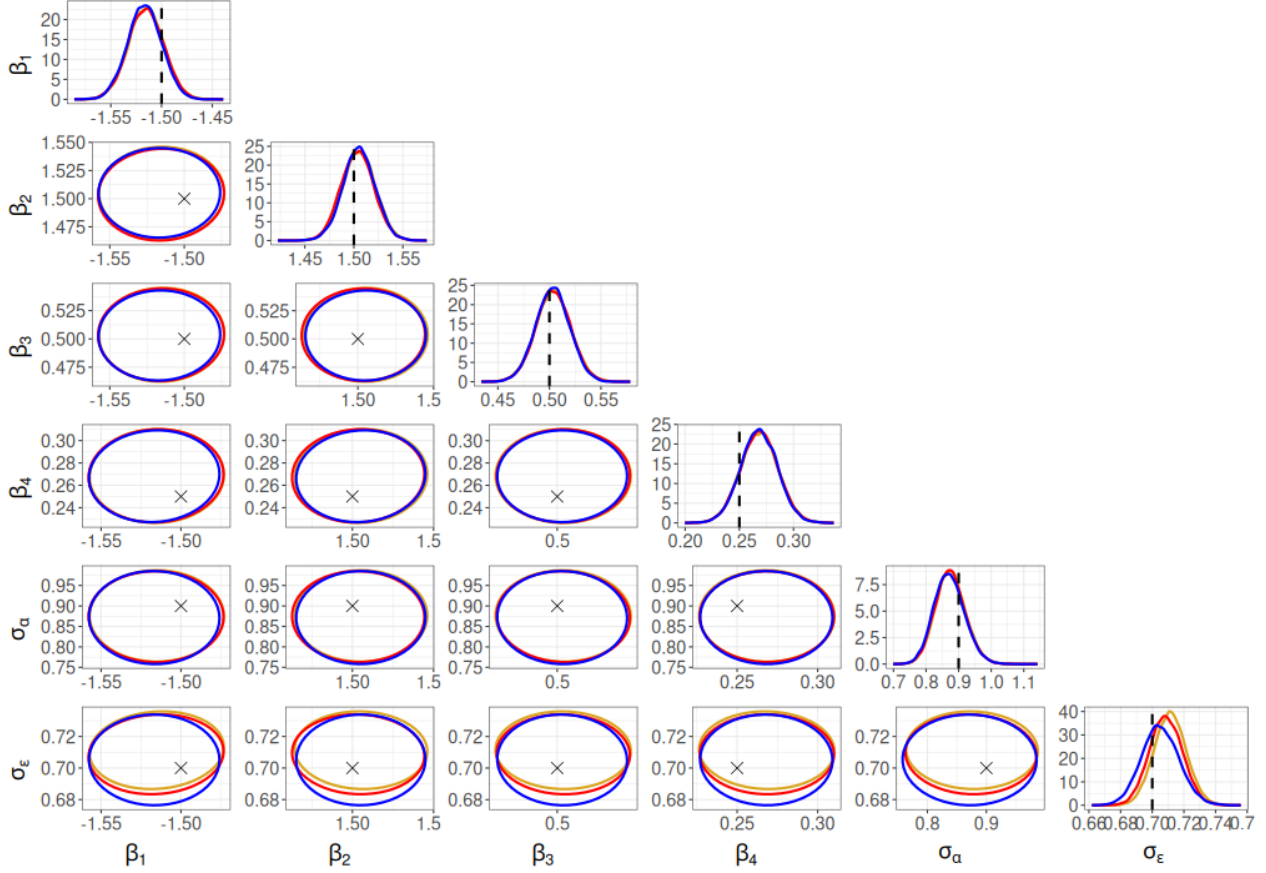


Figure 1: Exact posterior distributions (from HMC, in blue) and approximate posterior distributions (from R-VGAL with estimated gradients and Hessians in red, and from R-VGAL with exact gradients and Hessians in yellow) for the linear mixed model experiment. Diagonal panels: Marginal posterior distributions with true parameters denoted using dotted lines. Off-diagonal panels: Bivariate posterior distributions with true parameters denoted using the symbol \times .

Sects. 2.3.1 and 2.3.2. These identities require the expressions for $\nabla_{\boldsymbol{\theta}} \log p(\mathbf{y}_i, \alpha_i \mid \boldsymbol{\theta})$ and $\nabla_{\boldsymbol{\theta}}^2 \log p(\mathbf{y}_i, \alpha_i \mid \boldsymbol{\theta})$, which are provided in Sect. S1.2 of the online supplement.

The prior distribution we use, which is also the “initial” variational distribution, is

$$p(\boldsymbol{\theta}) = q_0(\boldsymbol{\theta}) = \text{Gau} \left(\begin{bmatrix} \mathbf{0} \\ \log(0.5^2) \end{bmatrix}, \begin{bmatrix} 10\mathbf{I}_4 & \mathbf{0} \\ \mathbf{0}^\top & 1 \end{bmatrix} \right). \quad (30)$$

A $\text{Gau}(\log(0.5^2), 1)$ prior distribution for ϕ_τ is equivalent to a log-normal prior distribution with mean 0.41 and variance 0.29 for τ^2 . The prior 2.5th and 97.5th percentiles for τ^2 are (0.035, 1.775). At each iteration $i = 1, \dots, 500$, we use $S_\alpha = 100$ Monte Carlo samples (of α_i) to approximate the gradient and Hessian of $\log p(\mathbf{y}_i \mid \boldsymbol{\theta})$ during importance sampling, and $S = 100$ samples (of $\boldsymbol{\theta}$) to approximate the expectations with respect to $q_{i-1}(\boldsymbol{\theta})$ in the R-VGAL updates of the mean and precision matrix.

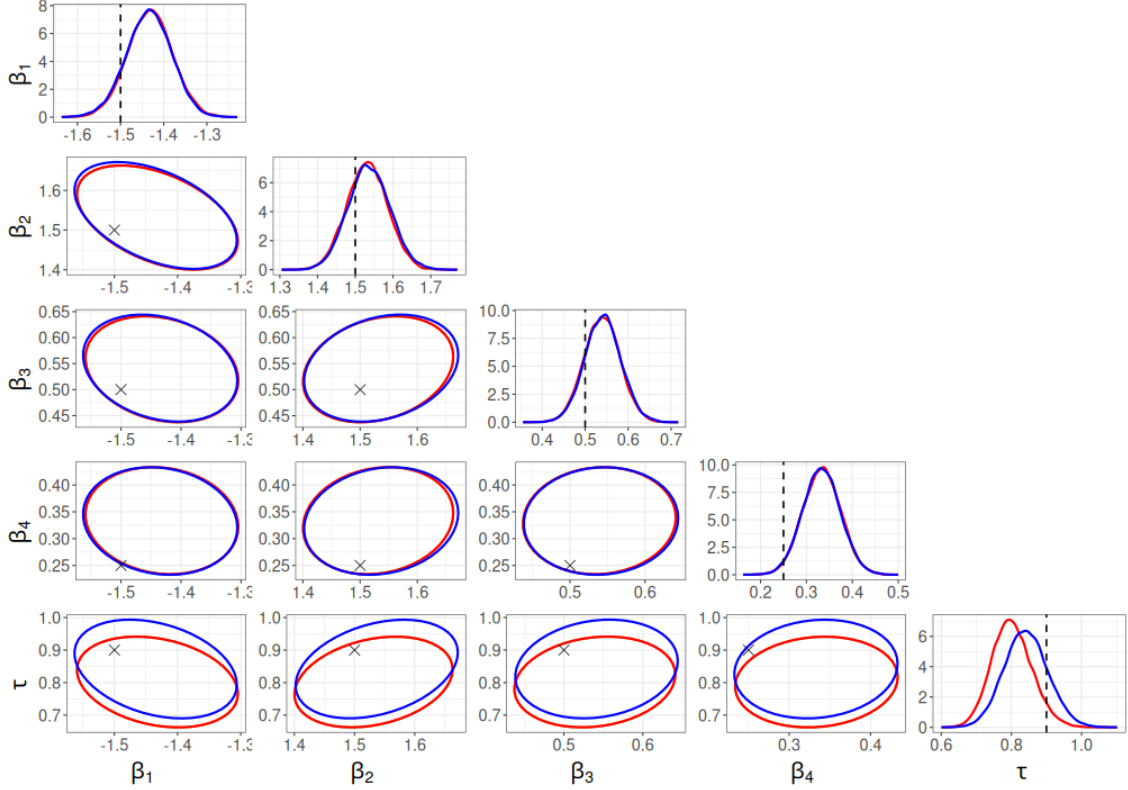


Figure 2: Exact posterior distributions from HMC (in blue) and approximate posterior distributions from R-VGAL with estimated gradients and Hessians (in red) for the logistic mixed model experiment. Diagonal panels: Marginal posterior distributions with true parameters denoted using dotted lines. Off-diagonal panels: Bivariate posterior distributions with true parameters denoted using the symbol \times .

Figure 2 shows the marginal posterior distributions of the parameters, along with bivariate posterior distributions as estimated using R-VGAL and HMC. The posterior distributions obtained using R-VGAL are again very similar to those obtained using HMC.

3.3 Poisson mixed model

We now apply R-VGAL to a model with bivariate random effects. For this example, we simulate data with $N = 200$ groups and $n = 10$ responses per group from the following Poisson mixed effect regression model:

$$y_{ij} \sim \text{Poisson}(\lambda_{ij}), \quad \lambda_{ij} = \exp(\mathbf{x}_{ij}^\top \boldsymbol{\beta} + \mathbf{z}_{ij}^\top \boldsymbol{\alpha}_i), \quad \boldsymbol{\alpha}_i \sim \text{Gau}(\mathbf{0}, \boldsymbol{\Sigma}_\alpha),$$

where $\mathbf{x}_{ij} \equiv (1, x_{ij,1})^\top$, with $x_{ij,1}$ drawn from a $\text{Gau}(0, 1)$ distribution, and $\mathbf{z}_{ij} \equiv (1, z_{ij,1})^\top$, with $z_{ij,1}$ drawn from a $\text{Gau}(0, 1)$ distribution, for $i = 1, \dots, N$ and $j = 1, \dots, n$. We denote the fixed and random effects as

$\boldsymbol{\beta} \equiv (\beta_0, \beta_1)^\top$ and $\boldsymbol{\alpha}_i \equiv (\alpha_{i,1}, \alpha_{i,2})^\top$, respectively. The true parameter values are

$$\boldsymbol{\beta} = (-1.5, -0.5)^\top, \quad \boldsymbol{\Sigma}_\alpha = \begin{bmatrix} 0.15 & 0.05 \\ 0.05 & 0.20 \end{bmatrix}.$$

We parameterise $\boldsymbol{\Sigma}_\alpha = \mathbf{L}\mathbf{L}^\top$, where \mathbf{L} denotes the lower Cholesky factor of $\boldsymbol{\Sigma}_\alpha$ and takes the form

$$\mathbf{L} = \begin{bmatrix} \exp(\zeta_{11}) & 0 \\ \zeta_{21} & \exp(\zeta_{22}) \end{bmatrix}.$$

In the algorithm, we consider the unconstrained parameters $\boldsymbol{\theta} = (\boldsymbol{\beta}^\top, \boldsymbol{\zeta}^\top)^\top$, where $\boldsymbol{\zeta} \equiv (\zeta_{11}, \zeta_{22}, \zeta_{21})^\top$. The gradient $\nabla_{\boldsymbol{\theta}} \log p(\mathbf{y}_i, \boldsymbol{\alpha}_i | \boldsymbol{\theta})$ and Hessian $\nabla_{\boldsymbol{\theta}}^2 \log p(\mathbf{y}_i, \boldsymbol{\alpha}_i | \boldsymbol{\theta})$, which are necessary in the computation of the gradient and Hessian of the group-specific log likelihood $\log p(\mathbf{y}_i | \boldsymbol{\theta})$, are provided in Sect. S1.3 of the online supplement.

We use the following prior/initial variational distribution:

$$p(\boldsymbol{\theta}) = q_0(\boldsymbol{\theta}) = \text{Gau} \left(\begin{bmatrix} \mathbf{0} \\ \mathbf{0} \end{bmatrix}, \begin{bmatrix} \mathbf{I}_2 & \mathbf{0} \\ \mathbf{0}^\top & 0.1\mathbf{I}_3 \end{bmatrix} \right).$$

Using a $\text{Gau}(0, 0.1)$ prior distribution for ζ_{11} , ζ_{22} and ζ_{21} leads to having 2.5th and 97.5th percentiles of (0.290, 3.485) for $\Sigma_{\alpha_{11}}$, (0.342, 3.577) for $\Sigma_{\alpha_{22}}$, and $(-0.713, 0.713)$ for the off-diagonal entries $\Sigma_{\alpha_{21}}$ and $\Sigma_{\alpha_{12}}$.

As with the linear and logistic examples, we use $S_\alpha = 100$ for the importance sampling step and $S = 100$ samples for approximating the expectations with respect to $q_{i-1}(\boldsymbol{\theta})$ in the R-VGAL updates. Figure 3 shows the marginal posterior distributions of the parameters, along with bivariate posterior distributions as estimated using R-VGAL and HMC. For all parameters, the R-VGAL and HMC posterior densities are very similar, though the posterior densities of $\Sigma_{\alpha_{11}}$ from both methods appear a bit biased.

To assess the robustness of the results in these simulation studies, we also include repeated simulation studies on the linear, logistic and Poisson mixed models in Sect. S4 of the online supplement. For each of these models, we simulate 100 datasets using the same parameter settings, and compare the posterior estimates from R-VGAL and HMC on these simulated datasets. We find that the R-VGAL and HMC posterior estimates are very similar across simulations for the linear and logistic models, while for the Poisson model, the estimates from the two methods are close for most simulations, with only a few cases where estimates

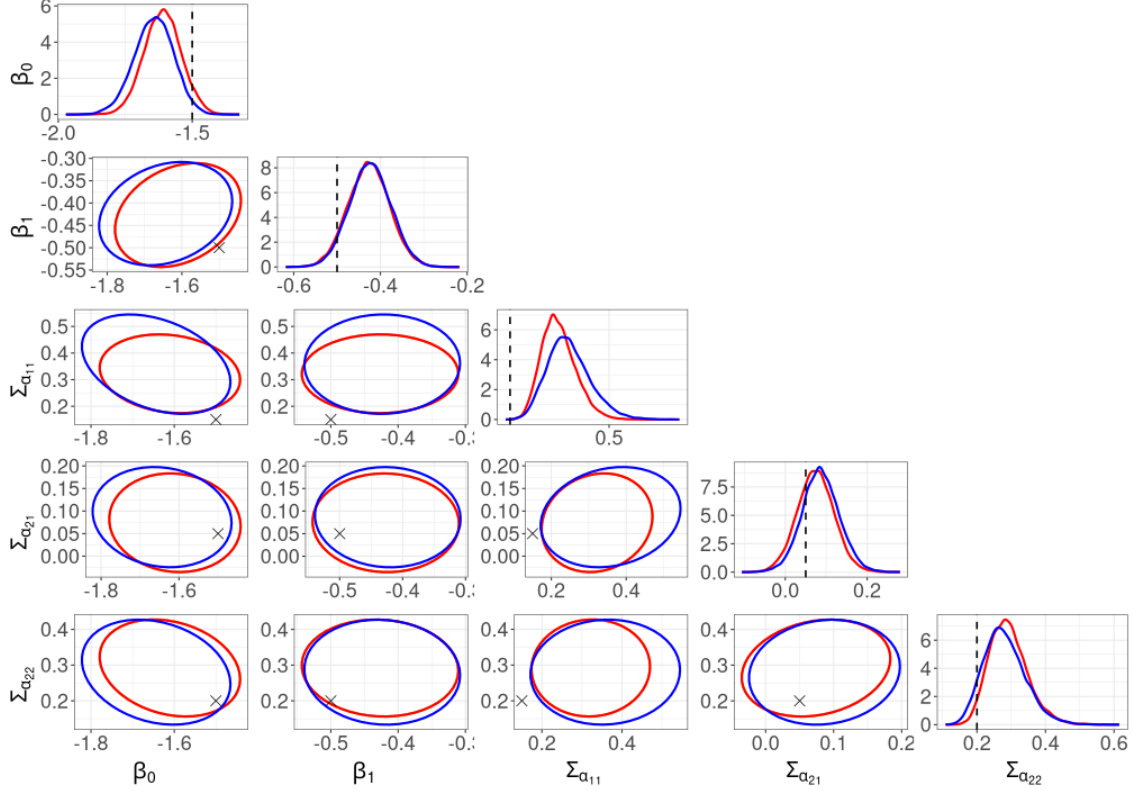


Figure 3: Exact posterior distributions from HMC (in blue) and approximate posterior distributions from R-VGAL with estimated gradients and Hessians (in red) for the Poisson mixed model experiment. Diagonal panels: Marginal posterior distributions with true parameters denoted using dotted lines. Off-diagonal panels: Bivariate posterior distributions with true parameters denoted using the symbol \times .

are slightly different. We also find that the posterior standard deviations from R-VGAL tend to be slightly smaller than those from HMC.

3.4 Real data examples

We now apply R-VGAL to two real datasets: the Six City dataset from Fitzmaurice and Laird (1993), and the Polypharmacy dataset from Hosmer et al. (2013).

For the Six City dataset, we follow Tran et al. (2017) and consider the random intercept logistic regression model

$$\log\left(\frac{\pi_{ij}}{1 - \pi_{ij}}\right) = \beta_0 + \beta_{age}\mathbf{Age}_{ij} + \beta_{smoke}\mathbf{Smoke}_{ij} + \alpha_i, \quad \alpha_i \sim \text{Gau}(0, \tau^2), \quad (31)$$

where $\pi_{ij} \equiv \Pr(y_{ij} = 1 \mid \boldsymbol{\beta}, \tau^2)$, with $\boldsymbol{\beta} \equiv (\beta_0, \beta_{age}, \beta_{smoke})^\top$, for $i = 1, \dots, 537$ and $j = 1, \dots, 4$. The binary response variable $y_{ij} = 1$ if child i is wheezing at time point j , and 0 otherwise. The covariate \mathbf{Age}_{ij} is the

age of child i at time point j , centred at 9 years, while the covariate $\text{Smoke}_{ij} = 1$ if the mother of child i is smoking at time point j , and 0 otherwise. Finally, α_i is the random effect associated with the i th child. The parameters of the model are $\boldsymbol{\theta} = (\boldsymbol{\beta}^\top, \phi_\tau)^\top$, where $\phi_\tau \equiv \log(\tau^2)$.

For the Polypharmacy dataset, we consider the random intercept logistic regression model from Tan and Nott (2018):

$$\log\left(\frac{\pi_{ij}}{1 - \pi_{ij}}\right) = \beta_0 + \beta_{\text{gender}}\text{Gender}_i + \beta_{\text{race}}\text{Race}_i + \beta_{\text{age}}\text{Age}_{ij} + \beta_{M1}\text{MHV1}_{ij} \\ + \beta_{M2}\text{MHV2}_{ij} + \beta_{M3}\text{MHV3}_{ij} + \beta_{IM}\text{INPTMHV}_{ij} + \alpha_i, \quad \alpha_i \sim \text{Gau}(0, \tau^2), \quad (32)$$

where $\pi_{ij} \equiv \Pr(y_{ij} = 1 \mid \boldsymbol{\beta}, \tau^2)$, $\boldsymbol{\beta} \equiv (\beta_0, \beta_{\text{gender}}, \beta_{\text{race}}, \beta_{\text{age}}, \beta_{M1}, \beta_{M2}, \beta_{M3}, \beta_{IM})^\top$, for $i = 1, \dots, 500$ and $j = 1, \dots, 7$. The response variable y_{ij} is 1 if subject i in year j is taking drugs from three or more different classes (of drugs), and 0 otherwise. The covariate $\text{Gender}_i = 1$ if subject i is male, and 0 if female, while $\text{Race}_i = 0$ if the race of subject i is white, and 1 otherwise. The covariate Age_{ij} is the age (in years and months, to two decimal places) of subject i in year j . The number of outpatient mental health visits (MHV) for subject i in year j is split into three dummy variables: $\text{MHV1}_{ij} = 1$ if $1 \leq \text{MHV}_{ij} \leq 5$, and 0 otherwise; $\text{MHV2}_{ij} = 1$ if $6 \leq \text{MHV}_{ij} \leq 14$, and 0 otherwise; and $\text{MHV3}_{ij} = 1$ if $\text{MHV}_{ij} \geq 15$, and 0 otherwise. The covariate $\text{INPTMHV}_{ij} = 0$ if there were no inpatient mental health visits for subject i in year j , and 1 otherwise. Finally, α_i is a subject-level random effect for subject i . The parameters of the model are $\boldsymbol{\theta} = (\boldsymbol{\beta}^\top, \phi_\tau)^\top$, where $\phi_\tau \equiv \log(\tau^2)$.

We use similar priors/initial variational distributions for both examples. For the Six City dataset, the prior/initial variational distribution we use is

$$p(\boldsymbol{\theta}) = q_0(\boldsymbol{\theta}) = \text{Gau}\left(\begin{bmatrix} \mathbf{0} \\ 1 \end{bmatrix}, \begin{bmatrix} 10\mathbf{I}_3 & \mathbf{0} \\ \mathbf{0}^\top & 1 \end{bmatrix}\right), \quad (33)$$

and for the Polypharmacy dataset, we use

$$p(\boldsymbol{\theta}) = q_0(\boldsymbol{\theta}) = \text{Gau}\left(\begin{bmatrix} \mathbf{0} \\ 1 \end{bmatrix}, \begin{bmatrix} 10\mathbf{I}_8 & \mathbf{0} \\ \mathbf{0}^\top & 1 \end{bmatrix}\right). \quad (34)$$

A $\text{Gau}(1, 1)$ prior distribution for ϕ_τ leads to a log-normal prior distribution with mean 4.48 and variance 34.51 for τ^2 . Using this prior distribution, the 2.5th and 97.5th percentiles for τ^2 are (0.383, 19.297), which cover most values of τ^2 in practice. At each R-VGAL iteration, the gradient and Hessian of $\log p(\mathbf{y}_i \mid \boldsymbol{\theta})$ are

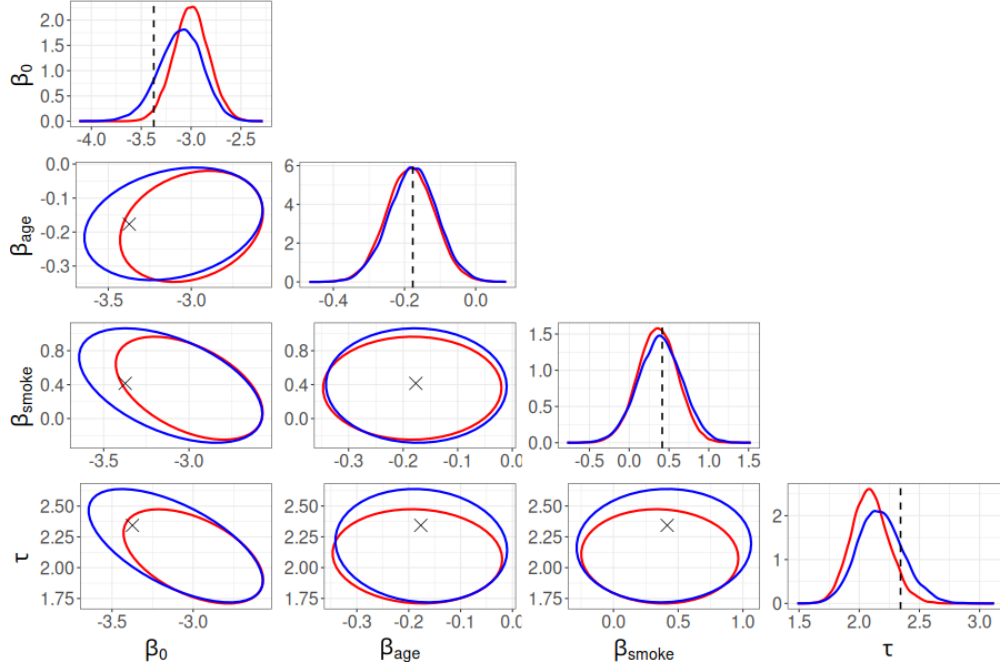


Figure 4: Exact posterior distributions from HMC (in blue) and approximate posterior distributions from R-VGAL with estimated gradients and Hessians (in red) for the experiment with the Six City dataset. Diagonal panels: Marginal posterior distributions with the maximum likelihood estimates marked using dotted lines. Off-diagonal panels: Bivariate posterior distributions with the maximum likelihood estimates marked using the symbol \times .

approximated using $S_\alpha = 200$ Monte Carlo samples (of α_i), and the expectations with respect to $q_{i-1}(\boldsymbol{\theta})$ in the R-VGAL updates are approximated using $S = 200$ Monte Carlo samples (of $\boldsymbol{\theta}$).

As there are no ground truths to these examples, we compare the posterior density estimates from R-VGAL to those from HMC. In addition, we also compute the maximum likelihood estimates using the `lme4` package in R. Figures 4 and 5 show the marginal posterior distributions with maximum likelihood estimates of the parameters, along with bivariate posterior distributions estimated using R-VGAL and HMC for the Six City and Polypharmacy datasets, respectively. In the Six City example, there is a slight difference in the marginal and bivariate posterior densities from R-VGAL and HMC for the fixed effect β_{smoke} , but the posterior densities for other parameters are very similar between the two methods. For the intercept β_0 and the random effect standard deviation τ , the posterior modes of HMC are closer to the maximum likelihood estimates than the posterior modes of R-VGAL, but for the other parameters, the posterior modes from both R-VGAL and HMC are close to the maximum likelihood estimates. For the Polypharmacy example, there are slight differences between the R-VGAL and HMC marginal and bivariate posterior densities for the intercept β_0 and the fixed effects β_{gender} and β_{race} , but for other parameters, the posterior densities are comparable between the two methods. The posterior modes of both R-VGAL and HMC are close to the



Figure 5: Exact posterior distributions from HMC (in blue) and approximate posterior distributions from R-VGAL with estimated gradients and Hessians (in red) for the experiment with the Polypharmacy dataset. Diagonal panels: Marginal posterior distributions with the maximum likelihood estimates marked using dotted lines. Off-diagonal panels: Bivariate posterior distributions with the maximum likelihood estimates marked using the symbol \times .

maximum likelihood estimates for all parameters in this example.

3.5 Computing time

Table 1 compares the computing time (in minutes) of R-VGAL and HMC for all simulated and real data examples that we have discussed in Sect. 3 and Sect. S6 of the online supplement, and includes the corresponding dataset size for each example. The last column in the table shows the average time taken (in seconds) for a single iteration of R-VGAL. For the linear example, where we run R-VGAL with both the theoretical and estimated gradients/Hessians, the displayed time is that of R-VGAL with the estimated gradients/Hessians. All experiments were carried out on the High Performance Computer system of the National Institute for Applied Statistics Research Australia, with an NVIDIA Tesla V100 PCIe 32GB graphics processing unit (GPU). The GPU was used to parallelise the computations in the importance sampling step, so that the gradient and Hessian of the joint log-likelihood $\log p(\mathbf{y}_i, \boldsymbol{\alpha}_i^{(s)} | \boldsymbol{\theta})$, $s = 1, \dots, S_\alpha$, and their

	N	n	HMC (min)	R-VGAL (min)	One R-VGAL iteration (s)
Linear (simulated data)	200	10	2.5	0.6	0.17
Logistic (simulated data)	500	10	7.2	1.1	0.13
Poisson (simulated data)	200	10	11.3	3.1	1.05
Logistic (Six City)	537	4	3.4	1.2	0.13
Logistic (Polypharmacy)	500	7	18.5	2.4	0.29
Poisson (Epilepsy)*	59	4	3.3	1.2	1.25
Logistic (simulated data)*	5000	10	133.6	16.8	0.20

Table 1: Computing time (in minutes) for R-VGAL and HMC on simulated and real datasets, with accompanying dataset sizes. Timings for one R-VGAL update is shown (in seconds). Examples with the * symbol are in the online supplement.

corresponding weights \mathcal{W}_i , are computed all at once. The GPU was also used to parallelise over the Monte Carlo samples used in the estimation of the expectations with respect to $q_{i-1}(\cdot)$ in Algorithm 1. We use the R interface to Tensorflow (Abadi et al., 2015) to facilitate GPU computations.

The table shows that the R-VGAL algorithm is generally 3 to 8 times faster than HMC. This is substantial given that our code is not as highly optimised as that in Stan. The difference in computing times also becomes more notable with a bigger dataset: in the logistic example with 50000 synthetic observations (see Sect. S6.2 of the online supplement), R-VGAL takes only 17 minutes to produce posterior estimates, while HMC takes more than 2 hours. Furthermore, since R-VGAL is a sequential algorithm, posterior approximations from R-VGAL can be easily updated as new observations become available. To incorporate an additional observation, R-VGAL needs to perform a single update, while an algorithm like HMC requires rerunning the entire sampling procedure.

4 Conclusion

In this article, we propose a sequential variational Bayes algorithm for estimating parameters in GLMMs based on an extension of the R-VGA algorithm of Lambert et al. (2022). The original R-VGA algorithm requires the gradient and Hessian of the partial log-likelihood at each observation, which are computationally intractable for most GLMMs. To overcome this, we use Fisher’s and Louis’ identities to obtain unbiased estimates of the gradient and Hessian, which can be used in place of the closed form gradient and Hessian in the R-VGAL algorithm.

We apply R-VGAL to the linear, logistic and Poisson mixed effect models with simulated and real datasets. In all examples, we compare the posterior distributions of the parameters estimated using R-VGAL to those obtained using HMC (Neal, 2011; Betancourt and Girolami, 2015). The examples show that R-VGAL yields comparable posterior estimates to HMC while being substantially faster, and the R-VGAL posterior modes

are very close to the maximum likelihood estimates for most parameters in the models we consider. R-VGAL would be especially useful in situations where new observations are being continuously collected.

In the current paper, we assume that the random effects are independent and identically distributed between subjects or groups. We discuss the potential application of R-VGAL to models with more complicated random effect structures, such as crossed or nested effects, in Sect. S7 of the online supplement. Future work will attempt to extend R-VGAL to cases where the random effects are temporally correlated. This will expand the set of models on which R-VGAL can be used to include time series and state space models.

Acknowledgements

This work was supported by ARC SRIEAS Grant SR200100005 Securing Antarctica’s Environmental Future. Andrew Zammit-Mangion’s research was also supported by ARC Discovery Early Career Research Award DE180100203. The authors would also like to thank two anonymous reviewers for their insightful and constructive comments.

References

- Abadi, M., Agarwal, A., Barham, P., Brevdo, E., Chen, Z., Citro, C., Corrado, G. S., Davis, A., Dean, J., Devin, M., Ghemawat, S., Goodfellow, I., Harp, A., Irving, G., Isard, M., Jia, Y., Jozefowicz, R., Kaiser, L., Kudlur, M., Levenberg, J., Mané, D., Monga, R., Moore, S., Murray, D., Olah, C., Schuster, M., Shlens, J., Steiner, B., Sutskever, I., Talwar, K., Tucker, P., Vanhoucke, V., Vasudevan, V., Viégas, F., Vinyals, O., Warden, P., Wattenberg, M., Wicke, M., Yu, Y., and Zheng, X. (2015). TensorFlow: Large-scale machine learning on heterogeneous systems. Software available from tensorflow.org.
- Bates, D., Mächler, M., Bolker, B., and Walker, S. (2015). Fitting linear mixed-effects models using lme4. *Journal of Statistical Software*, 67(1):1–48.
- Betancourt, M. and Girolami, M. (2015). Hamiltonian Monte Carlo for hierarchical models. *Current Trends in Bayesian Methodology with Applications*, 79(30):2–4.
- Blei, D. M., Kucukelbir, A., and McAuliffe, J. D. (2017). Variational inference: a review for statisticians. *Journal of the American Statistical Association*, 112(518):859–877.
- Bonnet, G. (1964). Transformations des signaux aléatoires a travers les systemes non linéaires sans mémoire. In *Annales des Télécommunications*, volume 19, pages 203–220. Springer.

- Bottou, L. (2010). Large-scale machine learning with stochastic gradient descent. In *Proceedings of COMP-STAT'2010: 19th International Conference on Computational Statistics*, pages 177–186. Springer, New York, NY.
- Breslow, N. E. and Clayton, D. G. (1993). Approximate inference in generalized linear mixed models. *Journal of the American Statistical Association*, 88(421):9–25.
- Broderick, T., Boyd, N., Wibisono, A., Wilson, A. C., and Jordan, M. I. (2013). Streaming variational Bayes. In *Proceedings of the 26th International Conference on Neural Information Processing Systems - Volume 2, NIPS'13*, page 1727–1735. Curran Associates Inc., Red Hook, NY.
- Cappé, O., Moulines, E., and Rydén, T. (2005). *Inference in Hidden Markov Models*. Springer, New York, NY.
- Crowder, M. J. (1979). Inference about the intraclass correlation coefficient in the beta-binomial ANOVA for proportions. *Journal of the Royal Statistical Society B*, 41(2):230–234.
- Demidenko, E. (2013). *Mixed Models: Theory and Applications with R*. John Wiley & Sons, Hoboken, NJ.
- Dempster, A. P., Laird, N. M., and Rubin, D. B. (1977). Maximum likelihood from incomplete data via the EM algorithm. *Journal of the Royal Statistical Society B*, 39(1):1–22.
- Faraway, J. J. (2016). *Extending the Linear Model with R: Generalized Linear, Mixed Effects and Nonparametric Regression Models*. CRC Press, New York, NY, 2nd edition.
- Fitzmaurice, G. M. and Laird, N. M. (1993). A likelihood-based method for analysing longitudinal binary responses. *Biometrika*, 80(1):141–151.
- Fong, Y., Rue, H., and Wakefield, J. (2010). Bayesian inference for generalized linear mixed models. *Biostatistics*, 11(3):397–412.
- Gelman, A., Carlin, J. B., Stern, H. S., Dunson, D. B., Vehtari, A., and Rubin, D. B. (2013). *Bayesian Data Analysis*. CRC Press, New York, NY, 3rd edition.
- Gelman, A. and Hill, J. (2007). *Data Analysis Using Regression and Multilevel/Hierarchical Models*. Cambridge University Press, New York, NY.
- Gelman, A. and Rubin, D. B. (1992). Inference from iterative simulation using multiple sequences. *Statistical Science*, 7(4):457–472.

- Goldstein, H. (1991). Nonlinear multilevel models, with an application to discrete response data. *Biometrika*, 78(1):45–51.
- Gunawan, D., Kohn, R., and Nott, D. (2021). Variational Bayes approximation of factor stochastic volatility models. *International Journal of Forecasting*, 37(4):1355–1375.
- Hoffman, M. D., Blei, D. M., Wang, C., and Paisley, J. (2013). Stochastic variational inference. *Journal of Machine Learning Research*, 14:1303–1347.
- Hosmer, D. W., Lemeshow, S., and Sturdivant, R. X. (2013). *Applied Logistic Regression*. John Wiley & Sons, Hoboken, NJ, 3rd edition.
- Jansen, M. G. H. (1994). Parameters of the latent distribution in Rasch’s Poisson counts model. In Fischer, G. H. and Laming, D., editors, *Contributions to Mathematical Psychology, Psychometrics, and Methodology*, pages 319–326. Springer, New York, NY.
- Kingma, D. P. and Welling, M. (2013). Auto-encoding variational Bayes. *arXiv preprint arXiv:1312.6114*.
- Lambert, M., Bonnabel, S., and Bach, F. (2022). The recursive variational Gaussian approximation (RVGA). *Statistics and Computing*, 32(1).
- Naylor, J. C. and Smith, A. F. (1982). Applications of a method for the efficient computation of posterior distributions. *Journal of the Royal Statistical Society C*, 31(3):214–225.
- Neal, R. (2011). MCMC using Hamiltonian dynamics. In Brooks, S., Gelman, A., Jones, G. J., and Meng, X.-L., editors, *Handbook of Markov Chain Monte Carlo*. CRC Press, Boca Raton, FL.
- Nemeth, C., Fearnhead, P., and Mihaylova, L. (2016). Particle approximations of the score and observed information matrix for parameter estimation in state–space models with linear computational cost. *Journal of Computational and Graphical Statistics*, 25(4):1138–1157.
- Ong, V. M.-H., Nott, D. J., and Smith, M. S. (2018). Gaussian variational approximation with a factor covariance structure. *Journal of Computational and Graphical Statistics*, 27(3):465–478.
- Ormerod, J. T. and Wand, M. P. (2010). Explaining variational approximations. *The American Statistician*, 64(2):140–153.
- Papaspiliopoulos, O., Stumpf-Fétizon, T., and Zanella, G. (2023). Scalable Bayesian computation for crossed and nested hierarchical models. *Electronic Journal of Statistics*, 17(2):3575–3612.

- Pinheiro, J. and Bates, D. (2006). *Mixed-effects Models in S and S-PLUS*. Springer Science and Business Media, New York, NY.
- Price, R. (1958). A useful theorem for nonlinear devices having Gaussian inputs. *IRE Transactions on Information Theory*, 4(2):69–72.
- R Core Team (2022). *R: A Language and Environment for Statistical Computing*. R Foundation for Statistical Computing, Vienna, Austria.
- Stan Development Team (2023). RStan: the R interface to Stan. R package version 2.21.8.
- Tan, L. S. and Nott, D. J. (2018). Gaussian variational approximation with sparse precision matrices. *Statistics and Computing*, 28(2018):259–275.
- Thall, P. F. and Vail, S. C. (1990). Some covariance models for longitudinal count data with overdispersion. *Biometrics*, 46(3):657–671.
- Tierney, L. and Kadane, J. B. (1986). Accurate approximations for posterior moments and marginal densities. *Journal of the American Statistical Association*, 81(393):82–86.
- Tokdar, S. T. and Kass, R. E. (2010). Importance sampling: a review. *WIREs Computational Statistics*, 2(1):54–60.
- Tomasetti, N., Forbes, C., and Panagiotelis, A. (2022). Updating variational Bayes: Fast sequential posterior inference. *Statistics and Computing*, 32(1).
- Tran, M.-N., Nott, D. J., and Kohn, R. (2017). Variational Bayes with intractable likelihood. *Journal of Computational and Graphical Statistics*, 26(4):873–882.
- Tran, M.-N., Nott, D. J., Kuk, A. Y., and Kohn, R. (2016). Parallel variational Bayes for large datasets with an application to generalized linear mixed models. *Journal of Computational and Graphical Statistics*, 25(2):626–646.
- Tuerlinckx, F., Rijmen, F., Verbeke, G., and De Boeck, P. (2006). Statistical inference in generalized linear mixed models: A review. *British Journal of Mathematical and Statistical Psychology*, 59(2):225–255.
- Verbeke, G., Molenberghs, G., and Verbeke, G. (1997). *Linear Mixed Models for Longitudinal Data*. Springer, New York, NY.
- Wakefield, J. (2013). *Bayesian and Frequentist Regression Methods*. Springer, New York, NY.

West, B. T., Welch, K. B., and Galecki, A. T. (2014). *Linear Mixed Models: A Practical Guide Using Statistical Software*. CRC Press, Boca Raton, FL.

Zhao, Y., Staudenmayer, J., Coull, B. A., and Wand, M. P. (2006). General design Bayesian generalized linear mixed models. *Statistical Science*, 21(1):35–51.

S1 Appendix A: Gradient and Hessian derivations

S1.1 Derivation of gradient and Hessian expressions for the linear mixed model

In the linear mixed model, the theoretical gradient and Hessian for the likelihood at observation i for $i = 1, \dots, N$ are available. This section gives the expressions for both the theoretical gradient and Hessian, as well as their approximations when using Fisher's and Louis' identities.

S1.1.1 Theoretical gradient and Hessian

The "partial" log-likelihood for observations from the i th group is given by

$$\log p(\mathbf{y}_i | \boldsymbol{\theta}) = -\frac{n}{2} \log(2\pi) - \frac{1}{2} \log |\boldsymbol{\Sigma}_{y|\theta}| - \frac{1}{2} (\mathbf{y}_i - \mathbf{X}_i \boldsymbol{\beta})^\top \boldsymbol{\Sigma}_{y|\theta}^{-1} (\mathbf{y}_i - \mathbf{X}_i \boldsymbol{\beta}), \quad i = 1, \dots, N, \quad (\text{S1})$$

where $\boldsymbol{\Sigma}_{y|\theta} = \exp(\phi_\alpha) \mathbf{z}_i \mathbf{z}_i^\top + \exp(\phi_\epsilon) \mathbf{I}_n$.

The gradient of the log-likelihood with respect to the parameters $\boldsymbol{\theta}$ is given by

$$\nabla_{\boldsymbol{\theta}} \log p(\mathbf{y}_i | \boldsymbol{\theta}) = (\nabla_{\boldsymbol{\beta}} \log p(\mathbf{y}_i | \boldsymbol{\theta}))^\top, \nabla_{\phi_\alpha} \log p(\mathbf{y}_i | \boldsymbol{\theta}), \nabla_{\phi_\epsilon} \log p(\mathbf{y}_i | \boldsymbol{\theta})^\top,$$

where the components are, respectively,

$$\nabla_{\boldsymbol{\beta}} \log p(\mathbf{y}_i | \boldsymbol{\theta}) = \mathbf{X}_i^\top \boldsymbol{\Sigma}_{y|\theta}^{-1} (\mathbf{y}_i - \mathbf{X}_i \boldsymbol{\beta}) \quad (\text{S2})$$

$$\nabla_{\phi_\alpha} \log p(\mathbf{y}_i | \boldsymbol{\theta}) = -\frac{1}{2} \text{Tr} \left(\boldsymbol{\Sigma}_{y|\theta}^{-1} \frac{\partial \boldsymbol{\Sigma}_{y|\theta}}{\partial \phi_\alpha} \right) + \frac{1}{2} (\mathbf{y}_i - \mathbf{X}_i \boldsymbol{\beta})^\top \boldsymbol{\Sigma}_{y|\theta}^{-1} \frac{\partial \boldsymbol{\Sigma}_{y|\theta}}{\partial \phi_\alpha} \boldsymbol{\Sigma}_{y|\theta}^{-1} (\mathbf{y}_i - \mathbf{X}_i \boldsymbol{\beta}) \quad (\text{S3})$$

$$\nabla_{\phi_\epsilon} \log p(\mathbf{y}_i | \boldsymbol{\theta}) = -\frac{1}{2} \text{Tr} \left(\boldsymbol{\Sigma}_{y|\theta}^{-1} \frac{\partial \boldsymbol{\Sigma}_{y|\theta}}{\partial \phi_\epsilon} \right) + \frac{1}{2} (\mathbf{y}_i - \mathbf{X}_i \boldsymbol{\beta})^\top \boldsymbol{\Sigma}_{y|\theta}^{-1} \frac{\partial \boldsymbol{\Sigma}_{y|\theta}}{\partial \phi_\epsilon} \boldsymbol{\Sigma}_{y|\theta}^{-1} (\mathbf{y}_i - \mathbf{X}_i \boldsymbol{\beta}), \quad (\text{S4})$$

with

$$\frac{\partial \boldsymbol{\Sigma}_{y|\theta}}{\partial \phi_\alpha} = \exp(\phi_\alpha) \mathbf{z}_i \mathbf{z}_i^\top, \quad \frac{\partial \boldsymbol{\Sigma}_{y|\theta}}{\partial \phi_\epsilon} = \exp(\phi_\epsilon) \mathbf{I}_n. \quad (\text{S5})$$

The Hessian is given by

$$\nabla_{\boldsymbol{\theta}}^2 \log p(\mathbf{y}_i | \boldsymbol{\theta}) = \begin{bmatrix} \nabla_{\boldsymbol{\beta}}^2 \log p(\mathbf{y}_i | \boldsymbol{\theta}) & \nabla_{\boldsymbol{\beta}} \nabla_{\phi_\alpha} \log p(\mathbf{y}_i | \boldsymbol{\theta}) & \nabla_{\boldsymbol{\beta}} \nabla_{\phi_\epsilon} \log p(\mathbf{y}_i | \boldsymbol{\theta}) \\ \nabla_{\boldsymbol{\beta}} \nabla_{\phi_\alpha} \log p(\mathbf{y}_i | \boldsymbol{\theta})^\top & \nabla_{\phi_\alpha}^2 \log p(\mathbf{y}_i | \boldsymbol{\theta}) & \nabla_{\phi_\alpha} \nabla_{\phi_\epsilon} \log p(\mathbf{y}_i | \boldsymbol{\theta}) \\ \nabla_{\boldsymbol{\beta}} \nabla_{\phi_\epsilon} \log p(\mathbf{y}_i | \boldsymbol{\theta})^\top & \nabla_{\phi_\alpha} \nabla_{\phi_\epsilon} \log p(\mathbf{y}_i | \boldsymbol{\theta}) & \nabla_{\phi_\epsilon}^2 \log p(\mathbf{y}_i | \boldsymbol{\theta}) \end{bmatrix}. \quad (\text{S6})$$

The diagonal terms in the Hessian are the second derivatives

$$\nabla_{\boldsymbol{\beta}}^2 \log p(\mathbf{y}_i | \boldsymbol{\theta}) = -\mathbf{X}_i^\top \boldsymbol{\Sigma}_{y|\theta}^{-1} \mathbf{X}_i, \quad (\text{S7})$$

$$\nabla_{\phi_\alpha}^2 \log p(\mathbf{y}_i | \boldsymbol{\theta}) = -\frac{1}{2} \text{Tr}(\mathbf{G}_{\phi_\alpha}) + \frac{1}{2} (\mathbf{y}_i - \mathbf{X}_i \boldsymbol{\beta})^\top \mathbf{H}_{\phi_\alpha} (\mathbf{y}_i - \mathbf{X}_i \boldsymbol{\beta}), \quad (\text{S8})$$

where

$$\mathbf{G}_{\phi_\alpha} = -\boldsymbol{\Sigma}_{y|\theta}^{-1} \frac{\partial \boldsymbol{\Sigma}_{y|\theta}}{\partial \phi_\alpha} \boldsymbol{\Sigma}_{y|\theta}^{-1} \frac{\partial \boldsymbol{\Sigma}_{y|\theta}}{\partial \phi_\alpha} + \boldsymbol{\Sigma}_{y|\theta}^{-1} \frac{\partial^2 \boldsymbol{\Sigma}_{y|\theta}}{\partial \phi_\alpha^2} \quad (\text{S9})$$

$$\mathbf{H}_{\phi_\alpha} = -2\boldsymbol{\Sigma}_{y|\theta}^{-1} \frac{\partial \boldsymbol{\Sigma}_{y|\theta}}{\partial \phi_\alpha} \boldsymbol{\Sigma}_{y|\theta}^{-1} \frac{\partial \boldsymbol{\Sigma}_{y|\theta}}{\partial \phi_\alpha} \boldsymbol{\Sigma}_{y|\theta}^{-1} + \boldsymbol{\Sigma}_{y|\theta}^{-1} \frac{\partial^2 \boldsymbol{\Sigma}_{y|\theta}}{\partial \phi_\alpha^2} \boldsymbol{\Sigma}_{y|\theta}^{-1}, \quad (\text{S10})$$

with $\frac{\partial^2 \boldsymbol{\Sigma}_{y|\theta}}{\partial \phi_\alpha^2} = \exp(\phi_\alpha) \mathbf{z}_i \mathbf{z}_i^\top$. The expression for $\nabla_{\phi_\epsilon}^2 \log p(\mathbf{y}_i | \boldsymbol{\theta})$ is the same as in (S8), but with all derivatives with respect to ϕ_α replaced by those with respect to ϕ_ϵ . Note that $\frac{\partial^2 \boldsymbol{\Sigma}_{y|\theta}}{\partial \phi_\epsilon^2} = \exp(\phi_\epsilon) \mathbf{I}_n$.

The off-diagonal terms in the Hessian are

$$\begin{aligned} \nabla_{\boldsymbol{\beta}} \nabla_{\phi_\alpha} \log p(\mathbf{y}_i | \boldsymbol{\theta}) &= -\mathbf{X}_i^\top \boldsymbol{\Sigma}_{y|\theta}^{-1} \frac{\partial \boldsymbol{\Sigma}_{y|\theta}}{\partial \phi_\alpha} \boldsymbol{\Sigma}_{y|\theta}^{-1} (\mathbf{y}_i - \mathbf{X}_i \boldsymbol{\beta}) \\ \nabla_{\boldsymbol{\beta}} \nabla_{\phi_\epsilon} \log p(\mathbf{y}_i | \boldsymbol{\theta}) &= -\mathbf{X}_i^\top \boldsymbol{\Sigma}_{y|\theta}^{-1} \frac{\partial \boldsymbol{\Sigma}_{y|\theta}}{\partial \phi_\epsilon} \boldsymbol{\Sigma}_{y|\theta}^{-1} (\mathbf{y}_i - \mathbf{X}_i \boldsymbol{\beta}) \\ \nabla_{\phi_\alpha} \nabla_{\phi_\epsilon} \log p(\mathbf{y}_i | \boldsymbol{\theta}) &= -\frac{1}{2} \text{Tr}(\mathbf{G}_{\phi_\alpha \phi_\epsilon}) + \frac{1}{2} (\mathbf{y}_i - \mathbf{X}_i \boldsymbol{\beta})^\top \mathbf{H}_{\phi_\alpha \phi_\epsilon} (\mathbf{y}_i - \mathbf{X}_i \boldsymbol{\beta}), \end{aligned}$$

where

$$\mathbf{G}_{\phi_\alpha \phi_\epsilon} = -\boldsymbol{\Sigma}_{y|\theta}^{-1} \frac{\partial \boldsymbol{\Sigma}_{y|\theta}}{\partial \phi_\alpha} \boldsymbol{\Sigma}_{y|\theta}^{-1} \frac{\partial \boldsymbol{\Sigma}_{y|\theta}}{\partial \phi_\epsilon} \quad (\text{S11})$$

$$\mathbf{H}_{\phi_\alpha \phi_\epsilon} = -\boldsymbol{\Sigma}_{y|\theta}^{-1} \frac{\partial \boldsymbol{\Sigma}_{y|\theta}}{\partial \phi_\alpha} \boldsymbol{\Sigma}_{y|\theta}^{-1} \frac{\partial \boldsymbol{\Sigma}_{y|\theta}}{\partial \phi_\epsilon} \boldsymbol{\Sigma}_{y|\theta}^{-1} - \boldsymbol{\Sigma}_{y|\theta}^{-1} \frac{\partial \boldsymbol{\Sigma}_{y|\theta}}{\partial \phi_\epsilon} \boldsymbol{\Sigma}_{y|\theta}^{-1} \frac{\partial \boldsymbol{\Sigma}_{y|\theta}}{\partial \phi_\alpha} \boldsymbol{\Sigma}_{y|\theta}^{-1}. \quad (\text{S12})$$

S1.1.2 Expressions for the gradient and Hessian using Fisher's and Louis' identities

Fisher's identity (19) requires the gradient $\nabla_{\boldsymbol{\theta}} \log p(\mathbf{y}_i, \alpha_i | \boldsymbol{\theta})$, while Louis' identity (22) requires the Hessian $\nabla_{\boldsymbol{\theta}}^2 \log p(\mathbf{y}_i, \alpha_i | \boldsymbol{\theta})$. We now give the expression for these quantities for the linear mixed model considered in Sect. 3.1.

For $i = 1, \dots, N$, the gradient $\nabla_{\boldsymbol{\theta}} \log p(\mathbf{y}_i, \alpha_i | \boldsymbol{\theta})$ can be written as

$$\nabla_{\boldsymbol{\theta}} \log p(\mathbf{y}_i, \alpha_i | \boldsymbol{\theta}) = \nabla_{\boldsymbol{\theta}} \log p(\mathbf{y}_i | \alpha_i, \boldsymbol{\theta}) + \nabla_{\boldsymbol{\theta}} \log p(\alpha_i | \boldsymbol{\theta}), \quad (\text{S13})$$

$$= \nabla_{\boldsymbol{\theta}} \log p(\mathbf{y}_i | \alpha_i, \boldsymbol{\beta}, \phi_\epsilon) + \nabla_{\boldsymbol{\theta}} \log p(\alpha_i | \phi_\alpha), \quad (\text{S14})$$

where

$$\log p(\mathbf{y}_i | \alpha_i, \boldsymbol{\beta}, \phi_\epsilon) = -\frac{n}{2} \log(2\pi) - \frac{1}{2} \log |\exp(\phi_\epsilon) \mathbf{I}_n| - \frac{1}{2 \exp(\phi_\epsilon)} (\mathbf{y}_i - \mathbf{X}_i \boldsymbol{\beta} - \mathbf{z}_i \alpha_i)^\top (\mathbf{y}_i - \mathbf{X}_i \boldsymbol{\beta} - \mathbf{z}_i \alpha_i), \quad (\text{S15})$$

and

$$\log p(\alpha_i | \phi_\alpha) = -\frac{1}{2} \log(2\pi) - \frac{\phi_\alpha}{2} - \frac{\alpha_i^2}{2 \exp(\phi_\alpha)}. \quad (\text{S16})$$

Thus, the gradient of the joint $\nabla_{\boldsymbol{\theta}} \log p(\mathbf{y}_i, \alpha_i | \boldsymbol{\theta})$ is

$$\nabla_{\boldsymbol{\theta}} \log p(\mathbf{y}_i, \alpha_i | \boldsymbol{\theta}) = (\nabla_{\boldsymbol{\beta}} \log p(\mathbf{y}_i, \alpha_i | \boldsymbol{\theta}))^\top, \nabla_{\phi_\alpha} \log p(\mathbf{y}_i, \alpha_i | \boldsymbol{\theta}), \nabla_{\phi_\epsilon} \log p(\mathbf{y}_i, \alpha_i | \boldsymbol{\theta})^\top, \quad (\text{S17})$$

where each component is given by

$$\begin{aligned} \nabla_{\boldsymbol{\beta}} \log p(\mathbf{y}_i, \alpha_i | \boldsymbol{\theta}) &= \nabla_{\boldsymbol{\beta}} \log p(\mathbf{y}_i | \alpha_i, \boldsymbol{\beta}, \phi_\epsilon) \\ &= \frac{1}{\exp(\phi_\epsilon)} \mathbf{X}_i^\top (\mathbf{y}_i - \mathbf{X}_i \boldsymbol{\beta} - \mathbf{z}_i \alpha_i), \end{aligned} \quad (\text{S18})$$

$$\begin{aligned} \nabla_{\phi_\alpha} \log p(\mathbf{y}_i, \alpha_i | \boldsymbol{\theta}) &= \nabla_{\phi_\alpha} \log p(\alpha_i | \phi_\alpha) \\ &= -\frac{1}{2} + \frac{\alpha_i^2}{2 \exp(\phi_\alpha)}, \end{aligned} \quad (\text{S19})$$

$$\begin{aligned} \nabla_{\phi_\epsilon} \log p(\mathbf{y}_i, \alpha_i | \boldsymbol{\theta}) &= \nabla_{\phi_\epsilon} \log p(\mathbf{y}_i | \alpha_i, \boldsymbol{\beta}, \phi_\epsilon) \\ &= -\frac{n}{2} + \frac{1}{2 \exp(\phi_\epsilon)} (\mathbf{y}_i - \mathbf{X}_i \boldsymbol{\beta} - \mathbf{z}_i \alpha_i)^\top (\mathbf{y}_i - \mathbf{X}_i \boldsymbol{\beta} - \mathbf{z}_i \alpha_i). \end{aligned} \quad (\text{S20})$$

Similarly, the approximation of the Hessian using Louis' identity requires $\nabla_{\boldsymbol{\theta}}^2 \log p(\mathbf{y}_i, \alpha_i | \boldsymbol{\theta})$, in particular,

$$\nabla_{\boldsymbol{\theta}}^2 \log p(\mathbf{y}_i, \alpha_i | \boldsymbol{\theta}) = \begin{bmatrix} \nabla_{\boldsymbol{\beta}}^2 \log p(\mathbf{y}_i, \alpha_i | \boldsymbol{\theta}) & \nabla_{\boldsymbol{\beta}} \nabla_{\phi_\alpha} \log p(\mathbf{y}_i, \alpha_i | \boldsymbol{\theta}) & \nabla_{\boldsymbol{\beta}} \nabla_{\phi_\epsilon} \log p(\mathbf{y}_i, \alpha_i | \boldsymbol{\theta}) \\ \nabla_{\boldsymbol{\beta}} \nabla_{\phi_\alpha} \log p(\mathbf{y}_i, \alpha_i | \boldsymbol{\theta})^\top & \nabla_{\phi_\alpha}^2 \log p(\mathbf{y}_i, \alpha_i | \boldsymbol{\theta}) & \nabla_{\phi_\alpha} \nabla_{\phi_\epsilon} \log p(\mathbf{y}_i, \alpha_i | \boldsymbol{\theta}) \\ \nabla_{\boldsymbol{\beta}} \nabla_{\phi_\epsilon} \log p(\mathbf{y}_i, \alpha_i | \boldsymbol{\theta})^\top & \nabla_{\phi_\alpha} \nabla_{\phi_\epsilon} \log p(\mathbf{y}_i, \alpha_i | \boldsymbol{\theta})^\top & \nabla_{\phi_\epsilon}^2 \log p(\mathbf{y}_i, \alpha_i | \boldsymbol{\theta}) \end{bmatrix}. \quad (\text{S21})$$

The components of (S21) are given by

$$\nabla_{\boldsymbol{\beta}}^2 \log p(\mathbf{y}_i, \alpha_i | \boldsymbol{\theta}) = -\frac{1}{\exp(\phi_\epsilon)} \mathbf{X}_i^\top \mathbf{X}_i, \quad (\text{S22})$$

$$\nabla_{\phi_\alpha}^2 \log p(\mathbf{y}_i, \alpha_i | \boldsymbol{\theta}) = -\frac{\alpha_i^2}{2 \exp(\phi_\alpha)}, \quad (\text{S23})$$

$$\nabla_{\phi_\epsilon}^2 \log p(\mathbf{y}_i, \alpha_i | \boldsymbol{\theta}) = -\frac{1}{2 \exp(\phi_\epsilon)} (\mathbf{y}_i - \mathbf{X}_i \boldsymbol{\beta} - \mathbf{z}_i \alpha_i)^\top (\mathbf{y}_i - \mathbf{X}_i \boldsymbol{\beta} - \mathbf{z}_i \alpha_i), \quad (\text{S24})$$

$$\nabla_{\boldsymbol{\beta}} \nabla_{\phi_\alpha} \log p(\mathbf{y}_i, \alpha_i | \boldsymbol{\theta}) = \mathbf{0}, \quad (\text{S25})$$

$$\nabla_{\boldsymbol{\beta}} \nabla_{\phi_\epsilon} \log p(\mathbf{y}_i, \alpha_i | \boldsymbol{\theta}) = -\frac{1}{\exp(\phi_\epsilon)} \mathbf{X}_i^\top (\mathbf{y}_i - \mathbf{X}_i \boldsymbol{\beta} - \mathbf{z}_i \alpha_i), \quad (\text{S26})$$

$$\nabla_{\phi_\alpha} \nabla_{\phi_\epsilon} \log p(\mathbf{y}_i, \alpha_i | \boldsymbol{\theta}) = 0. \quad (\text{S27})$$

S1.2 Derivation of gradient and Hessian expressions for the logistic mixed model

The parameters of interest are $\boldsymbol{\theta} = (\boldsymbol{\beta}^\top, \phi_\tau)^\top$, where $\phi_\tau = \log(\tau^2)$. The likelihood function $p(\mathbf{y}_i | \boldsymbol{\theta})$ is not available in closed form for this model, so the gradient and Hessian of the log likelihood with respect to the parameters $\boldsymbol{\theta}$ need to be approximated via Fisher's and Louis' identities.

The evaluation of Fisher's identity requires the gradient $\nabla_{\boldsymbol{\theta}} \log p(\mathbf{y}_i, \alpha_i | \boldsymbol{\theta})$, where

$$\begin{aligned} \log p(\mathbf{y}_i, \alpha_i | \boldsymbol{\theta}) &= \log p(\mathbf{y}_i | \alpha_i, \boldsymbol{\theta}) + \log p(\alpha_i | \boldsymbol{\theta}) \\ &= \log p(\mathbf{y}_i | \alpha_i, \boldsymbol{\beta}) + \log p(\alpha_i | \phi_\tau). \end{aligned}$$

Individually,

$$\log p(\mathbf{y}_i | \alpha_i, \boldsymbol{\beta}) = \sum_{j=1}^n y_{ij} \log \left(\frac{1}{1 + \exp(-(\mathbf{x}_{ij}^\top \boldsymbol{\beta} + \alpha_i))} \right) + (1 - y_{ij}) \log \left(1 - \frac{1}{1 + \exp(-(\mathbf{x}_{ij}^\top \boldsymbol{\beta} + \alpha_i))} \right)$$

and

$$\log p(\alpha_i | \phi_\tau) = -\frac{1}{2} \log(2\pi) - \frac{\phi_\tau}{2} - \frac{1}{2} \frac{\alpha_i^2}{\exp(\phi_\tau)}.$$

The components of $\nabla_{\boldsymbol{\theta}} \log p(\mathbf{y}_i, \alpha_i | \boldsymbol{\theta}) = (\nabla_{\boldsymbol{\beta}} \log p(\mathbf{y}_i, \alpha_i | \boldsymbol{\theta}))^\top, \nabla_{\phi_\tau} \log p(\mathbf{y}_i, \alpha_i | \boldsymbol{\theta})^\top$ are derived below:

$$\begin{aligned} \nabla_{\boldsymbol{\beta}} \log p(\mathbf{y}_i, \alpha_i | \boldsymbol{\theta}) &= \nabla_{\boldsymbol{\beta}} \log p(\mathbf{y}_i | \alpha_i, \boldsymbol{\beta}) \quad (\text{since } \log p(\alpha_i | \boldsymbol{\theta}) \text{ does not depend on } \boldsymbol{\beta}) \\ &= \sum_{j=1}^n y_{ij} [1 + \exp(-(\mathbf{x}_{ij}^\top \boldsymbol{\beta} + \alpha_i))] \frac{\partial}{\partial \boldsymbol{\beta}} \left(\frac{1}{1 + \exp(-(\mathbf{x}_{ij}^\top \boldsymbol{\beta} + \alpha_i))} \right) \\ &\quad - \sum_{j=1}^n (1 - y_{ij}) \frac{1 + \exp(-(\mathbf{x}_{ij}^\top \boldsymbol{\beta} + \alpha_i))}{\exp(-(\mathbf{x}_{ij}^\top \boldsymbol{\beta} + \alpha_i))} \frac{\partial}{\partial \boldsymbol{\beta}} \left(\frac{1}{1 + \exp(-(\mathbf{x}_{ij}^\top \boldsymbol{\beta} + \alpha_i))} \right), \end{aligned} \quad (\text{S28})$$

where

$$\frac{\partial}{\partial \boldsymbol{\beta}} \left(\frac{1}{1 + \exp(-(\mathbf{x}_{ij}^\top \boldsymbol{\beta} + \alpha_i))} \right) = \mathbf{x}_{ij} \frac{\exp(-(\mathbf{x}_{ij}^\top \boldsymbol{\beta} + \alpha_i))}{[1 + \exp(-(\mathbf{x}_{ij}^\top \boldsymbol{\beta} + \alpha_i))]^2}. \quad (\text{S29})$$

Substituting (S29) into (S28) and reducing terms gives

$$\nabla_{\boldsymbol{\beta}} \log p(\mathbf{y}_i, \alpha_i | \boldsymbol{\theta}) = \sum_{j=1}^n y_{ij} \mathbf{x}_{ij} \frac{\exp(-(\mathbf{x}_{ij}^\top \boldsymbol{\beta} + \alpha_i))}{1 + \exp(-(\mathbf{x}_{ij}^\top \boldsymbol{\beta} + \alpha_i))} - \sum_{j=1}^n (1 - y_{ij}) \mathbf{x}_{ij} \frac{1}{1 + \exp(-(\mathbf{x}_{ij}^\top \boldsymbol{\beta} + \alpha_i))} \quad (\text{S30})$$

$$= \sum_{j=1}^n \mathbf{x}_{ij} \left[y_{ij} - \frac{1}{1 + \exp(-(\mathbf{x}_{ij}^\top \boldsymbol{\beta} + \alpha_i))} \right]. \quad (\text{S31})$$

The other component of $\nabla_{\boldsymbol{\theta}} \log p(\mathbf{y}_i, \alpha_i | \boldsymbol{\theta})$ is

$$\begin{aligned} \nabla_{\phi_\tau} \log p(\mathbf{y}_i, \alpha_i | \boldsymbol{\theta}) &= \nabla_{\phi_\tau} \log p(\alpha_i | \phi_\tau) \quad (\text{since } \log p(\mathbf{y}_i | \alpha_i, \boldsymbol{\beta}) \text{ does not depend on } \phi_\tau) \\ &= -\frac{1}{2} + \frac{\alpha_i^2}{2 \exp(\phi_\tau)}. \end{aligned} \quad (\text{S32})$$

Evaluation of Louis' identity similarly requires

$$\nabla_{\boldsymbol{\theta}}^2 \log p(\mathbf{y}_i, \alpha_i | \boldsymbol{\theta}) = \begin{bmatrix} \nabla_{\boldsymbol{\beta}}^2 \log p(\mathbf{y}_i, \alpha_i | \boldsymbol{\theta}) & \nabla_{\boldsymbol{\beta}} \nabla_{\phi_\tau} \log p(\mathbf{y}_i, \alpha_i | \boldsymbol{\theta}) \\ \nabla_{\boldsymbol{\beta}} \nabla_{\phi_\tau} \log p(\mathbf{y}_i, \alpha_i | \boldsymbol{\theta})^\top & \nabla_{\phi_\tau}^2 \log p(\mathbf{y}_i, \alpha_i | \boldsymbol{\theta}) \end{bmatrix}, \quad (\text{S33})$$

the components of which are

$$\nabla_{\boldsymbol{\beta}}^2 \log p(\mathbf{y}_i, \alpha_i | \boldsymbol{\theta}) = \sum_{j=1}^n \frac{\partial}{\partial \boldsymbol{\beta}^\top} \left(\frac{\mathbf{x}_{ij}}{1 + \exp(-(\mathbf{x}_{ij}^\top \boldsymbol{\beta} + \alpha_i))} \right) = - \sum_{j=1}^n \mathbf{x}_{ij} \mathbf{x}_{ij}^\top \frac{\exp(-(\mathbf{x}_{ij}^\top \boldsymbol{\beta} + \alpha_i))}{[1 + \exp(-(\mathbf{x}_{ij}^\top \boldsymbol{\beta} + \alpha_i))]^2}, \quad (\text{S34})$$

$$\nabla_{\phi_\tau}^2 \log p(\mathbf{y}_i, \alpha_i | \boldsymbol{\theta}) = -\frac{\alpha_i^2}{2 \exp(\phi_\tau)}, \quad (\text{S35})$$

$$\nabla_{\boldsymbol{\beta}} \nabla_{\phi_\tau} \log p(\mathbf{y}_i, \alpha_i | \boldsymbol{\theta}) = \mathbf{0}. \quad (\text{S36})$$

S1.3 Derivation of gradient and Hessian expressions for the Poisson mixed model

In this section, we derive the gradient and Hessian for the Poisson model with bivariate random effects in Sect. 3.3. We note that the formula for the gradient in this section can be generalised to an arbitrary number of random effects.

The parameters of interest in this model are the fixed effects, $\boldsymbol{\beta}$, and the lower-diagonal elements of the Cholesky factor \mathbf{L} of the random effect covariance matrix $\boldsymbol{\Sigma}_\alpha$. We parameterise \mathbf{L} as

$$\mathbf{L} = \begin{bmatrix} \exp(\zeta_{11}) & 0 \\ \zeta_{21} & \exp(\zeta_{22}) \end{bmatrix}, \quad (\text{S37})$$

and collect the parameters in a vector $\boldsymbol{\theta} = (\boldsymbol{\beta}^\top, \boldsymbol{\zeta})^\top$, where $\boldsymbol{\zeta} \equiv (\zeta_{11}, \zeta_{22}, \zeta_{21})^\top$. The likelihood function $p(\mathbf{y}_i | \boldsymbol{\theta})$ is not available in closed form for this model, so the gradient and Hessian of the log likelihood with respect to the parameters $\boldsymbol{\theta}$ need to be approximated via Fisher's and Louis' identities.

The evaluation of Fisher's identity requires the gradient of $\log p(\mathbf{y}_i, \boldsymbol{\alpha}_i | \boldsymbol{\theta})$, where

$$\begin{aligned} \log p(\mathbf{y}_i, \boldsymbol{\alpha}_i | \boldsymbol{\theta}) &= \log p(\mathbf{y}_i | \boldsymbol{\alpha}_i, \boldsymbol{\beta}) + \log p(\boldsymbol{\alpha}_i | \boldsymbol{\zeta}) \\ &= \sum_{j=1}^n [y_{ij}(\mathbf{x}_{ij}^\top \boldsymbol{\beta} + \mathbf{z}_{ij}^\top \boldsymbol{\alpha}_i) - \exp(\mathbf{x}_{ij}^\top \boldsymbol{\beta} + \mathbf{z}_{ij}^\top \boldsymbol{\alpha}_i)] \\ &\quad - \frac{r}{2} \log(2\pi) - \frac{1}{2} \log |\boldsymbol{\Sigma}_\alpha| - \frac{1}{2} \boldsymbol{\alpha}_i^\top \boldsymbol{\Sigma}_\alpha^{-1} \boldsymbol{\alpha}_i, \end{aligned} \quad (\text{S38})$$

for $i = 1, \dots, N$, $j = 1, \dots, n$, and where r is the number of random effects. The gradient is

$$\nabla_{\boldsymbol{\theta}} \log p(\mathbf{y}_i, \boldsymbol{\alpha}_i | \boldsymbol{\theta}) = (\nabla_{\boldsymbol{\beta}} \log p(\mathbf{y}_i, \boldsymbol{\alpha}_i | \boldsymbol{\theta}), \nabla_{\boldsymbol{\zeta}} \log p(\mathbf{y}_i, \boldsymbol{\alpha}_i | \boldsymbol{\theta}))^\top.$$

As $\log p(\boldsymbol{\alpha}_i | \boldsymbol{\zeta})$ does not depend on $\boldsymbol{\beta}$, the gradient with respect to $\boldsymbol{\beta}$ is simply

$$\nabla_{\boldsymbol{\beta}} \log p(\mathbf{y}_i, \boldsymbol{\alpha}_i | \boldsymbol{\theta}) = \nabla_{\boldsymbol{\beta}} \log p(\mathbf{y}_i | \boldsymbol{\alpha}_i, \boldsymbol{\beta}) = \sum_{j=1}^n [y_{ij} - \exp(\mathbf{x}_{ij}^\top \boldsymbol{\beta} + \mathbf{z}_{ij}^\top \boldsymbol{\alpha}_i)] \mathbf{x}_{ij}. \quad (\text{S39})$$

Similarly, as $\log p(\mathbf{y}_i | \boldsymbol{\alpha}_i, \boldsymbol{\beta})$ does not depend on $\boldsymbol{\zeta}$, the gradient with respect to $\boldsymbol{\zeta}$ reduces to

$$\begin{aligned}\nabla_{\boldsymbol{\zeta}} \log p(\mathbf{y}_i, \boldsymbol{\alpha}_i | \boldsymbol{\theta}) &= \nabla_{\boldsymbol{\zeta}} \log p(\boldsymbol{\alpha}_i | \boldsymbol{\zeta}) \\ &= \text{Tr}(\mathbf{A}^\top \nabla_{\zeta_{kl}} \mathbf{L}), \quad k = 1, 2, l < k,\end{aligned}$$

where $\mathbf{A} = -\mathbf{L}^{-\top} + \mathbf{L}^{-\top} \mathbf{L}^{-1} \boldsymbol{\alpha}_i \boldsymbol{\alpha}_i^\top \mathbf{L}^{-\top}$, with $\mathbf{M}^{-\top}$ denoting the inverse of the transpose of a matrix \mathbf{M} , and

$$\nabla_{\zeta_{kl}} \mathbf{L} = \begin{cases} \mathbf{J}_{kk}^* & \text{if } k = l, \\ \mathbf{J}_{kl} & \text{otherwise,} \end{cases} \quad (\text{S40})$$

for $k = 1, 2, l < k$, where \mathbf{J}_{kl} is a 2×2 matrix that has 1 in the (k, l) th element and 0 elsewhere, and \mathbf{J}_{kk}^* is a 2×2 matrix that has $\exp(\zeta_{kk})$ in the (k, k) th element and 0 elsewhere.

The Hessian for the subject-specific log likelihood is

$$\begin{aligned}\nabla_{\boldsymbol{\theta}}^2 \log p(\mathbf{y}_i, \boldsymbol{\alpha}_i | \boldsymbol{\theta}) &= \begin{bmatrix} \nabla_{\boldsymbol{\beta}}^2 \log p(\mathbf{y}_i, \boldsymbol{\alpha}_i | \boldsymbol{\theta}) & \nabla_{\boldsymbol{\zeta}} \nabla_{\boldsymbol{\beta}} \log p(\mathbf{y}_i, \boldsymbol{\alpha}_i | \boldsymbol{\theta})^\top \\ \nabla_{\boldsymbol{\zeta}} \nabla_{\boldsymbol{\beta}} \log p(\mathbf{y}_i, \boldsymbol{\alpha}_i | \boldsymbol{\theta}) & \nabla_{\boldsymbol{\zeta}}^2 \log p(\mathbf{y}_i, \boldsymbol{\alpha}_i | \boldsymbol{\theta}) \end{bmatrix} \\ &= \begin{bmatrix} \nabla_{\boldsymbol{\beta}}^2 \log p(\mathbf{y}_i, \boldsymbol{\alpha}_i | \boldsymbol{\theta}) & \mathbf{0}_{4 \times 3} \\ \mathbf{0}_{3 \times 4} & \nabla_{\boldsymbol{\zeta}}^2 \log p(\mathbf{y}_i, \boldsymbol{\alpha}_i | \boldsymbol{\theta}) \end{bmatrix},\end{aligned}$$

where $\mathbf{0}_{m \times n}$ is a matrix of size $m \times n$. Here the cross-derivative $\nabla_{\boldsymbol{\zeta}} \nabla_{\boldsymbol{\beta}} \log p(\mathbf{y}_i, \boldsymbol{\alpha}_i | \boldsymbol{\theta})$ is zero because $\nabla_{\boldsymbol{\beta}} \log p(\mathbf{y}_i, \boldsymbol{\alpha}_i | \boldsymbol{\theta})$ does not depend on $\boldsymbol{\zeta}$. The remaining components of the Hessian matrix are

$$\nabla_{\boldsymbol{\beta}}^2 \log p(\mathbf{y}_i, \boldsymbol{\alpha}_i | \boldsymbol{\theta}) = \sum_{j=1}^n [y_{ij} - \exp(\mathbf{x}_{ij}^\top \boldsymbol{\beta} + \mathbf{z}_{ij}^\top \boldsymbol{\alpha}_i)] \mathbf{x}_{ij} \mathbf{x}_{ij}^\top, \quad (\text{S41})$$

and

$$\nabla_{\boldsymbol{\zeta}}^2 \log p(\mathbf{y}_i, \boldsymbol{\alpha}_i | \boldsymbol{\theta}) = \begin{bmatrix} \nabla_{\zeta_{11}}^2 \log p(\mathbf{y}_i, \boldsymbol{\alpha}_i | \boldsymbol{\theta}) & \nabla_{\zeta_{22}} \nabla_{\zeta_{11}} \log p(\mathbf{y}_i, \boldsymbol{\alpha}_i | \boldsymbol{\theta})^\top & \nabla_{\zeta_{21}} \nabla_{\zeta_{11}} \log p(\mathbf{y}_i, \boldsymbol{\alpha}_i | \boldsymbol{\theta})^\top \\ \nabla_{\zeta_{22}} \nabla_{\zeta_{11}} \log p(\mathbf{y}_i, \boldsymbol{\alpha}_i | \boldsymbol{\theta}) & \nabla_{\zeta_{22}}^2 \log p(\mathbf{y}_i, \boldsymbol{\alpha}_i | \boldsymbol{\theta})^\top & \nabla_{\zeta_{21}} \nabla_{\zeta_{22}} \log p(\mathbf{y}_i, \boldsymbol{\alpha}_i | \boldsymbol{\theta})^\top \\ \nabla_{\zeta_{21}} \nabla_{\zeta_{11}} \log p(\mathbf{y}_i, \boldsymbol{\alpha}_i | \boldsymbol{\theta}) & \nabla_{\zeta_{21}} \nabla_{\zeta_{22}} \log p(\mathbf{y}_i, \boldsymbol{\alpha}_i | \boldsymbol{\theta})^\top & \nabla_{\zeta_{21}}^2 \log p(\mathbf{y}_i, \boldsymbol{\alpha}_i | \boldsymbol{\theta})^\top \end{bmatrix}$$

where

$$\nabla_{\zeta_{kl}}^2 \log p(\mathbf{y}_i, \boldsymbol{\alpha}_i | \boldsymbol{\theta}) = \text{Tr}((\nabla_{\zeta_{kl}} \mathbf{A})^\top \nabla_{\zeta_{kl}} \mathbf{L} + \mathbf{A}^\top \nabla_{\zeta_{kl}}^2 \mathbf{L}), \quad k = 1, 2, l < k. \quad (\text{S42})$$

Separately,

$$\nabla_{\zeta_{kl}}^2 \mathbf{L} = \begin{cases} \mathbf{J}_{kk}^*, & \text{if } k = l \\ \mathbf{0}_{2 \times 2}, & \text{otherwise,} \end{cases} \quad (\text{S43})$$

and

$$\begin{aligned} \nabla_{\zeta_{kl}} \mathbf{A} &= \nabla_{\zeta_{kl}} (-\mathbf{L}^{-\top} + \mathbf{L}^{-\top} \mathbf{L}^{-1} \boldsymbol{\alpha}_i \boldsymbol{\alpha}_i^{\top} \mathbf{L}^{-\top}) \\ &= -\nabla_{\zeta_{kl}} \mathbf{L}^{-\top} + (\nabla_{\zeta_{kl}} \mathbf{L}^{-\top}) \mathbf{B} + \mathbf{L}^{-\top} \nabla_{\zeta_{kl}} \mathbf{B}, \end{aligned} \quad (\text{S44})$$

where $\mathbf{B} = \mathbf{L}^{-1} \boldsymbol{\alpha}_i \boldsymbol{\alpha}_i^{\top} \mathbf{L}^{-\top}$, and $\nabla_{\zeta_{kl}} \mathbf{B} = (\nabla_{\zeta_{kl}} \mathbf{L}^{-1}) \boldsymbol{\alpha}_i \boldsymbol{\alpha}_i^{\top} \mathbf{L}^{-\top} + \mathbf{L}^{-1} \boldsymbol{\alpha}_i \boldsymbol{\alpha}_i^{\top} (\nabla_{\zeta_{kl}} \mathbf{L}^{-\top})$, for $k = 1, 2, l < k$.

We derive the terms $\nabla_{\zeta_{kl}} \mathbf{L}^{-\top}$ individually:

$$\begin{aligned} \nabla_{\zeta_{11}} \mathbf{L}^{-\top} &= \begin{bmatrix} -\exp(-\zeta_{11}) & 0 \\ \zeta_{21} \exp(-\zeta_{11} - \zeta_{22}) & 0 \end{bmatrix}, \\ \nabla_{\zeta_{22}} \mathbf{L}^{-\top} &= \begin{bmatrix} 0 & 0 \\ \zeta_{21} \exp(-\zeta_{11} - \zeta_{22}) & -\exp(-\zeta_{22}) \end{bmatrix}, \\ \nabla_{\zeta_{21}} \mathbf{L}^{-\top} &= \begin{bmatrix} 0 & 0 \\ -\exp(-\zeta_{11} - \zeta_{22}) & 0 \end{bmatrix}. \end{aligned}$$

S2 Variance of the R-VGAL posterior densities for various Monte Carlo sample sizes

In this section, we study the effects of increasing the number of samples S , for estimating the expectations in the variational mean and precision matrix updates, and S_α , for estimating the gradient of the log-likelihood on the R-VGAL posterior estimates. The results are obtained using the simulated logistic data in Sect. 3.2 and the Polypharmacy dataset in Sect. 3.4 of the main paper. Similar results are obtained for other datasets. For all simulations in this section, we use the damped R-VGAL algorithm in Sect. 2.4 with $n_{damp} = 10$ observations and $K = 4$ damping steps per observation.

S2.1 Simulated logistic data

The simulated data used in this section is the same as that used in Sect. 3.2 of the main paper. The same values for S and S_α are used and they are taken from the set $\{50, 100, 500, 1000\}$. For each pair of S and S_α values, we independently run R-VGAL 10 times on the simulated dataset, and plot the posterior densities from all 10 runs for each parameter. These posterior densities are shown in Figures S1 to S4. For comparison, the HMC posterior distributions (from a single run, with 2 chains and 20000 total posterior samples after burn-in) are also plotted in each figure.

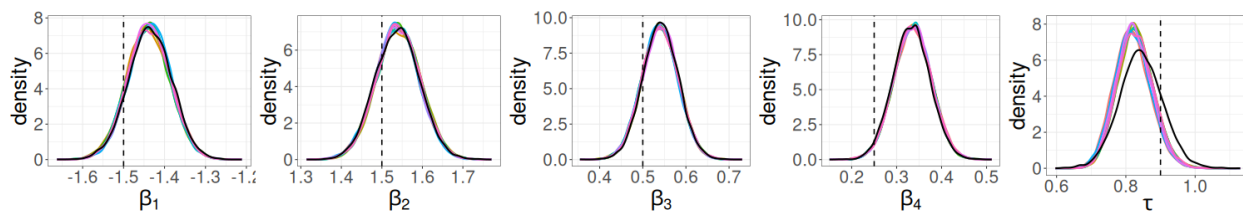


Figure S1: R-VGAL posterior distributions from 10 runs on simulated logistic data are plotted in colour. Damping is done on the first 10 observations, and the Monte Carlo sample sizes are $S = 50$ and $S_\alpha = 50$. HMC posterior distributions are plotted in black for comparison.

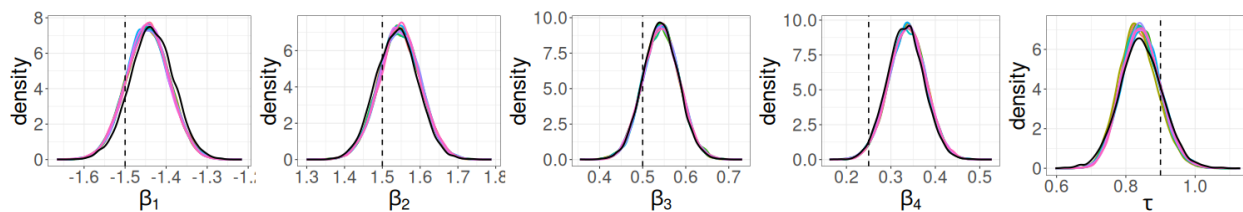


Figure S2: R-VGAL posterior distributions from 10 runs on simulated logistic data are plotted in colour. Damping is done on the first 10 observations, and the Monte Carlo sample sizes are $S = 100$ and $S_\alpha = 100$. HMC posterior distributions are plotted in black for comparison.

As the Monte Carlo sample sizes increase, the R-VGAL posterior density estimates get closer and closer to

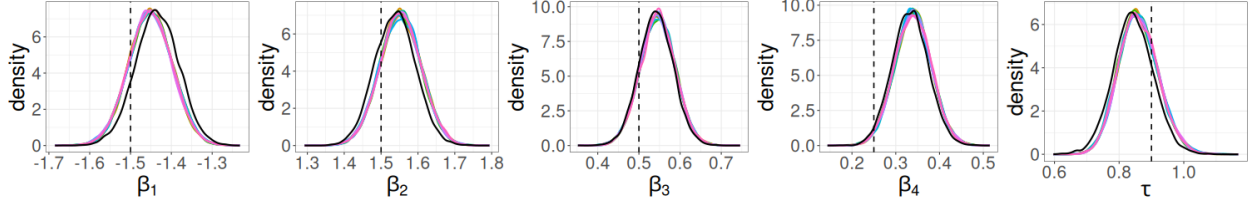


Figure S3: R-VGAL posterior distributions from 10 runs on simulated logistic data are plotted in colour. Damping is done on the first 10 observations, and the Monte Carlo sample sizes are $S = 500$ and $S_\alpha = 500$. HMC posterior distributions are plotted in black for comparison.

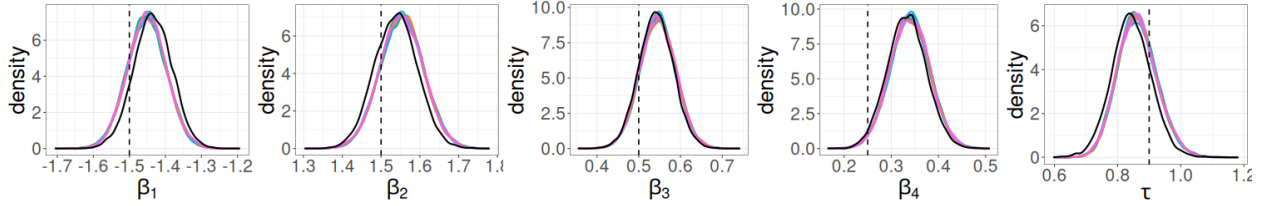


Figure S4: R-VGAL posterior distributions from 10 runs on simulated logistic data are plotted in colour. Damping is done on the first 10 observations, and the Monte Carlo sample sizes are $S = 1000$ and $S_\alpha = 1000$. HMC posterior distributions are plotted in black for comparison.

each other, which shows that increasing the values of S and S_α helps reduce the variability of the R-VGAL posterior estimates across multiple independent runs.

S2.2 Polypharmacy dataset

The Polypharmacy dataset used in this section is the same as that used in Sect. 3.4 of the main paper. Similar to Sect. S2.1, the same values for S and S_α are used and they are taken from the set $\{50, 100, 500, 1000\}$. We independently run R-VGAL 10 times on the Polypharmacy dataset for each pair of S and S_α values, and plot the posterior densities from all 10 runs for each parameter. These posteriors are shown in Figures S5 to S8. For comparison, the HMC posterior distributions (from a single run, with 2 chains and 20000 total posterior samples after burn-in) are also plotted.

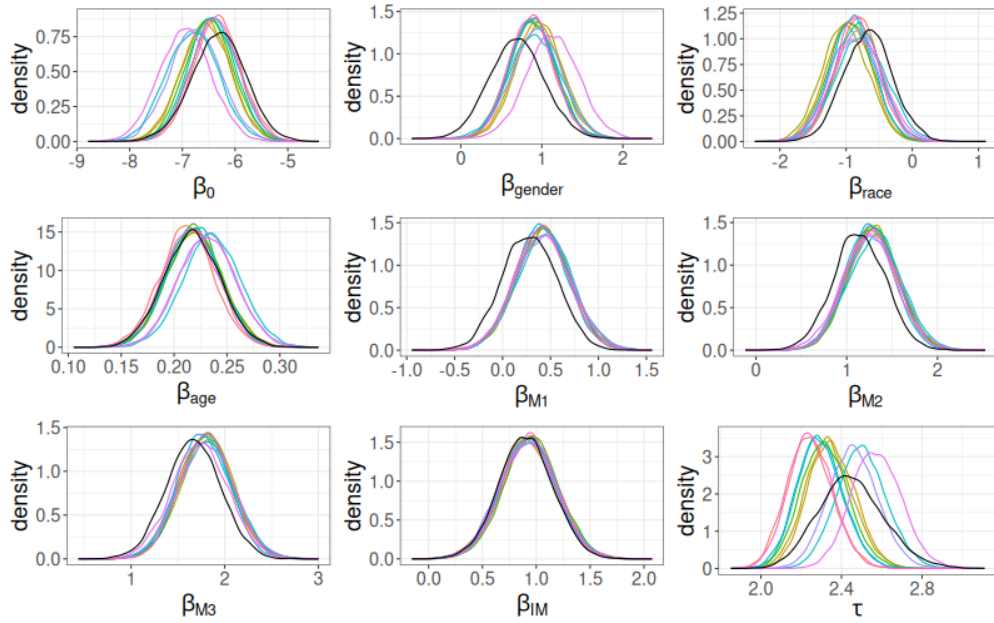


Figure S5: R-VGAL posterior distributions from 10 runs on the Polypharmacy dataset are plotted in colour. Damping is done on the first 10 observations, and the Monte Carlo sample sizes are $S = 50$ and $S_\alpha = 50$. HMC posterior distributions are plotted in black for comparison.

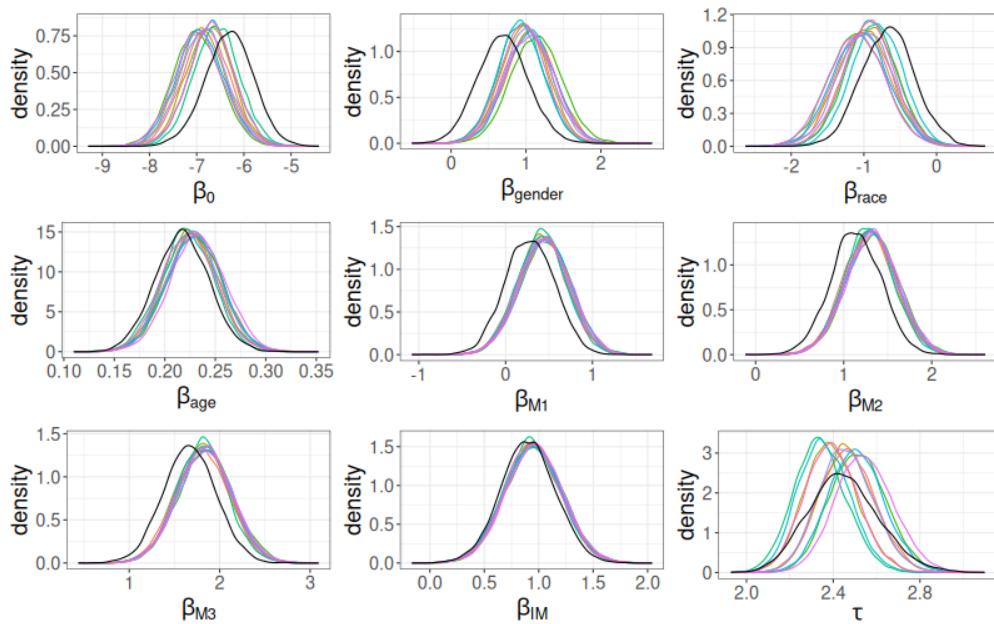


Figure S6: R-VGAL posterior distributions from 10 runs on the Polypharmacy dataset are plotted in colour. Damping is done on the first 10 observations, and the Monte Carlo sample sizes are $S = 100$ and $S_\alpha = 100$. HMC posterior distributions are plotted in black for comparison.

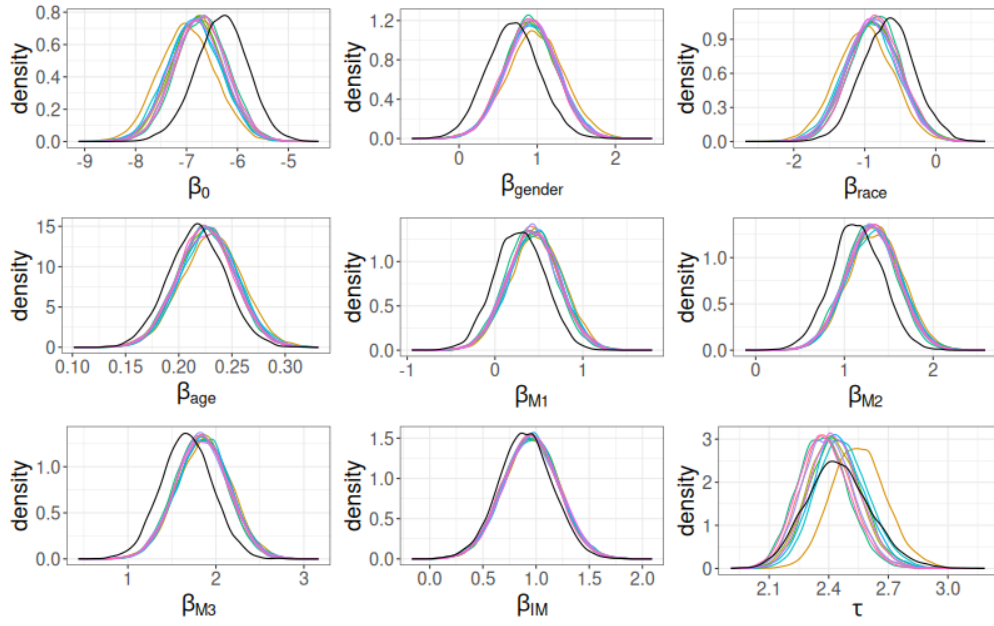


Figure S7: R-VGAL posterior distributions from 10 runs on the Polypharmacy dataset are plotted in colour. Damping is done on the first 10 observations, and the Monte Carlo sample sizes are $S = 500$ and $S_\alpha = 500$. HMC posterior distributions are plotted in black for comparison.

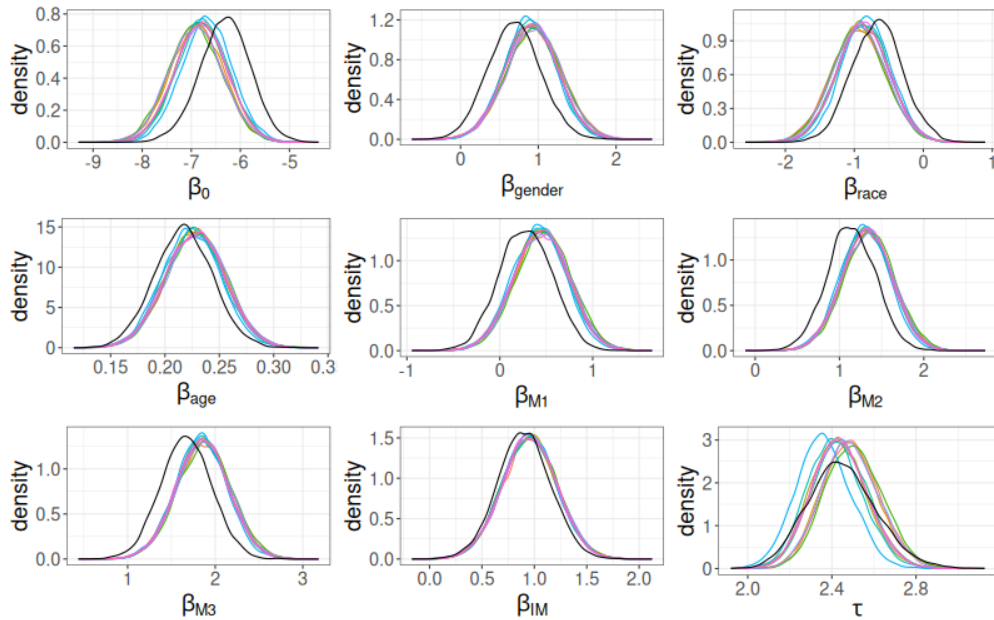


Figure S8: R-VGAL posterior distributions from 10 runs on the Polypharmacy dataset are plotted in colour. Damping is done on the first 10 observations, and the Monte Carlo sample sizes are $S = 1000$ and $S_\alpha = 1000$. HMC posterior distributions are plotted in black for comparison.

As with the previous example, the results in this example also show that increasing the values of S and S_α reduces the variability of the R-VGAL posterior estimates across multiple runs. This phenomenon is particularly pronounced for the random effect standard deviation τ . Suitable values for S and S_α are likely to be application-dependent. However, from our studies, we conclude that S and S_α need to be at least 100 for the Monte Carlo sample sizes not to have a substantial effect on the final estimates.

S3 Robustness check of the R-VGAL algorithm

In this section, we use the Polypharmacy dataset in Sect. 3.4 to check the robustness of the R-VGAL algorithm given different orderings of the data. The simulations in this section show that R-VGAL can be unstable while traversing the first few observations, which makes it sensitive to the ordering of observations. This instability can, however, be alleviated with the damped R-VGAL algorithm, as described in Sect. 2.4 of the main paper.

Figures S9 and S10 show the R-VGAL posterior density estimates from 10 independent runs using the original ordering of the data and a random ordering of the data, respectively. In both simulations, the number of Monte Carlo samples S to estimate the expectation with respect to $q_{i-1}(\boldsymbol{\theta})$ and the number of samples S_α to estimate the gradients/Hessians are fixed to 100. In both figures, the HMC posterior densities for each parameter are plotted in black for comparison. The figures show that the R-VGAL estimates are quite far away from those of HMC estimates when using the original ordering of the data, while the R-VGAL estimates are reasonably close to those of HMC when using the random ordering of the data. This suggests that the R-VGAL estimates are not robust with respect to the ordering of the data.

To confirm that the source of variability in the R-VGAL estimates is from different data orderings and not from the low number of Monte Carlo samples, we increase the number of Monte Carlo samples S and S_α . Figures S11 and S12 show the R-VGAL posterior density estimates from 10 independent runs using the original ordering of the data and a random ordering of the data, respectively, with the Monte Carlo sample sizes set to $S = S_\alpha = 1000$. The posterior densities for each parameter are different for the two orderings; for instance, with the original ordering, the posterior of τ is centred around 4.5, while with the random ordering, the posterior of τ is centred around 2.4.

A plot of the trajectory of the variational mean across R-VGAL iterations reveals that R-VGAL is unstable during the first few iterations. The blue lines in Figures S13 and S14 show the trajectories of the variational mean for each of the parameters across 10 independent runs of the R-VGAL algorithm, on the original

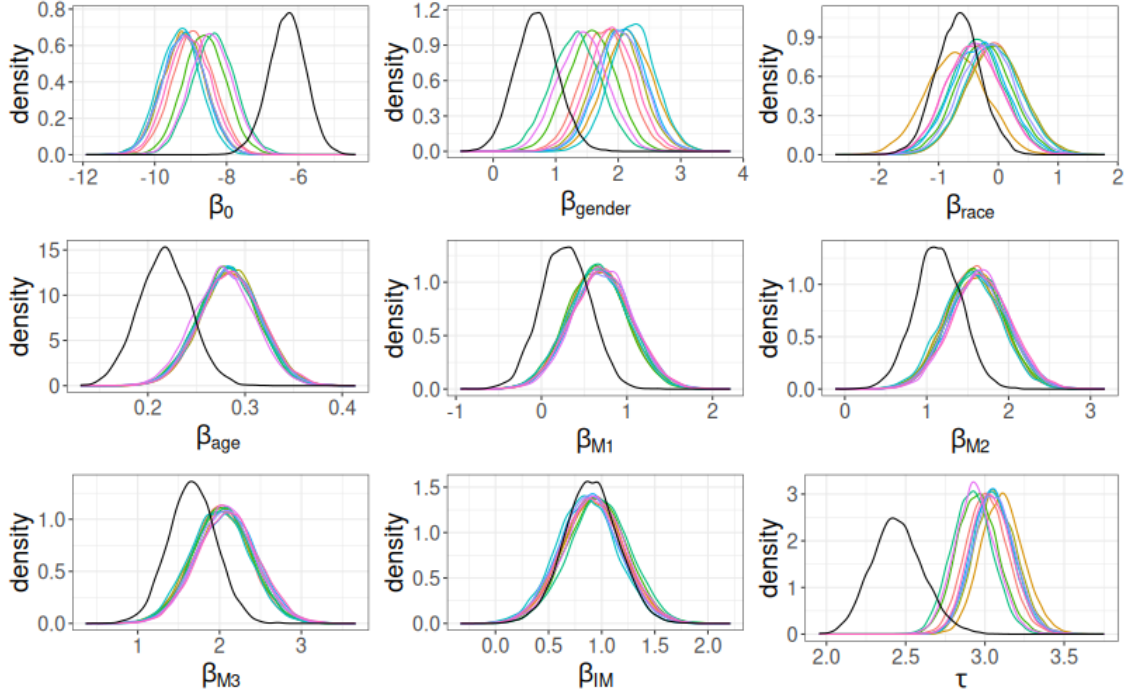


Figure S9: R-VGAL posterior distributions from 10 independent runs using the original ordering of the data are plotted in different colours. The Monte Carlo sample sizes are $S = 100, S_\alpha = 100$. HMC posterior distributions are plotted in black for comparison.

ordering and on a random ordering of the data, respectively. The initial trajectories of the fixed effect parameters in Figure S13 vary significantly (for example, between -50 and 0 for the intercept β_0), and the trajectory of τ is dragged up to nearly 7 before progressively dropping towards 4. This potentially contributes to the biased posterior mean of τ . In Figure S14, where the data were randomly reordered, the trajectories of the parameters are less variable initially, which then allows the variational mean to converge towards the true values more rapidly. This shows that the R-VGAL algorithm is unstable while traversing the first few observations, making the algorithm sensitive to the ordering of the data.

We propose a damping approach (in Sect. 2.4 of the main paper) to make the R-VGAL algorithm more robust. By damping the first few observations, the R-VGAL posterior estimates become much more consistent across different data orderings. Figures S15 and S16 show the posterior density estimates from 10 independent runs of the R-VGAL algorithm using the original ordering of the data and a random ordering of the data, respectively, with damping done on the first 10 observations, and with Monte Carlo sample sizes $S = S_\alpha = 100$. These figures show that the posterior density estimates of R-VGAL with damping are consistent across two different orderings of the data, and also consistent with those obtained from HMC.

Figures S17 and S18 display the R-VGAL posterior densities using the original ordering and the random

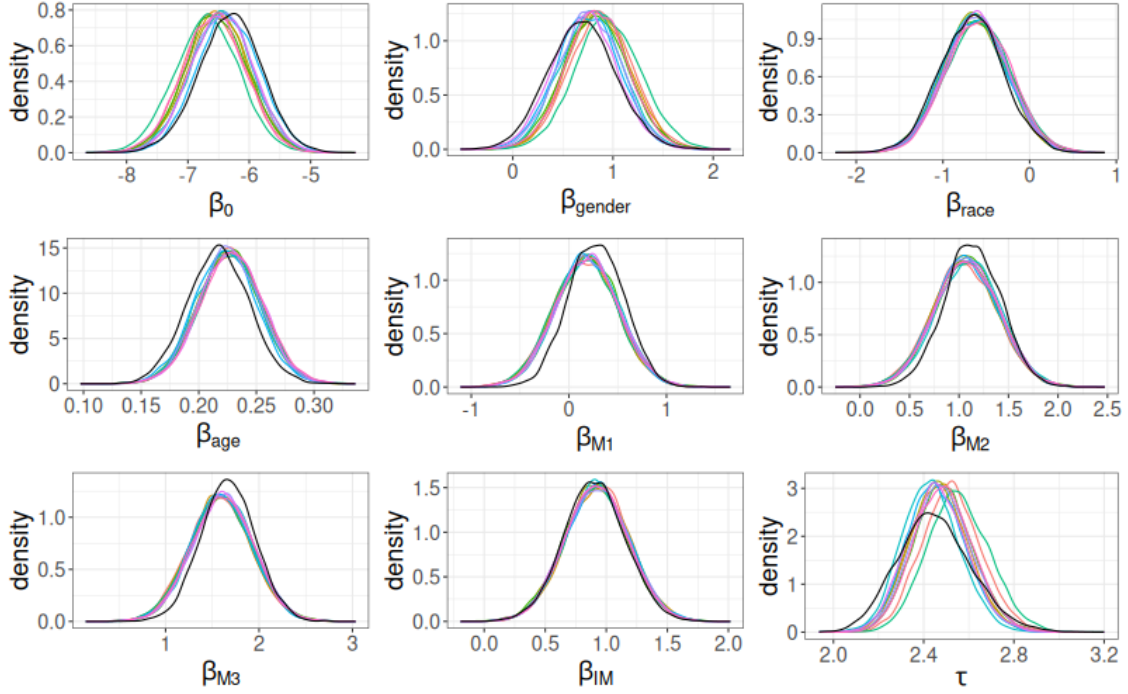


Figure S10: R-VGAL posterior distributions from 10 independent runs using the random ordering of the data are plotted in different colours. The Monte Carlo sample sizes are $S = 100$, and $S_\alpha = 100$. HMC posterior distributions are plotted in black for comparison.

ordering of the data, respectively, with damping done on the first 10 observations, and Monte Carlo sample sizes increased to $S = S_\alpha = 1000$. There is now very little difference between the posterior densities using the original and the random ordering of the dataset. The red lines in Figures S13 and S14 show the parameter trajectories obtained from damped R-VGAL, on the original ordering and the random ordering of the data, respectively. The trajectories with damping (plotted in red) are much more stable than those without damping (plotted in blue), especially during the first few iterations. These figures suggest that damping is effective in reducing the variability of R-VGAL estimates while traversing the first few observations and increases the algorithm's robustness to different data orderings. Other random orderings of the data give similar results.

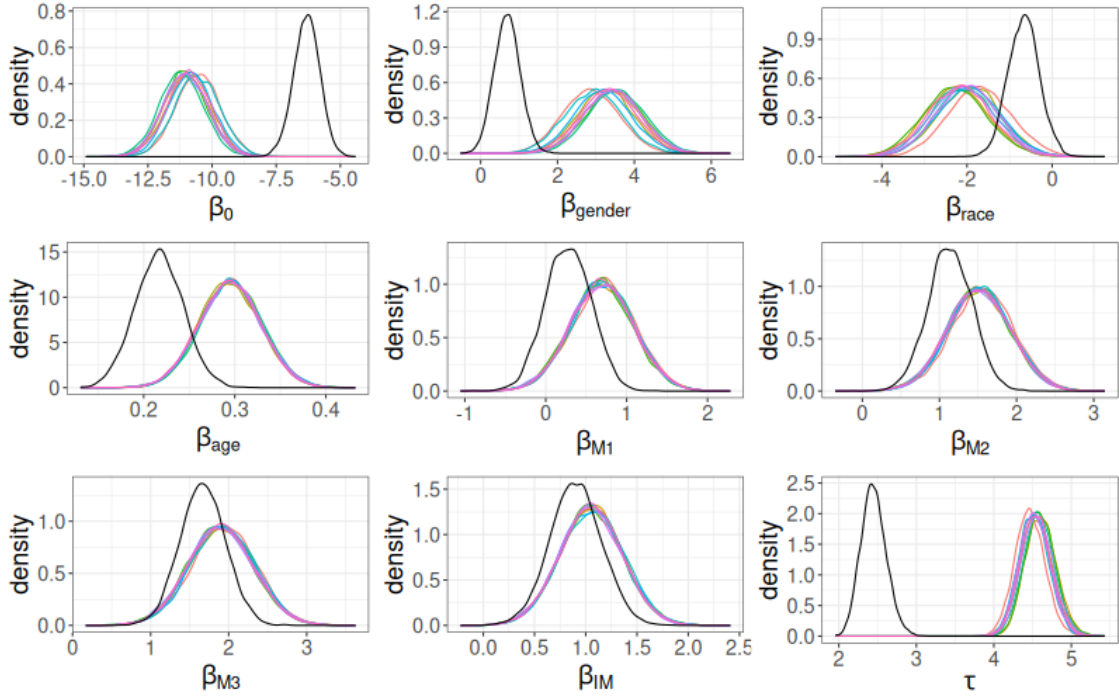


Figure S11: R-VGAL posterior distributions from 10 independent runs using the original ordering of the data are plotted in colour. The Monte Carlo sample sizes are $S = 1000$, $S_\alpha = 1000$. HMC posterior distributions are plotted in black for comparison.

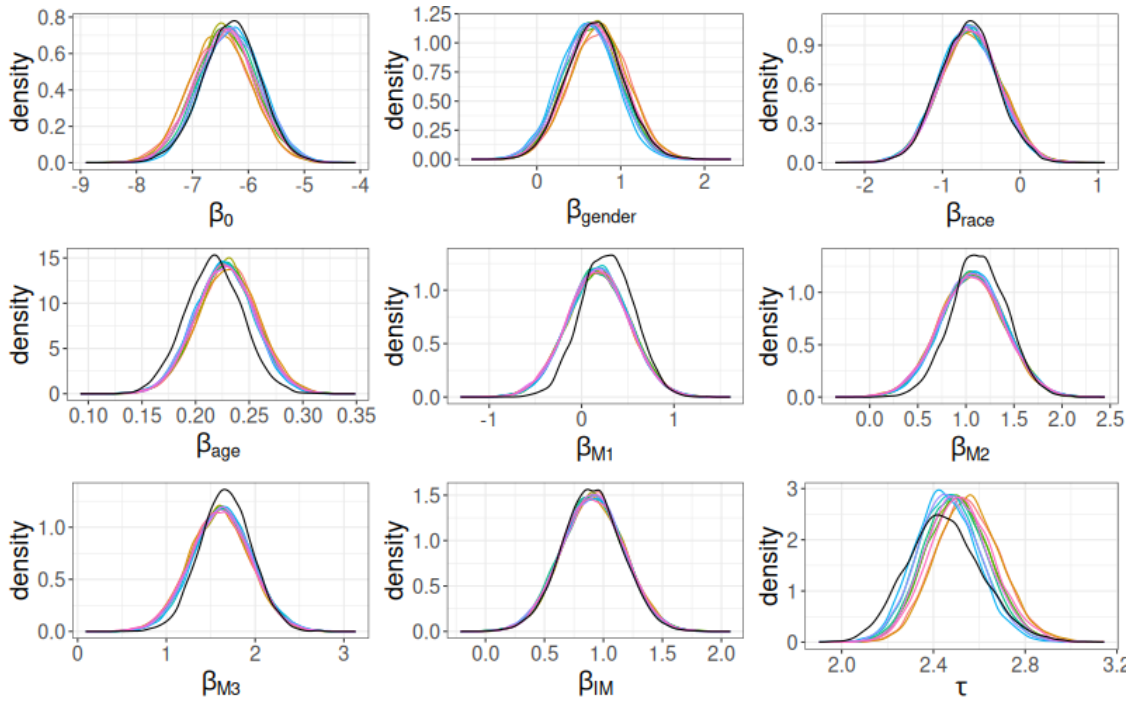


Figure S12: R-VGAL posterior distributions from 10 independent runs using the random ordering of the data are plotted in colour. The Monte Carlo sample sizes are $S = 1000$, $S_\alpha = 1000$. HMC posterior distributions are plotted in black for comparison.

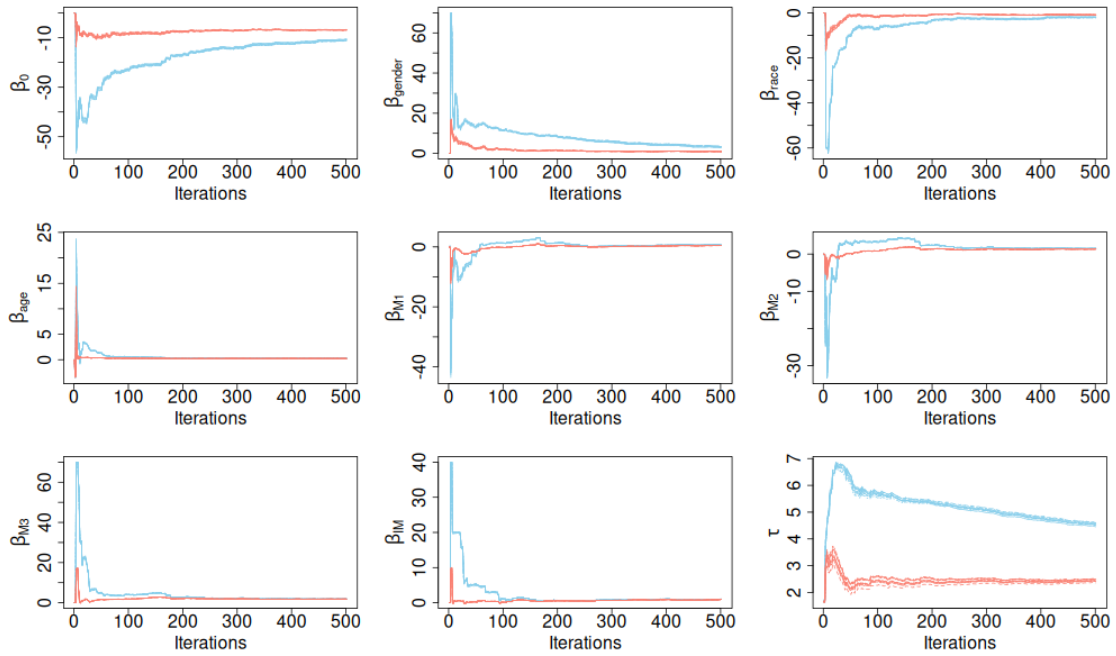


Figure S13: Trajectories of the variational mean without damping (in blue) and with damping (in red) for each parameter across 10 independent runs of R-VGAL on the original ordering of the data. The Monte Carlo sample sizes are $S = 1000$ and $S_\alpha = 1000$.

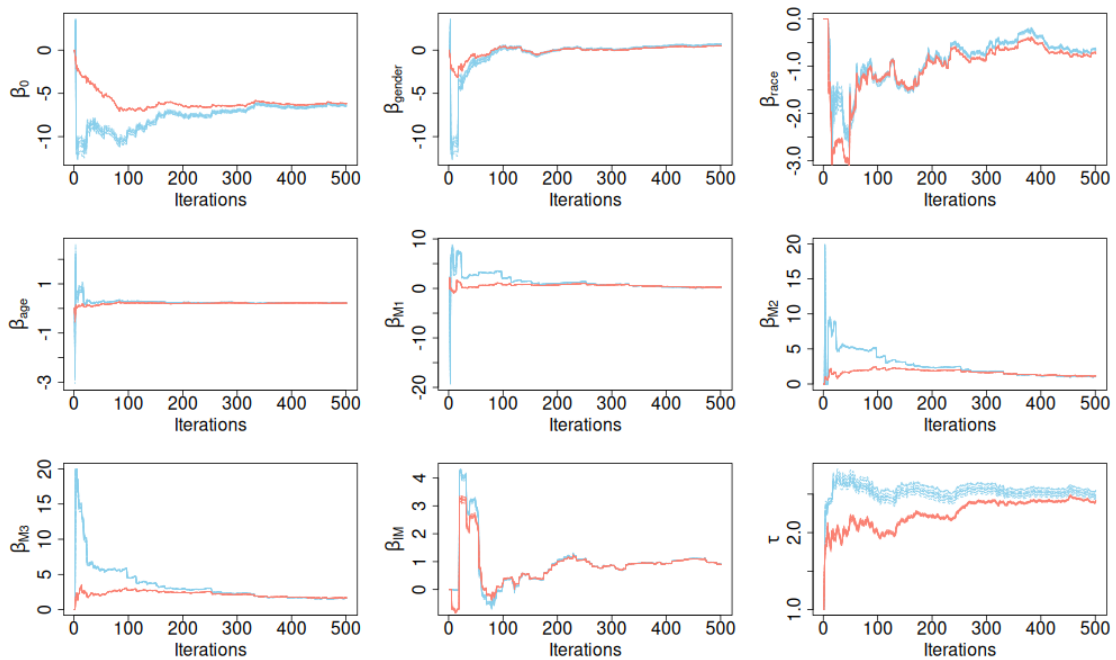


Figure S14: Trajectories of the variational mean without damping (in blue) and with damping (in red) for each parameter across 10 independent runs of R-VGAL on the random ordering of the data. The Monte Carlo sample sizes are $S = 1000$ and $S_\alpha = 1000$.

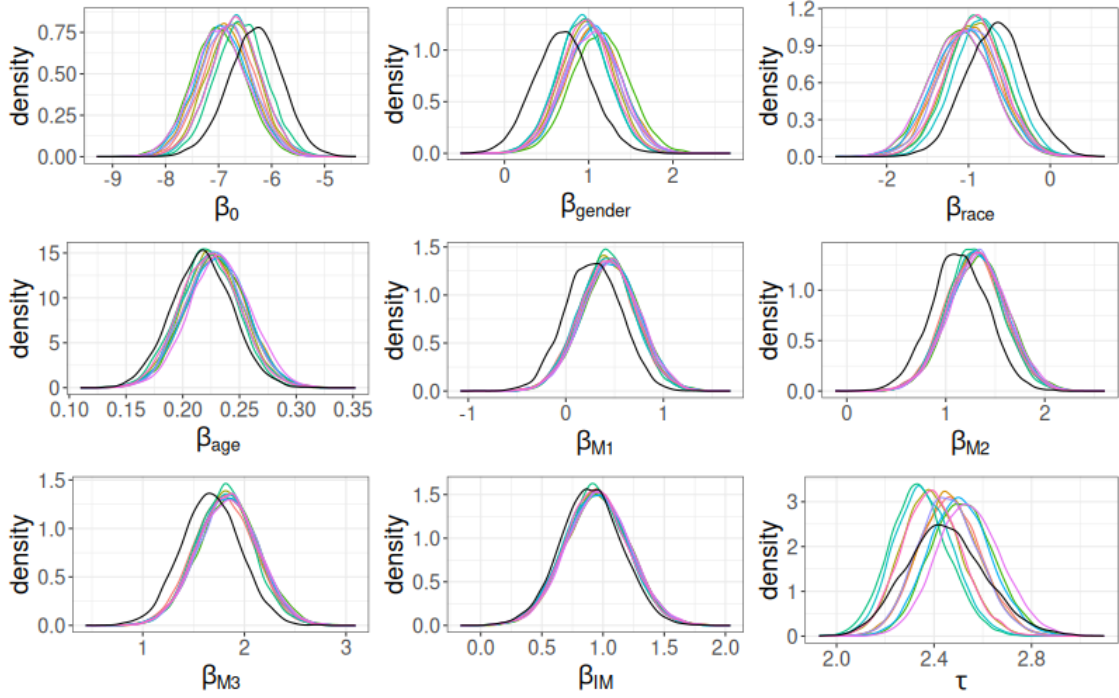


Figure S15: R-VGAL posterior distributions from 10 independent runs using the original ordering of the data are plotted in colour. Damping is done on the first 10 observations. The Monte Carlo sample sizes are $S = 100, S_\alpha = 100$. HMC posterior distributions are plotted in black for comparison.

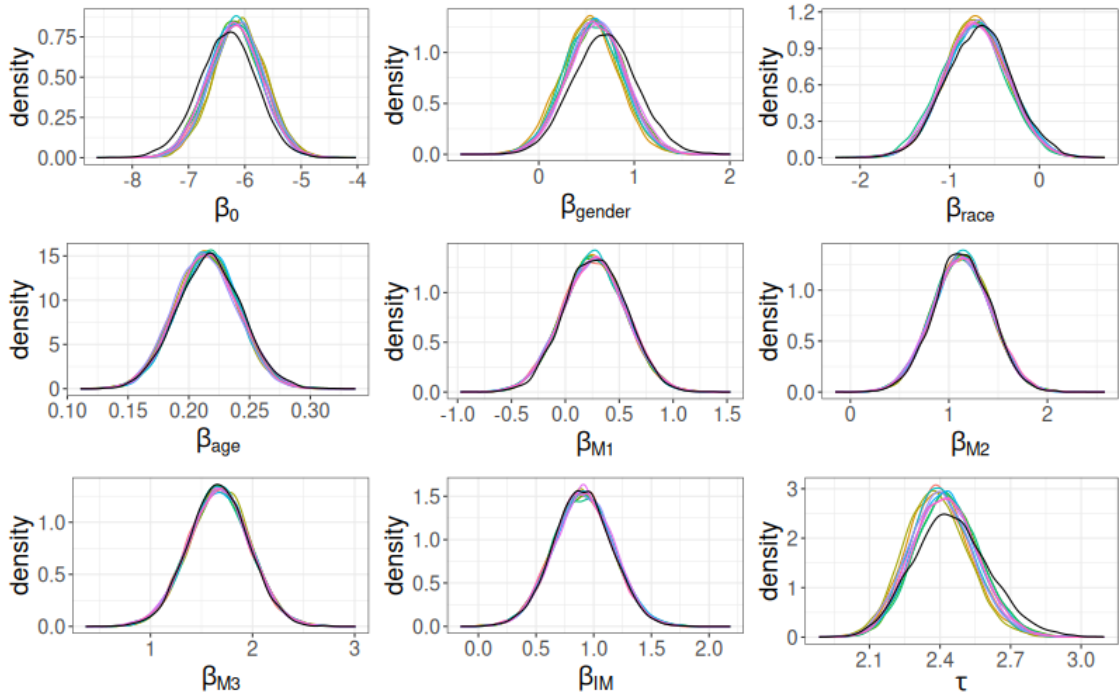


Figure S16: R-VGAL posterior distributions from 10 independent runs using a random reordering of the data are plotted in colour. Damping is done on the first 10 observations. The Monte Carlo sample sizes are $S = 100, S_\alpha = 100$. HMC posterior distributions are plotted in black for comparison.

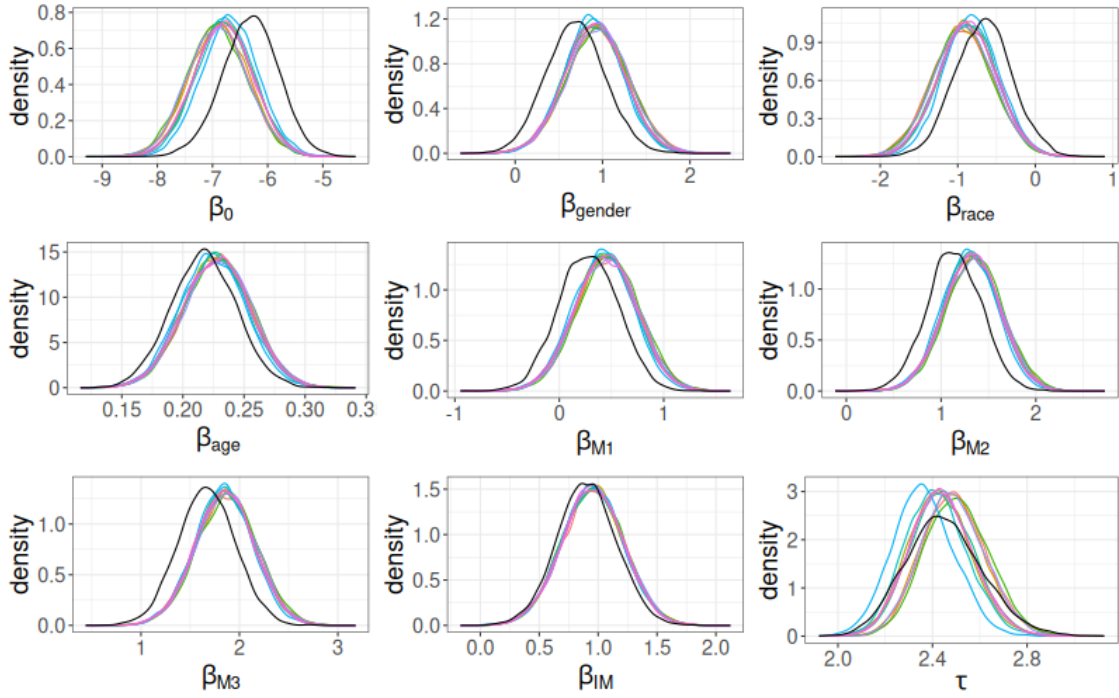


Figure S17: R-VGAL posterior distributions from 10 independent runs using the original ordering of the data are plotted in colour. Damping is done on the first 10 observations. The Monte Carlo sample sizes are $S = 1000, S_\alpha = 1000$. HMC posterior distributions are plotted in black for comparison.

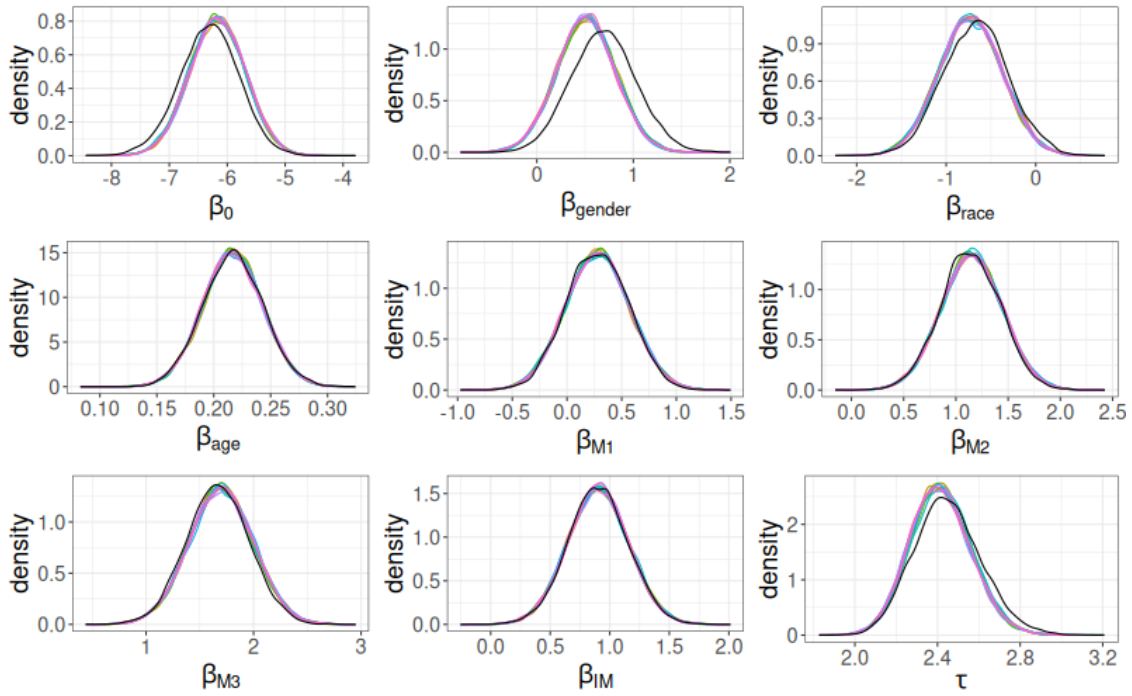


Figure S18: R-VGAL posterior distributions from 10 independent runs using a random reordering of the data are plotted in colour. Damping is done on the first 10 observations. The Monte Carlo sample sizes are $S = 1000, S_\alpha = 1000$. HMC posterior distributions are plotted in black for comparison.

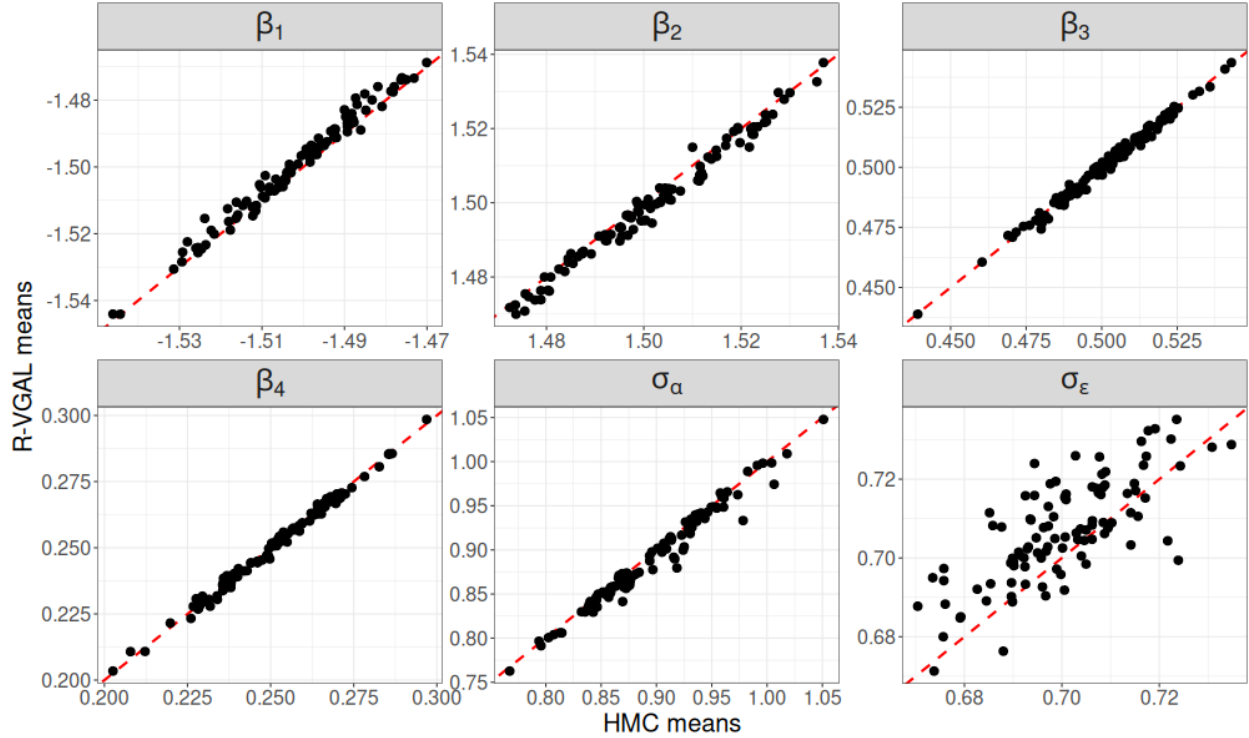


Figure S19: Plot of the R-VGAL posterior means against those from HMC for 100 datasets simulated from the linear mixed model.

S4 Repeated simulations

In this section, for each of the linear, logistic and Poisson mixed models, we simulate 100 datasets with the same parameter settings. We run R-VGAL and HMC on each of the 100 datasets, and compare their posterior density estimates.

S4.1 Repeated simulations from the linear mixed model

The synthetic datasets in this section are simulated according to the number of observations and parameter values detailed in Sect. 3.1. Figure S19 plots the R-VGAL posterior means against those from HMC for each of the 100 simulated datasets. The red dotted diagonal line marks the “ideal” scenario where the posterior means from the two methods are equal. Figure S20 plots the ratio between the R-VGAL and HMC posterior standard deviations, with the dotted horizontal line marking the ideal ratio of one. Figure S21 compares the distribution of the differences between the R-VGAL means and the true parameter values to the distribution of the differences between the HMC means and the true parameter values. We see that posterior means and standard deviations from the two methods are very similar across the 100 replicated datasets.

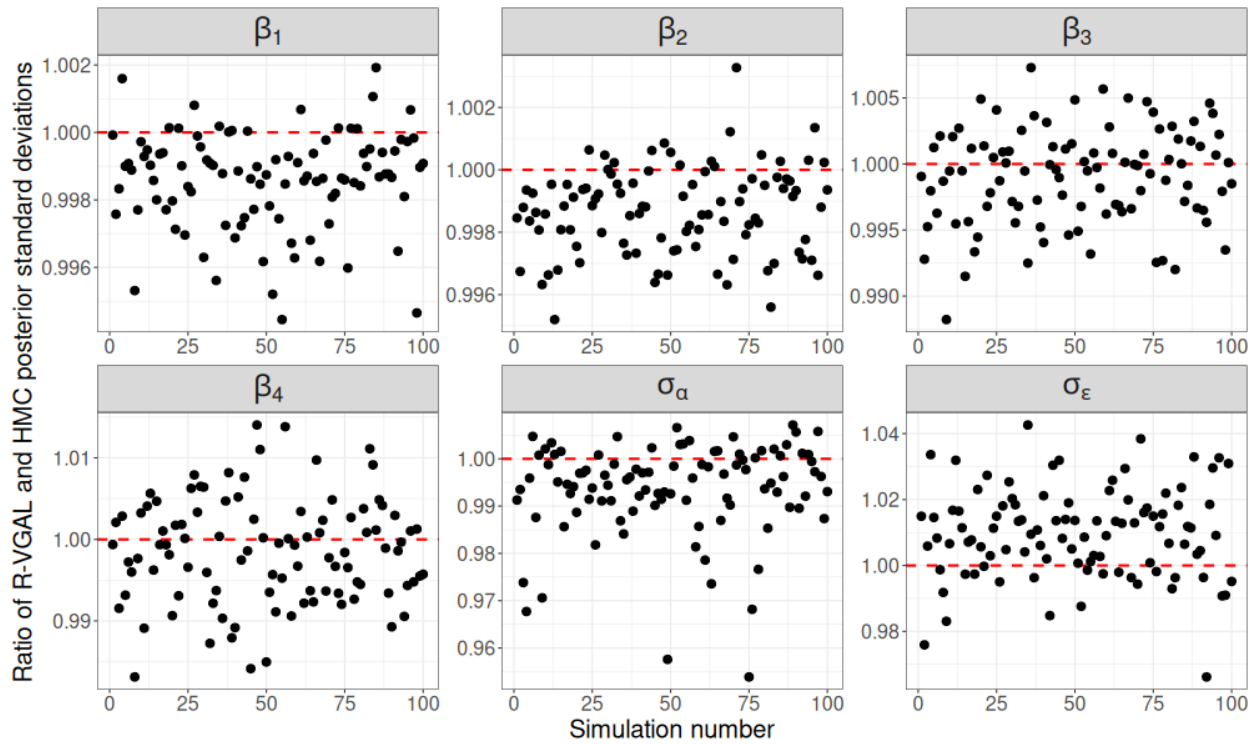


Figure S20: Plot of the ratio between the R-VGAL posterior standard deviations and those from HMC for 100 datasets simulated from the linear mixed model.

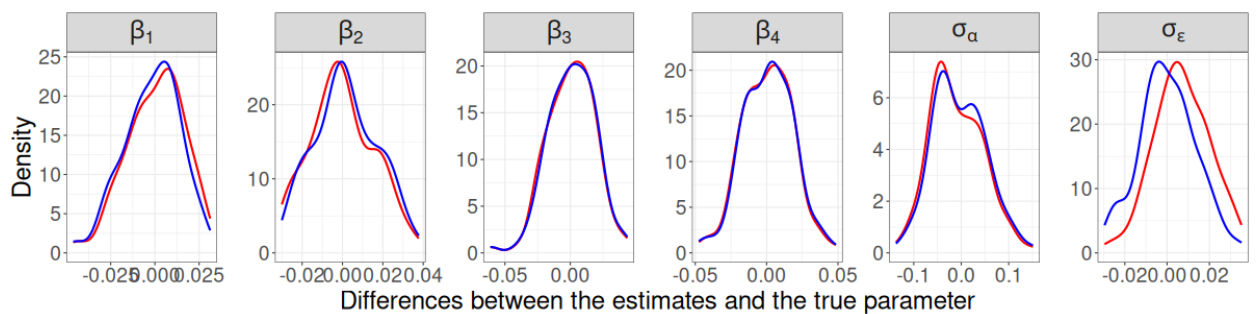


Figure S21: Comparison of the distribution of the differences between the R-VGAL posterior means and the true parameters (in red), against the distribution of the differences between the HMC posterior means and the true parameters (in blue), for 100 datasets simulated from the linear mixed model.

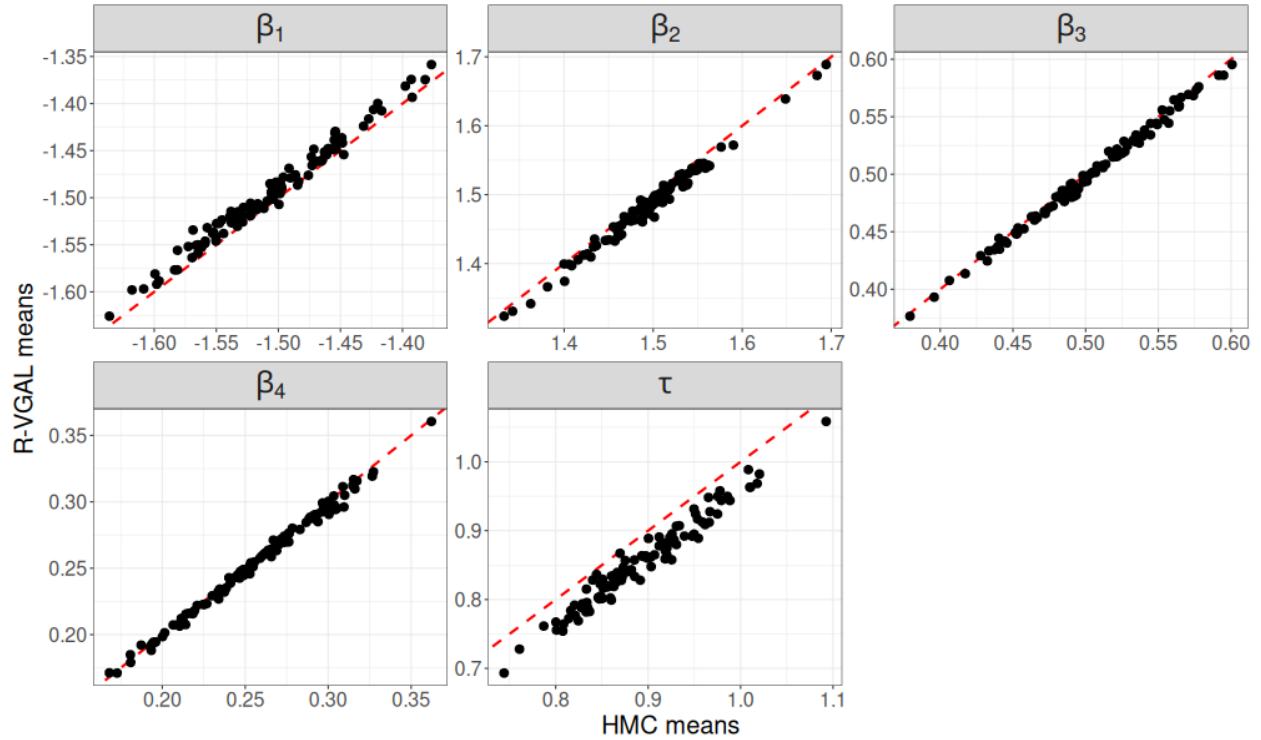


Figure S22: Plot of the R-VGAL posterior means against those from HMC for 100 datasets simulated from the logistic mixed model.

S4.2 Repeated simulations from the logistic mixed model

The synthetic datasets in this section are simulated according to the number of observations and parameter values detailed in Sect. 3.2. As with the previous section, we present plots comparing the R-VGAL and HMC posterior means in Figure S22, the ratio between the R-VGAL and HMC posterior standard deviations in Figure S23, and the distributions of the differences between each method's posterior mean estimates and the true parameters in Figure S24. The R-VGAL and HMC posterior means are similar, though R-VGAL tends to slightly underestimate the random effect variance when compared to HMC.

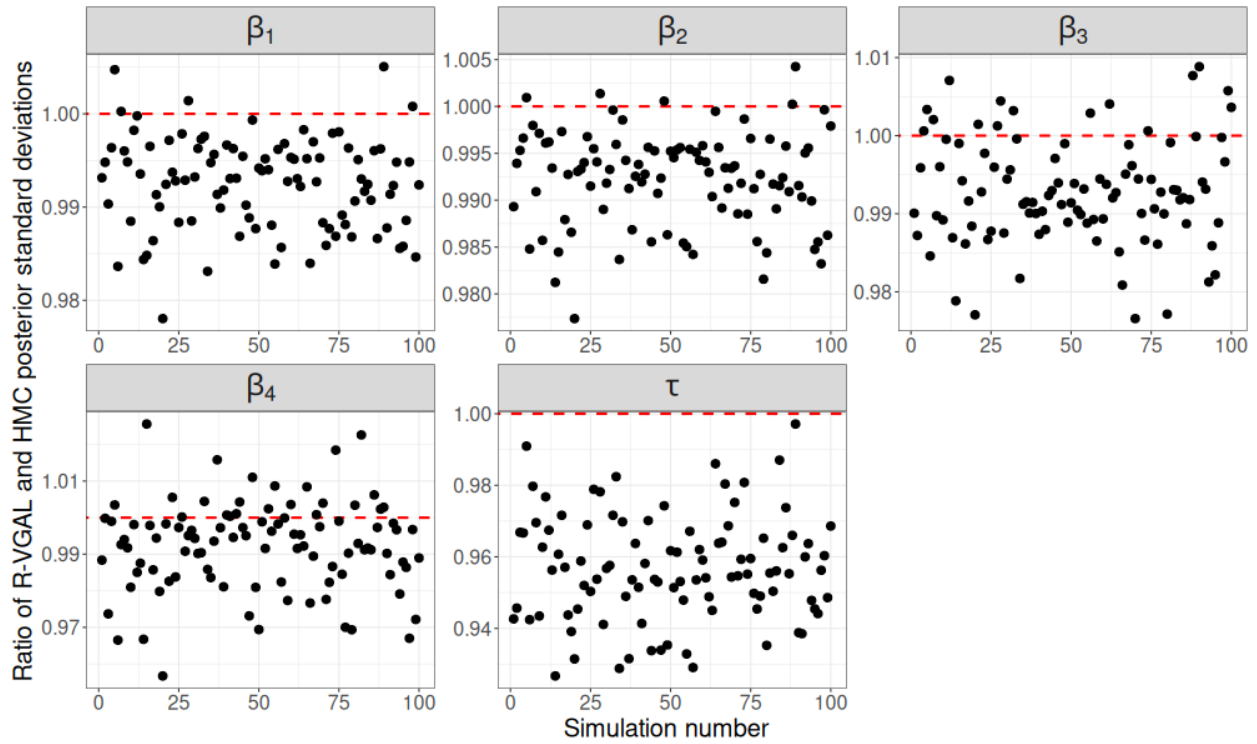


Figure S23: Plot of the ratio between the R-VGAL posterior standard deviations and those from HMC for 100 datasets simulated from the logistic mixed model.

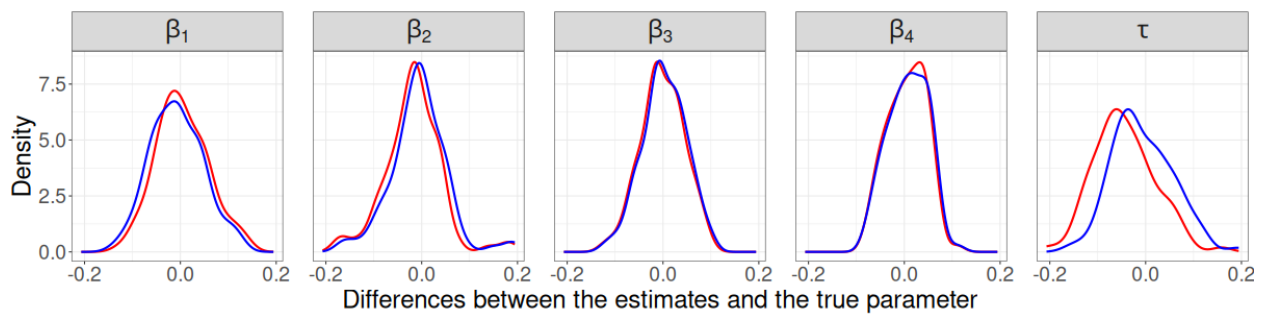


Figure S24: Comparison of the distribution of the differences between the R-VGAL posterior means and the true parameters (in red), against the distribution of the differences between the HMC posterior means and the true parameters (in blue), for 100 datasets simulated from the logistic mixed model.

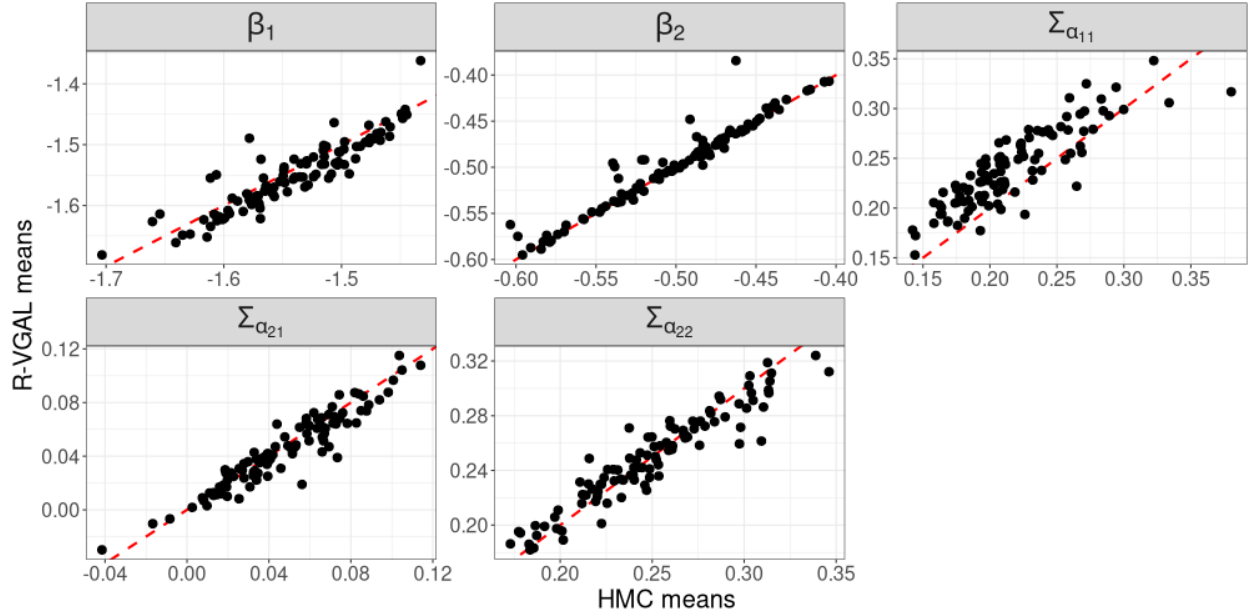


Figure S25: Plot of the R-VGAL and HMC posterior means for 100 datasets simulated from the Poisson mixed model.

S4.3 Repeated simulations on the Poisson mixed model

The synthetic datasets in this section are simulated according to the number of observations and parameter values detailed in Sect. 3.3. As with the previous sections, we present plots comparing the R-VGAL and HMC posterior means in Figure S25, the ratio between the R-VGAL and HMC posterior standard deviations in Figure S26, and the distributions of the differences between each method’s posterior mean estimates and the true parameters in Figure S27. The R-VGAL and HMC posterior means and standard deviations are quite similar across simulations, although R-VGAL has a mild tendency for overestimating the parameter $\Sigma_{\alpha_{11}}$ and underestimating the posterior variance of $\Sigma_{\alpha_{11}}$ and $\Sigma_{\alpha_{22}}$ compared to HMC.

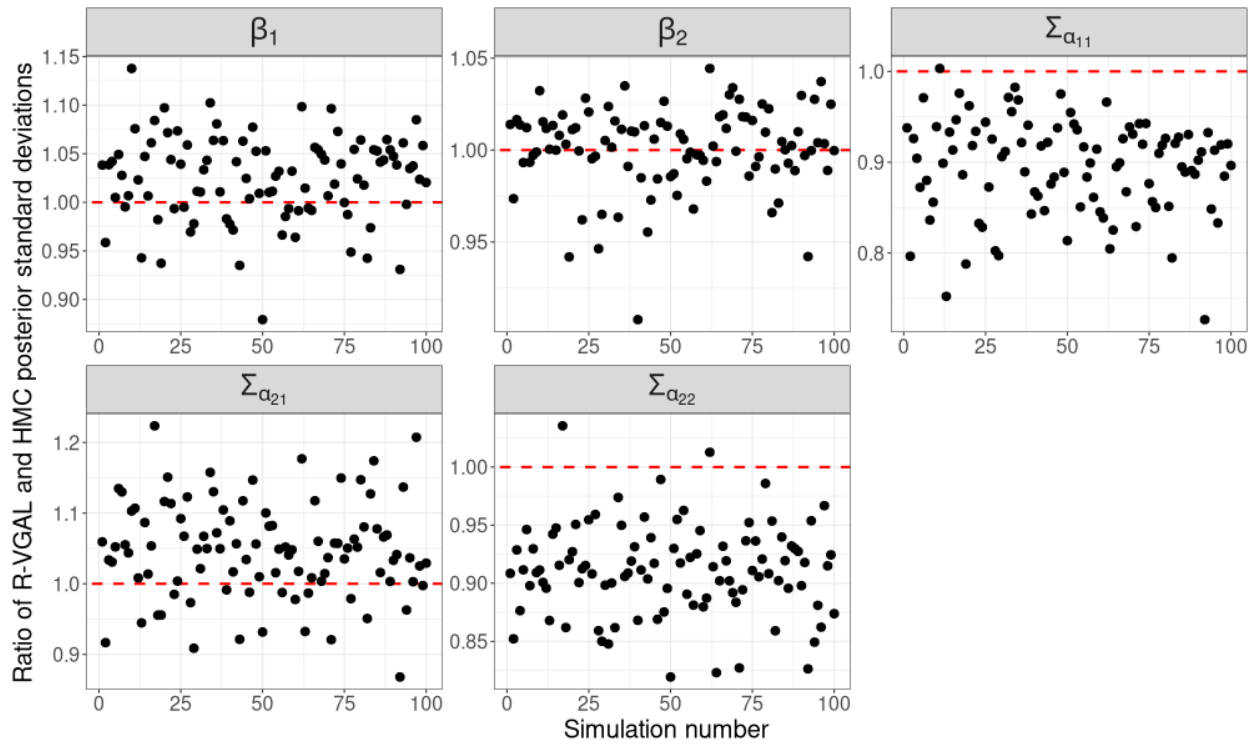


Figure S26: Plot of the ratio between the R-VGAL and HMC posterior standard deviations for 100 datasets simulated from the Poisson mixed model.

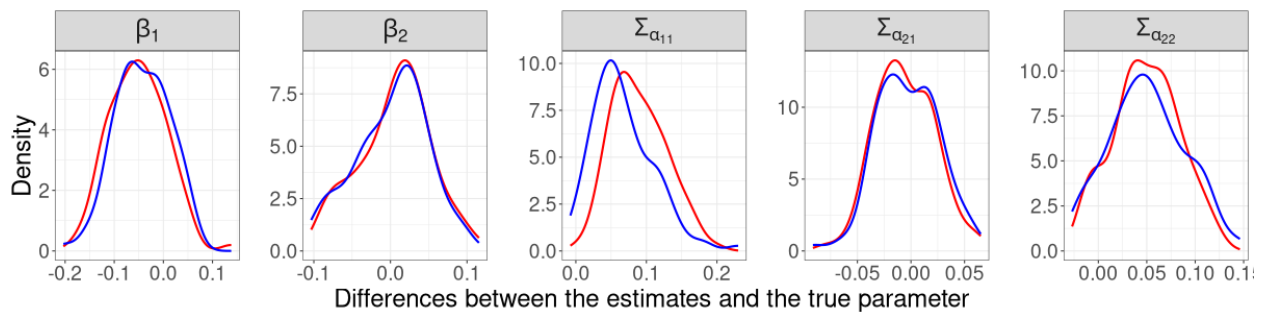


Figure S27: Comparison of the distribution of the differences between the R-VGAL posterior means and the true parameters (in red), against the distribution of the differences between the HMC posterior means and the true parameters (in blue), for 100 datasets simulated from the Poisson mixed model.

S5 Convergence statistics for HMC

This section contains some statistics on the convergence of HMC in the simulated and real data examples in Sect. 3. In particular, we show the effective sample size (ESS) and \hat{R} values obtained from the `RStan` diagnostics. The ESS is a measure of the number of uncorrelated posterior samples, and the higher the ESS the better; see Gelman et al. (2013) for further details on how STAN calculates ESS. The \hat{R} statistic proposed by Gelman and Rubin (1992) measures the ratio of the average variance of samples within each chain to the variance of the pooled samples across chains; an \hat{R} close to 1 indicates that the chains have converged. Gelman and Rubin (1992) recommends that the independent Markov chains be initialized with diffuse starting values for the parameters and sampled until all values for \hat{R} are below 1.1.

The ESS and \hat{R} values for each parameter in each of the examples we considered in Sect. 3 are shown in Table S1.

Example	Parameter	ESS	\hat{R}
Linear	β_1	42590.45	0.9999355
Linear	β_2	46091.76	0.9999275
Linear	β_3	45614.94	0.9999371
Linear	β_4	44814.06	0.9999292
Linear	σ_α	39572.87	0.9999377
Linear	σ_ϵ	36754.35	0.9999034
Logistic	β_1	14116.662	1.0002822
Logistic	β_2	12974.649	1.0000641
Logistic	β_3	26374.149	1.0001275
Logistic	β_4	31828.214	0.9999238
Logistic	τ	3700.836	1.0004196
Poisson	β_1	14313.12	1.0000291
Poisson	β_2	14433.41	1.0001494
Poisson	$\Sigma_{\alpha_{11}}$	20022.85	1.0000592
Poisson	$\Sigma_{\alpha_{21}}$	17313.42	1.0004479
Poisson	$\Sigma_{\alpha_{22}}$	19660.59	0.9999396
Six City	β_1	2041.219	1.0001195
Six City	β_2	21906.059	0.9999014
Six City	β_3	6902.207	0.9999044
Six City	τ	1406.197	1.0007235
Polypharmacy	β_0	8724.835	1.0001990
Polypharmacy	β_{gender}	7868.562	1.0003835
Polypharmacy	β_{race}	8810.641	1.0000568
Polypharmacy	β_{age}	17864.738	1.0000620
Polypharmacy	β_{M1}	17248.489	0.9999448
Polypharmacy	β_{M2}	15052.711	1.0000169
Polypharmacy	β_{M3}	14499.271	0.9999639
Polypharmacy	β_{IM}	31828.214	0.9999535
Polypharmacy	τ	37289.351	1.0001344

Table S1: Effective sample size and \hat{R} values for the parameters in each model.

S6 Additional examples

This section contains two additional examples: the first one applies the Poisson model in Sect. 3.3 of the main paper to the Epilepsy dataset from Thall and Vail (1990), and the second involves a bigger synthetic dataset simulated from the logistic mixed model in Sect. 3.2 of the main paper.

S6.1 Real data example: Poisson mixed model

In this example, we apply R-VGAL on the well-known Epilepsy dataset from Thall and Vail (1990). This dataset includes $N = 59$ epileptic patients who were treated with either a new drug (Progabide) or placebo in a clinical trial. The response variable is the number of seizures patients have during $n = 4$ follow-up periods. We index the patients as $i = 1, \dots, N$ and the responses for each patient as $j = 1, \dots, n$. We follow Tan and Nott (2018) and use the following covariates: the logarithm of 1/4 the number of baseline seizures (**Base**); the **Treatment**, coded as 1 for Progabide and 0 for placebo; the log-transformed and centred age, $\widetilde{\text{Age}}_i = \text{Age}_i - \frac{1}{N} \sum_{i=1}^N (\text{Age}_i)$, where Age_i is the logarithm of the age of the i th individual; and the follow up period, **Visit**, coded as **Visit** = -0.3 for the first visit, **Visit** = -0.1 for the second, **Visit** = 0.1 for the third and **Visit** = 0.3 for the fourth.

We consider the following model with random slope and random intercept:

$$y_{ij} \sim \text{Poisson}(\lambda_{ij}), \quad (\text{S45})$$

$$\log(\lambda_{ij}) = \beta_0 + \beta_{\text{base}} \text{Base}_i + \beta_{\text{treatment}} \text{Treatment}_i + \beta_{\text{age}} \widetilde{\text{Age}}_i + \beta_{\text{visit}} \text{Visit}_{ij} + \alpha_{i,1} + \alpha_{i,2} \text{Visit}_{ij}, \quad (\text{S46})$$

where $\boldsymbol{\alpha} \equiv (\alpha_{i,1}, \alpha_{i,2})^\top \sim \text{Gau}(\mathbf{0}, \boldsymbol{\Sigma}_\alpha)$, with $\boldsymbol{\Sigma}_\alpha = \mathbf{L}\mathbf{L}^\top$ and $\mathbf{L} = \begin{bmatrix} \exp(\zeta_{11}) & 0 \\ \zeta_{21} & \exp(\zeta_{22}) \end{bmatrix}$. In the algorithm, we consider the unconstrained parameters $\boldsymbol{\theta} = (\boldsymbol{\beta}^\top, \boldsymbol{\zeta}^\top)^\top$, where $\boldsymbol{\beta} \equiv (\beta_0, \beta_{\text{base}}, \beta_{\text{treatment}}, \beta_{\text{age}}, \beta_{\text{visit}})^\top$ and $\boldsymbol{\zeta} \equiv (\zeta_{11}, \zeta_{22}, \zeta_{21})^\top$. The gradient $\nabla_{\boldsymbol{\theta}} \log p(\mathbf{y}_i, \boldsymbol{\alpha}_i | \boldsymbol{\theta})$ and Hessian $\nabla_{\boldsymbol{\theta}}^2 \log p(\mathbf{y}_i, \boldsymbol{\alpha}_i | \boldsymbol{\theta})$, which are necessary in the computation of the gradient and Hessian of the subject-specific log likelihood $\log p(\mathbf{y}_i | \boldsymbol{\theta})$, are provided in Sect. S1.3 of the online supplement.

The initial variational distribution we use is

$$p(\boldsymbol{\theta}) = q_0(\boldsymbol{\theta}) = \text{Gau} \left(\begin{bmatrix} \mathbf{0} \\ \mathbf{0} \end{bmatrix}, \begin{bmatrix} \mathbf{I}_2 & \mathbf{0}_{2 \times 3} \\ \mathbf{0}_{3 \times 2} & 0.1\mathbf{I}_3 \end{bmatrix} \right).$$

Using a $\text{Gau}(0, 0.1)$ prior distribution for ζ_{11} , ζ_{22} and ζ_{21} leads to having 2.5th and 97.5th percentiles of

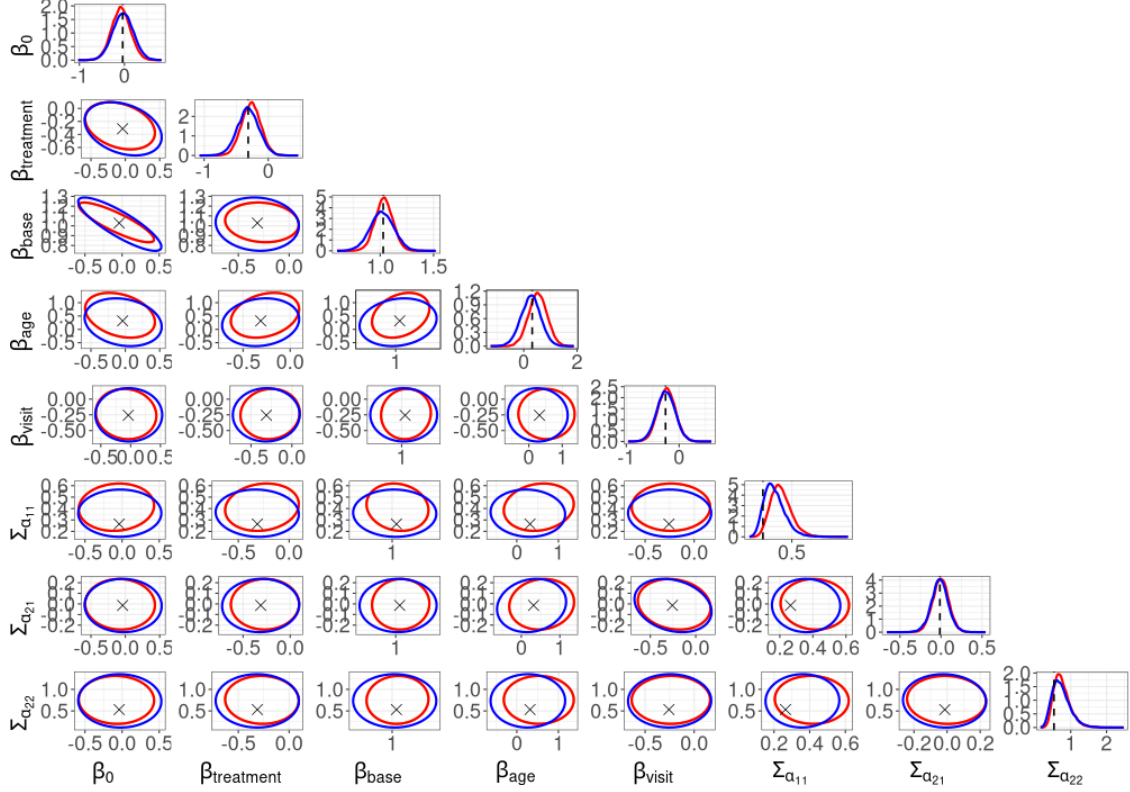


Figure S28: Exact posterior distributions from HMC (in blue) and approximate posterior distributions from R-VGAL with estimated gradients and Hessians (in red) for the Poisson mixed model experiment. Diagonal panels: Marginal posterior distributions with the maximum likelihood estimates marked using dotted lines. Off-diagonal panels: Bivariate posterior distributions with the maximum likelihood estimates marked using the symbol \times .

(0.290, 3.485) for $\Sigma_{\alpha_{11}}$, (0.342, 3.577) for $\Sigma_{\alpha_{22}}$, and (-0.713, 0.713) for the off-diagonal entries $\Sigma_{\alpha_{21}}$ and $\Sigma_{\alpha_{12}}$.

As with the simulated Poisson model in Sect. 3.3, we run damped R-VGAL with $n_{damp} = 10$ observations and $K = 4$ steps per observation. We use $S_\alpha = 200$ Monte Carlo samples in the importance sampling step, and $S = 200$ samples to approximate the expectations with respect to $q_{i-1}(\theta)$ in the R-VGAL updates of the variational mean and the precision matrix. Figure S28 shows the marginal posterior distributions with maximum likelihood estimates of the parameters, along with bivariate posterior distributions as estimated using R-VGAL and HMC. We find that the estimates from R-VGAL and HMC agree quite well for all parameters, and posterior modes for all parameters from both methods are close to the maximum likelihood estimates.

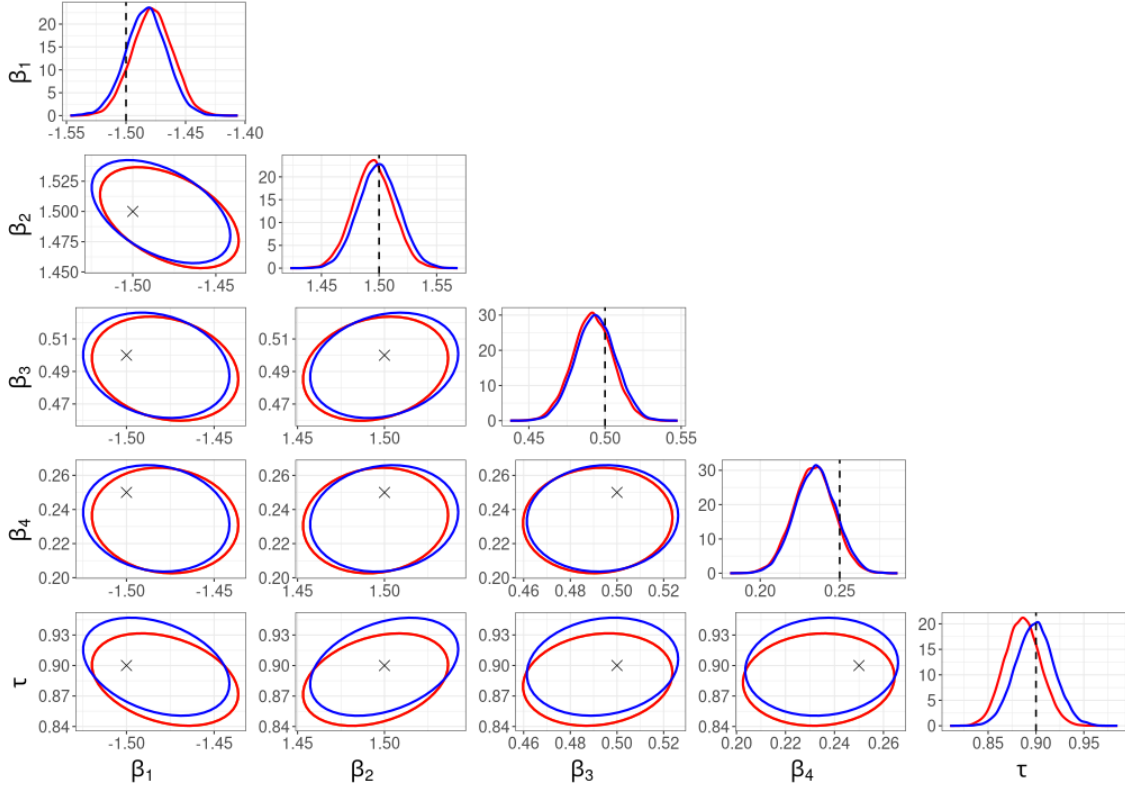


Figure S29: Exact posterior distributions from HMC (in blue) and approximate posterior distributions from R-VGAL with estimated gradients and Hessians (in red) for the logistic mixed model experiment with 50000 observations. Diagonal panels: Marginal posterior distributions with true parameters denoted using dotted lines. Off-diagonal panels: Bivariate posterior distributions with true parameters denoted using the symbol \times .

S6.2 Big data example: Logistic mixed model

For this experiment, we simulate data from the logistic mixed model in Sect. 3.2 with $N = 5000$ and $n = 10$, resulting in a total of 50000 observations. We find that it is necessary to increase the number of Monte Carlo samples to $S = 200$ and $S_\alpha = 200$ to achieve accurate posterior estimates in this example. The prior distribution and the settings for damping in R-VGAL are kept the same as in the example in Sect. 3.2.

Figure S29 shows the marginal posterior densities, along with bivariate posterior plots from R-VGAL and HMC. As with previous simulations, the posterior distributions obtained using R-VGAL are very similar to those obtained using HMC.

S7 Application of R-VGAL to models with other random effect structures

In the main paper, we considered the application of R-VGAL to models where the random effects are correlated within subjects (individuals), but independent between subjects. In practice, there are many cases where other random effect structures, such as crossed or nested random effects, are needed; see Pinheiro and Bates (2006); Gelman and Hill (2007); West et al. (2014) or Papaspiliopoulos et al. (2023) for examples. Here, we briefly discuss the application of R-VGAL to some classes of models with crossed or nested random effects. The implementation of R-VGAL to these models is left for future endeavours.

Models with crossed effects are often used to model data that can be organised in the form of contingency tables between categorical variables. For example, consider a study of annual income, in which a number of characteristics from participants are recorded using categorical variables, such as their age range, sex, ethnicity, and highest level of education. In this case, the data can be organised into a multi-dimensional contingency table between age range, sex, ethnicity, and level of education. Participants who have the same combination of characteristics may have similar income levels, and the correlation between people in the same set of categories may be modelled with the addition of category-specific random effects.

The notation we use in the following crossed effect model follows that in Chapter 11 of Gelman and Hill (2007) and Sect. 2 of Papaspiliopoulos et al. (2023). Suppose that there are K categorical variables, and the k th variable has L_k levels, for $k = 1, \dots, K$. The logarithm of the income of the i th individual may then be modelled as

$$y_i = \mathbf{x}_i^\top \boldsymbol{\beta} + \sum_{k=1}^K \alpha_{l_k[i]}^{(k)} + \epsilon_i, \quad \alpha_l^{(k)} \sim \text{Gau}(0, \sigma_\alpha^2), \quad \epsilon_i \sim \text{Gau}(0, \sigma_\epsilon^2), \quad (\text{S47})$$

for $i = 1, \dots, N$, where \mathbf{x}_i denotes a vector of covariates associated with the fixed effects $\boldsymbol{\beta}$, and $\alpha_l^{(k)}$ denotes the random effect associated with the l th level of the k th categorical variable. The notation $l_k[i]$ denotes the level of the k th category that the i th individual falls into; for example, if the first categorical variable in the model is age range, where the categories are 1 for 18–30 years old, 2 for 30–50 years old, and 3 for 50 years old and above, then $l_1[4] = 2$ means that the 4th individual in the dataset is in level 2 of the “age” variable (between 30 and 50 years old). Here we have assumed that the random effects $\alpha_l^{(k)}$ have the same variance for all $l = 1, \dots, L$ and $k = 1, \dots, K$. Thus the parameters of interest in this model are $\boldsymbol{\theta} = (\boldsymbol{\beta}^\top, \sigma_\alpha^2, \sigma_\epsilon^2)^\top$.

In this model, there are $G = L_1 \times L_2 \times \dots \times L_K$ combinations of levels. The R-VGAL updates would therefore be based on the log-likelihood of all individuals within the same combination (group). For each combination

(group) $g = 1, \dots, G$, the vector of responses of people in this group is denoted as \mathbf{y}_g . Then for each group $g = 1, \dots, G$, the gradient of the group-specific log likelihood can be expressed via Fisher's identity as

$$\nabla_{\boldsymbol{\theta}} \log p(\mathbf{y}_g | \boldsymbol{\theta}) = \int \nabla_{\boldsymbol{\theta}} \log p(\mathbf{y}_g, \alpha_{l_{1,g}}^{(1)}, \dots, \alpha_{l_{K,g}}^{(K)} | \boldsymbol{\theta}) p(\alpha_{l_{1,g}}^{(1)}, \dots, \alpha_{l_{K,g}}^{(K)} | \mathbf{y}_g, \boldsymbol{\theta}) d\alpha_{l_{1,g}}^{(1)} \dots d\alpha_{l_{K,g}}^{(K)}, \quad (\text{S48})$$

where, here, the notation $l_{k,g}$ denotes the level of the k th categorical variable associated with group g . The Hessian of the group log likelihood can be similarly expressed via Louis' identity (22), which we do not restate here. The gradient and Hessian of the group log likelihood can then be approximated using the importance-sampling-based approach described in Sects. 2.3.1 and 2.3.2. Note that there are analytical formulae for the gradient (and Hessian) in this case, as the model is linear; but this approach is applicable to a wide class of GLMMs with crossed random effects.

R-VGAL is also applicable to models with nested random effects. One popular example of such models is that of students being nested within classes, which are then nested within schools (see, for example, Chapter 4 of West et al. (2014)). Suppose that we are interested in the final exam marks of Year 12 students across a number of schools in the year 2023. If we write the final mark of the k th student in the j th class at the i th school as y_{ijk} , for $i = 1, \dots, N$, $j = 1, \dots, n_i$ and $k = 1, \dots, n_{ij}$, then a simple linear model with one random intercept at both the school level and the class level is

$$y_{ijk} = \mathbf{x}_{ijk}^{\top} \boldsymbol{\beta} + \alpha_i + \gamma_{ij} + \epsilon_{ijk}, \quad \alpha_i \sim \text{Gau}(0, \sigma_{\alpha}^2), \quad \gamma_{ij} \sim \text{Gau}(0, \sigma_{\gamma}^2), \quad \epsilon_{ijk} \sim \text{Gau}(0, \sigma_{\epsilon}^2), \quad (\text{S49})$$

where \mathbf{x}_{ijk} is a vector of fixed covariates for the k th student (which may include, for instance, the average number of hours they spend studying per week, or the average number of hours slept per night), $\boldsymbol{\beta}$ are the corresponding fixed effects, α_i is the random effect associated with the school that the student attends, γ_{ij} is the random effect associated with the class they are in at their school, and ϵ_{ijk} is an error term associated with each student.

At the class level, the model (S49) may be written as

$$\mathbf{y}_{ij} = \mathbf{X}_{ij} \boldsymbol{\beta} + \mathbf{1}_{n_{ij}} \alpha_i + \mathbf{1}_{n_{ij}} \gamma_{ij} + \boldsymbol{\epsilon}_{ij}, \quad \alpha_i \sim \text{Gau}(0, \sigma_{\alpha}^2), \quad \gamma_{ij} \sim \text{Gau}(0, \sigma_{\gamma}^2), \quad \boldsymbol{\epsilon}_{ij} \sim \text{Gau}(\mathbf{0}, \boldsymbol{\Sigma}_{\epsilon,i}), \quad (\text{S50})$$

where $\mathbf{y}_{ij} \equiv (y_{ij1}, \dots, y_{ijn_{ij}})^{\top}$ is a vector containing final exam marks for all students in class j of school i , $\mathbf{X}_i \equiv (\mathbf{x}_{ij1}^{\top}, \dots, \mathbf{x}_{ijn_{ij}}^{\top})^{\top}$ is a design matrix containing fixed covariates from all students in class j of school i , $\mathbf{1}_d$ denotes a $d \times 1$ vector of ones, and $\boldsymbol{\epsilon}_{ij} \equiv (\epsilon_{ij1}, \dots, \epsilon_{ijn_{ij}})^{\top}$, for classes $j = 1, \dots, n_i$ and schools $i = 1, \dots, N$. For simplicity, we assume here that the error terms $\epsilon_{ijk}, k = 1, \dots, n_{ij}$, are uncorrelated, so

that $\Sigma_{\epsilon,i} = \sigma_\epsilon^2 \mathbf{I}_{n_{class,i}}$, where \mathbf{I}_d denotes a $d \times d$ identity matrix, and $n_{class,i}$ is the number of students in each class at school i , which we assume does not change with class; that is, we let $n_{ij} = n_{class,i}$, for $j = 1, \dots, n_i$ and $i = 1, \dots, N$.

We will now go one step further and write the model at the school level as

$$\mathbf{y}_i = \mathbf{X}_i \boldsymbol{\beta} + \mathbf{Z}_i \alpha_i + \mathbf{W}_i \boldsymbol{\gamma}_i + \boldsymbol{\epsilon}_i, \quad \alpha_i \sim \text{Gau}(0, \sigma_\alpha^2), \quad \boldsymbol{\gamma}_i \sim \text{Gau}(\mathbf{0}, \boldsymbol{\Sigma}_{\gamma_i}), \quad \boldsymbol{\epsilon}_i \sim \text{Gau}(\mathbf{0}, \mathbf{I}_{n_i} \otimes \boldsymbol{\Sigma}_{\epsilon,i}), \quad (\text{S51})$$

where \otimes denotes the Kronecker product between two matrices, $\mathbf{X}_i \equiv (\mathbf{X}_{i1}, \dots, \mathbf{X}_{in_i})^\top$, $\mathbf{Z}_i \equiv \mathbf{1}_{n_i n_{class,i}}$, $\mathbf{W}_i = \mathbf{I}_{n_i} \otimes \mathbf{1}_{n_{class,i}}$, $\boldsymbol{\gamma}_i \equiv (\gamma_{i1}, \dots, \gamma_{in_i})^\top$ is a vector of all random effects from classes $j = 1, \dots, n_i$ in school i , and $\boldsymbol{\epsilon}_i \equiv (\boldsymbol{\epsilon}_{i1}^\top, \dots, \boldsymbol{\epsilon}_{in_i}^\top)^\top$ is a vector of random error terms for all students in school i , $i = 1, \dots, N$. Here we allow the random effects $\gamma_{ij}, j = 1, \dots, n_i$ to be correlated between classes in the same school, so that for each school $i = 1, \dots, N$, the covariance matrix $\boldsymbol{\Sigma}_{\gamma_i}$ is potentially dense. We also assume that the school-specific random effects α_i are independent and identically distributed for all schools $i = 1, \dots, N$.

The parameters of interest in this model are $\boldsymbol{\theta} = \{\boldsymbol{\beta}, \sigma_\alpha^2, \boldsymbol{\Sigma}_{\gamma_1}, \dots, \boldsymbol{\Sigma}_{\gamma_N}, \sigma_\epsilon^2\}$. To make inference on these parameters, the R-VGAL updates can be performed by processing the data one school at a time. That is, for $i = 1, \dots, N$, the R-VGAL updates are made in terms of the gradient and Hessian of the school-specific log-likelihood, $\nabla_{\boldsymbol{\theta}} \log p(\mathbf{y}_i | \boldsymbol{\theta})$ and $\nabla_{\boldsymbol{\theta}}^2 \log p(\mathbf{y}_i | \boldsymbol{\theta})$. Using Fisher's identity (19), the gradient $\nabla_{\boldsymbol{\theta}} \log p(\mathbf{y}_i | \boldsymbol{\theta})$ can be written as

$$\nabla_{\boldsymbol{\theta}} \log p(\mathbf{y}_i | \boldsymbol{\theta}) = \int p(\alpha_i, \boldsymbol{\gamma}_i | \boldsymbol{\theta}) \nabla_{\boldsymbol{\theta}} \log p(\mathbf{y}_i, \alpha_i, \boldsymbol{\gamma}_i | \boldsymbol{\theta}) d\alpha_i d\boldsymbol{\gamma}_i, \quad i = 1, \dots, N, \quad (\text{S52})$$

where the term $\log p(\mathbf{y}_i, \alpha_i, \boldsymbol{\gamma}_i | \boldsymbol{\theta})$ can be expanded further as

$$\log p(\mathbf{y}_i, \alpha_i, \boldsymbol{\gamma}_i | \boldsymbol{\theta}) = \log p(\mathbf{y}_i | \alpha_i, \boldsymbol{\gamma}_i, \boldsymbol{\theta}) + \log p(\alpha_i, \boldsymbol{\gamma}_i | \boldsymbol{\theta}), \quad (\text{S53})$$

with

$$p(\mathbf{y}_i | \alpha_i, \boldsymbol{\gamma}_i, \boldsymbol{\theta}) = \text{Gau}(\mathbf{X}_i \boldsymbol{\beta} + \mathbf{Z}_i \alpha_i + \mathbf{W}_i \boldsymbol{\gamma}_i, \boldsymbol{\Sigma}_{\epsilon,i} \otimes \mathbf{I}_{n_i}),$$

$$p(\alpha_i, \boldsymbol{\gamma}_i | \boldsymbol{\theta}) = \text{Gau} \left(\begin{bmatrix} 0 \\ \mathbf{0} \end{bmatrix}, \begin{bmatrix} \sigma_\alpha^2 & \mathbf{0}^\top \\ \mathbf{0} & \boldsymbol{\Sigma}_{\gamma_i} \end{bmatrix} \right), \quad i = 1, \dots, N,$$

based on (S51). Approximation of the gradient $\nabla_{\boldsymbol{\theta}} \log p(\mathbf{y}_i | \boldsymbol{\theta})$ can then proceed via the importance-sampling-based approach in Sect. 2.3.1, and a similar procedure for the Hessian $\nabla_{\boldsymbol{\theta}}^2 \log p(\mathbf{y}_i | \boldsymbol{\theta})$ can be done

as shown in Sect. 2.3.2. As the model is linear in this case, we note that the log-likelihood, gradient, and Hessian are available analytically. However, this approach is applicable to a wide class of GLMMs with nested random effects.